

# التصميم الأمثل للخزانات الحديدية المستطيلة المستندة

على أساس مرن اعتمادا على

التحليل ألالا خطي

رسالة

مقدمة الى كلية الهندسة في جامعة بابل

كجزء من متطلبات نيل درجة ماجستير

في الهندسة المدنية

(الهندسة الإنشائية)

من قبل

علي حسين عبيد عجام

بكالوريوس هندسة مدنية

إشراف

أ.م.د. مصطفى بلاسم داود

أ.م.د. نمير عبد الأمير علوش

آذار ٢٠٠٦

**OPTIMAL DESIGN OF STEEL RECTANGULAR  
TANKS ON ELASTIC FOUNDATION BASED  
ON NONLINEAR ANALYSIS**

**A THESIS**

**SUBMITTED TO THE COLLEGE OF**

**ENGINEERING OF THE UNIVERSITY OF BABYLON**

**IN PARTIAL FULFILLMENT OF THE REQUIREMENTS**

**FOR THE DEGREE OF MASTER OF SCIENCE**

**IN**

**CIVIL ENGINEERING**

**(STRUCTURAL ENGINEERING)**

**BY**

**ALI HUSSEIN ABEAD AJAAM**

**(B.Sc)**

**SUPERVISED BY**

**Asst. Prof. Dr. Nameer A. Alwash      Asst. Prof. Dr. Mustafa B. Dawood**

**MARCH ٢٠٠٦**

بِسْمِ اللّٰهِ الرَّحْمٰنِ الرَّحِیْمِ

وَيَسْأَلُونَكَ عَنِ الرُّوحِ قُلِ الرُّوحُ مِنْ

أَمْرِ رَبِّي وَمَا أُوتِيتُمْ مِنَ الْعِلْمِ إِلَّا قَلِيلًا

صَدَقَ اللّٰهُ الْعَظِيمَ

(سورة الإسراء الآية ٨٥)

## الخلاصة

هذا البحث معني بالتصميم الأمثل للذن للخرانات المستطيلة الشكل المستندة على أسس مرنة بالاعتماد على التحليل المرن-الذن باستخدام طريقة العناصر المحددة التزايدية-التكرارية. تم استخدام عنصر القشرة المستوية ( flat shell element ) ذو العقد الثمان مع تحديد خمس درجات للحرية في كل عقدة متعلقة بالازاحات الثلاث ودورانين للمتجه العمودي في كل عقدة.

تم في الدراسة الحالية اشتقاق المعادلات الأساسية الخاصة بالتصرف للذن للعنصر المحدد (finite element)، بالاعتماد على قاعدة فون-ميسيز للخضوع (von-Mises yield criterion) وقاعدة برندتل-روز للجريان للذن (Prandtl-Reuss flow rule). تم اتباع أسلوب الخطوة-خطوة مع التكرار المعدل لنيوتن رافسن (modified Newton-Raphson) في كل خطوة تحميل.

قد اخذ التأثير المتداخل بين التربة والمنشأ بنظر الاعتبار وذلك باعتبار اللوح الأرضي مستندا على أساس مرن لا خطي.

في حالة الأمثلية الإنشائية والتي هي أمثلية مقيدة لا خطية ، قد تم استخدام طريقة هوك وجيفس (Hooke and Jeeves) المعدلة وباعتبار حجم المنشأ كدالة الهدف و أبعاد المنشأ كمتغيرات التصميم مع قيود هندسية. أنجز التصميم للذن باستخدام محدد فون ميسيز (von-Mises) للخضوع بدلالة محصلات الإجهاد مع إدخال تأثير القوة المحورية.

لقد جرى تحليل العديد من الأمثلة المتعلقة بتحليل الخزانات المستطيلة والتي قد تم تحليلها سابقا من قبل باحثين آخرين باستخدام طريقة العناصر المحددة الحالية. كما جرى تناول التصميم الأمثل للخرانات المستطيلة المستندة على أنواع مختلفة الأسس المرنة غير الخطية. لقد أظهرت النتائج بأن الشكل الأفق لقاعدة الخزان هو الشكل المربع, نسبة العرض : العمق المثلى ( ٣ : ١ ) وجد كذلك بأن الحل الأمثل ليس حساسا جدا بتغير نوع التربة وذلك للمسائل التي تم دراستها في هذا البحث.

## **ABSTRACT**

**This research deals with the optimal plastic design of rectangular tank on elastic foundation based on elastic-plastic incremental-iterative finite element analysis. The eight-node flat shell element is used in which five degrees of freedom are specified at each nodal point, corresponding to its three displacements and the two rotations of the normal at the node.**

**Formulation is introduced for the basic equations relating to the incremental plasticity approach, based on von-Mises yield criterion and Prandtl-Reuss flow rule. Numerical solutions are obtained using a three-level process: subincrements within iteration within load increments. This process is improved through the application of modified Newton-Raphson iteration technique in each load increment.**

**The soil-structure interaction is taken into consideration by assuming that the floor slab is resting on non-linear elastic foundation.**

**For the structural optimization problem, which is dealt with as a constrained non-linear optimization, the so-**

**called Modified Hooke and Jeeves method is employed considering the volume of the structure as the objective function and dimensions as the design variables with geometrical constraints. A plastic design is carried out using von-Mises yield criterion in terms of stresses resultants while the effect of axial force is incorporated. A computer program has been developed for the foregoing method.**

**Several examples for the analysis of rectangular tank, those analyzed previously by others, are worked out using the present finite element analysis. Optimal design of rectangular tank resting on different types of non-linear elastic foundation is also carried out. The results show that the square shape forming the best plan shape, the optimal width:depth ratio is about (3:1) and it is found that the optimum solution is not so sensitive to the type of soil for the problems considered in this study.**

### **ACKNOWLEDGMENTS**

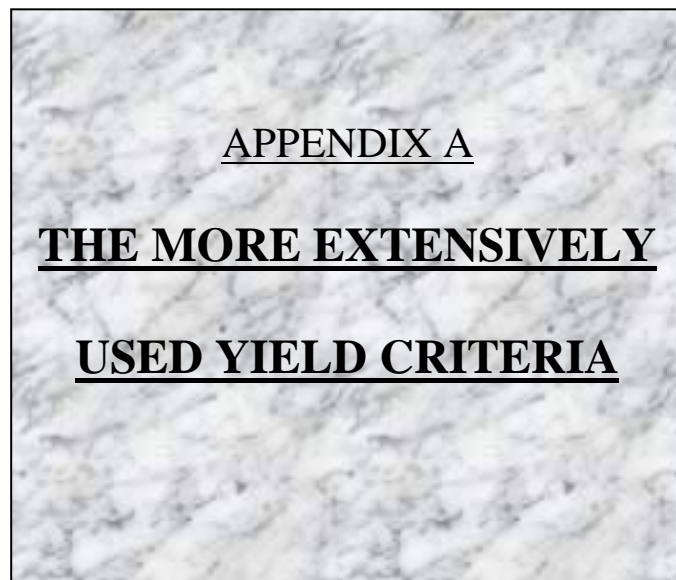
First of all, Praise to ALLAH, Lord of the whole creation

I would like to express my deepest thanks and appreciation to my supervisors **Asst. Prof. Dr. Nameer A. Alwash** and **Asst. Prof. Dr. Mustafa B. Dawood** for their valuable suggestions, encouragement, time and kind support

at every stage of this work; without their help, this mission would not have been accomplished.

I also wish to thank my parents and my wife for their constant support, assistance and understanding.

I extend my thanks to the staff of Civil Engineering Department at Babylon University. Special thanks to my friends Haider and Jawad for their aid. Finally, I would like to thank all friends and colleagues who helped in this work.



### **A.1 Tresca yield criterion:**

This yield criterion is also called the shear stress failure-yield criterion. The mathematical expression for such criterion could be given in terms of the principal stresses (  $\sigma_1, \sigma_2, \sigma_3$  ) as follows:

$$\bar{\sigma} = \max(|\sigma_1 - \sigma_2|, |\sigma_2 - \sigma_3|, |\sigma_3 - \sigma_1|) \quad \text{-----(A.1)}$$

The value of the maximum shear stress at yielding is given as:

$$\tau_o = \bar{\sigma} / 2 \quad \text{-----(A.2)}$$

The condition that is given in Eq.(A.1) is represented in cartesian arthogonal axes (  $\sigma_1, \sigma_2, \sigma_3$  ) by the hexagonal prism formed by the planes with equations

$$\sigma_1 - \sigma_2 = \pm \bar{\sigma}; \sigma_2 - \sigma_3 = \pm \bar{\sigma}; \sigma_3 - \sigma_1 = \pm \bar{\sigma} \quad \text{-----(A.3)}$$

When one of principal stresses vanishes, say  $\sigma_3$  , the surface reduced to the hexagon obtained by intersecting the prism with the plane  $\sigma_3=0$  . Figure(A.1 a).

The yield condition becomes

$$\bar{\sigma} = \max(|\sigma_1|, |\sigma_2|, |\sigma_1 - \sigma_2|) \quad \text{-----(A.4)}$$

### **A.2 von Mises yield criterion:**

More refined tests have shown (43) that the circular cylinder circumscribed to the considered hexagonal prism is a more exact “yield surface” for most metals. This surface represents the yield condition of von Mises. For this reason and the simplicity in the mathematical expression of this criterion, it is adopted in this thesis. The mathematical expression of this criterion in terms of principal stresses is:

$$\sigma_1^2 + \sigma_2^2 + \sigma_3^2 - \sigma_1\sigma_2 - \sigma_2\sigma_3 - \sigma_3\sigma_1 = \bar{\sigma}^2 \quad \text{-----}(A.5)$$

**For a stat of plane stress problem ( $\sigma_3=0$ ), condition (A.5) is represented by the ellipse of figure (A.1 b) with the equation**

$$\sigma_1^2 + \sigma_2^2 - \sigma_1\sigma_2 = \bar{\sigma}^2 \quad \text{-----}(A.6)$$

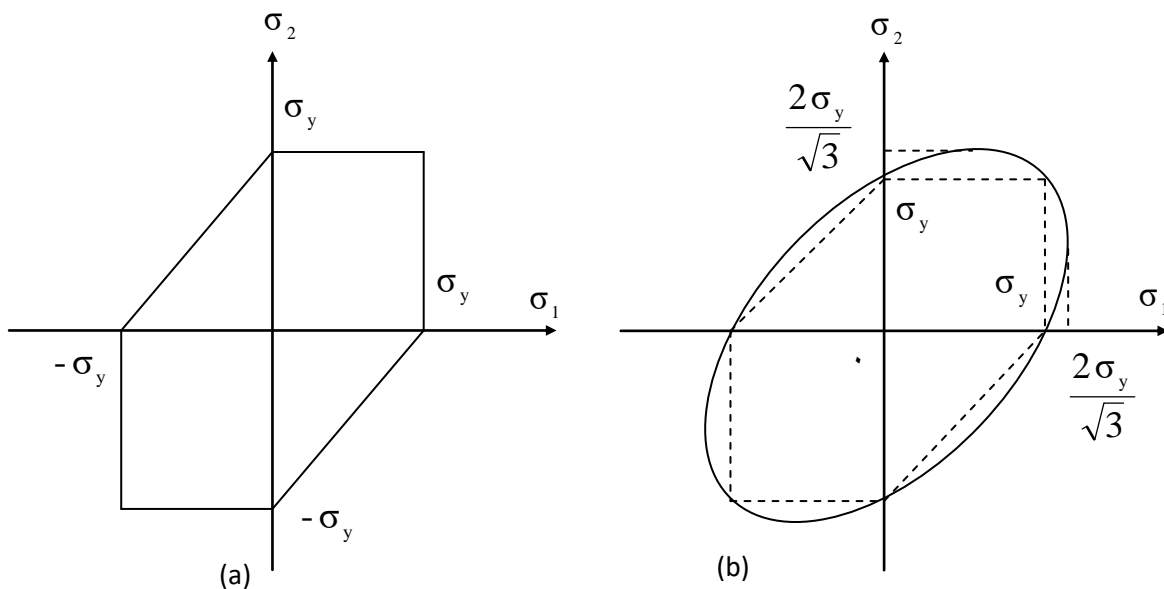


Figure (A.1): Yield curves for plane stress.

(a) Tresca condition.

## LIST OF CONTENTS

Subject	Page
Acknowledgments.....	I
Abstract.....	II
List of contents.....	III
List of Figures.....	V
List of Tables.....	VII
Notation.....	VIII
<b>CHAPTER ONE: INTRODUCTION</b>	
1.1 General.....	1
1.2 Structural optimization.....	2
1.3 Non-linear material analysis.....	3
1.4 Non-linear behavior of soil.....	3
1.5 Aims and layout of the present study.....	5
<b>CHAPTER TWO: LITERATURE REVIEW</b>	
2.1 General.....	6
2.2 Analysis of tanks.....	6
2.3 Optimal design of tanks.....	11
<b>CHAPTER THREE: FORMULATION OF FINITE</b>	16

## **ELEMENT ANALYSIS**

۳.۱ General.....	۱۶
۳.۲ Flat shell element.....	۱۷
۳.۳ Formulation of element stiffness matrix.....	۱۸
۳.۳.۱ Strains.....	۱۸
۳.۳.۲ Stresses.....	۲۰
۳.۳.۳ Isoparametric formulation.....	۲۱
۳.۳.۴ Numerical integration.....	۲۶
۳.۳.۵ Elastic foundation.....	۲۷
۳.۴ Transformation of the coordinates.....	۲۸
۳.۵ Formulation of the basic elastic-plastic equations	۳۰
۳.۶ An algorithm for the present incremental finite element analysis.....	۳۴
۳.۷ Computer program for analysis	۳۹
۳.۸ Non-linear behavior of soil.....	۴۴
۳.۸.۱ Soil characterization.....	۴۵
۳.۸.۲ Modeling of stress-strain curve of soil.....	۴۵
۳.۸.۲.۱ Hyperbolic stress-strain mode.....	۴۶
۳.۸.۲.۲ Polynomial model.....	۴۹

## **CHAPTER FOUR: OPTIMAL DESIGN**

۵۰

### **FORMULATION**

۴.۱ Optimization.....	۵۰
-----------------------	----

ξ.1.1 General.....	50
ξ.1.2 Direct Search Methods.....	51
ξ.1.3 Hooke and Jeeves Method.....	52
ξ.1.4 Dealing with Constraints.....	53
ξ.2 Plastic Design.....	56
ξ.2.1 General.....	56
ξ.2.2 Elastic-Plastic Behavior.....	56
ξ.2.3 Plastic Bending.....	61
ξ.2.4 Calculation of the Plastic Moment.....	60
ξ.2.4.1 General.....	60
ξ.2.4.2 Rectangular Section.....	60
ξ.2.4.3 Axial Force.....	67
ξ.2.5 Design technique.....	69
ξ.2.6 Computer Program.....	71
ξ.3 Load Factor.....	72
<b>CHAPTER FIVE: APPLICATIONS AND</b>	73

## DISCUSSION

ο.1 General.....	73
ο.2 Applications for testing the program.....	74
ο.2.1 Example No.1.....	74
ο.2.2 Example No.2.....	76
ο.2.3 Example No.3.....	78

ο.2.ε Example No. ε.....	80
ο.2.ο Example No. ο.....	81
ο.2.6 Example No. 6.....	80
ο.3 Optimal design application.....	88
ο.3.1 Open topped rectangular tank.....	88
ο.3.2 Closed rectangular tank.....	92

**CHAPTER SIX: CONCLUSIONS AND** 97

**RECOMMENDATIONS**

6.1 Conclusions.....	97
6.2 Recommendations for future research.....	98

**REFERENCES**..... 99

APPENDIX A:THE MORE EXTENSIVELY USED YIELD RITERIA	A.1
---	-----

**LIST OF FIGURES**

<b><u>Figure No.</u></b>	<b>Title</b>	<b><u>page</u></b>
1.1	Proposed hyperbolic stress-strain curve of soil.	ε
3.1	Flat shell element subject to in-plane and bending action.	17
3.2	Eight node quadrilateral in ζ , η space.	21
3.3	<b>Flat shell displacements in global</b>	26

## direction.

۳.۴	Four and nine gauss point positions for selective integration.	۲۷
۳.۵	Stress strain relation in uniaxial tension.	۳۳
۳.۶	Incremental technique with modified Newton-Raphson iteration for single degree of freedom.	۳۵
۳.۷	Scaling the stresses vector $\{\sigma_m\}$ at the end of subincrement (m) so as to satisfy the yield criterion.	۳۸
۳.۸	Flow chart of the developed program.	۴۰
۳.۹	Proposed hyperbolic stress-strain curve of soil.	۴۷
۳.۱۰	Hyperbolic load-settlement curve.	۴۸
۳.۱۱	Transformed hyperbolic load-settlement curve.	۴۹
۴.۱	Contour lines for function of two variables.	۵۱
۴.۲	Flow chart for Hooke and Jeeves method.	۵۴
۴.۳	Flow chart for an exploration.	۵۵
۴.۴	Uniaxial tensile specimen.	۵۷
۴.۵	Stress-strain diagram.	۵۷
۴.۶	Bauschinger Effect.	۵۹
۴.۷	Perfect elastic-plastic behavior.	۶۰
۴.۸	Stress-strain curves for different types of steel.	۶۱
۴.۹	Elastic stress and strain.	۶۲
۴.۱۰	Stress distribution at yield.	۶۳
۴.۱۱	Stress distribution after yield.	۶۳

ε.12	Constant yield stress at plastic stage.	74
ε.13	Formation of plastic hinge.	74
ε.14	Constant stress distribution.	70
ε.15	Rectangular section.	76
ε.16	The equivalent stresses.	78
ε.17	Diagram for equation.	79
ο.1	Simply supported square plate.	70
ο.2	Load verses central deflection for different mesh sizes.	70
ο.3	Load verses central deflection.	76
ο.4	Rectangular wall with hydrostatic pressure.	77
ο.5	Structure considered by Ng et al.	78
ο.6	load-displacement carve of simply supported box beam at midspan.	79
ο.7	Applied load on wall panel and floor slab.	80
ο.8	Bending moments obtained by finite element solution for rectangular tank filled with water when the bottom edge of the walls are fully clamped.(Example ε).	82
ο.9	Bending moments obtained by finite element solution for rectangular tank filled with water when the bottom edge of the tank is supported on dwarf walls around the edges.(Example ο).	83
ο.10	Distribution of plastic zones of an open-topped rectangular tank at failure stage.	84
ο.11.a	Finite elements groups for roof slab.	86

o.11.b	Finite elements groups for wall in x-direction.	86
o.11.c	Finite elements groups for floor slab.	87
o.11.d	Finite elements groups for wall in y-direction.	87
o.12	Tank on elastic foundation.	89
o.13	Mid wall horizontal deflection for different mesh sizes.	90
o.14	Volume of shell verses number of cycles for case No.1.	91
o.15	Volume of shell verses number of cycles.	91
o.16	Load-settlement curve of soil[dense sand].	94
o.17	Load-settlement curve of soil[loose sand].	94
o.18	Volume of shell verses number of cycles for (100m <sup>3</sup> ) closed tank.	90
o.19	Volume of shell verses number of cycles for (300m <sup>3</sup> ) closed tank.	90
o.20	Relation between optimum dimensions and tank volume.	96
o.21	Relation between optimum thicknesses and tank volume.	96
A.1	Yield curves for plane stress.	A.2

## LIST OF TABLES

<u>Table No.</u>	<u>Title</u>	<u>Page</u>
۲.۱	Types of tank considered in various codes.	۷
۵.۱	Bending moments in a rectangular wall loaded by hydrostatic pressure.	۷۷
۵.۲	Maximum absolute service bending moments in groups.	۸۸
۵.۳	Initial values of dimensions.	۹۰
۵.۴	Optimization results for case No. ۱.	۹۲
۵.۵	Optimization results for case No. ۲.	۹۲
۵.۶	Initial values of dimensions.	۹۳
۵.۷	Optimum dimensions for different storage capacity.	۹۳

## NOTATION

Symbol	Description
a,b	Constant can be obtained from plate-load test.
[B]	The constitutive strain-displacement matrix.
$b_i$	<b>Bound at the <math>i</math>th constraint.</b>
$b_i$	<b><math>i</math>th base point.</b>
D	<b>Depth.</b>

$\{dI_r\}_j$	<b>Vector of internal forces for each element in the local coordinates.</b>
$\{dI_r\}$	<b>Vector of internal forces for each element in the global coordinates.</b>
$\{dR\}_j$	<b>Vector of residual forces for the whole structure.</b>
$\{dIR\}_j$	<b>Vector of internal forces for the whole structure.</b>
$d\bar{\sigma}$	<b>Effective stress increment.</b>
$d\bar{\varepsilon}^p$	<b>Effective plastic strain increment.</b>
$d\lambda$	<b>A non-negative scalar.</b>
$\{d\sigma\}$	<b>Vector of stress increments.</b>
$\{d\varepsilon^e\}$	<b>Vector of elastic strain increments.</b>
$\{d\varepsilon^p\}$	<b>Vector of plastic strain increments.</b>
$\{d\varepsilon^{ep}\}$	<b>Vector of total strain increments.</b>
$E$	<b>Modulus of elasticity.</b>
$E_{sh}$	<b>Initial slope of strain hardening region.</b>
$e_i$	<b>Unit vector in the direction of the i-axes.</b>
$[E]$	<b>Elasticity matrix.</b>
$f$	<b>Objective function.</b>
$G$	<b>Shear modulus of elasticity.</b>
$g_i$	<b>i-th constraint.</b>
$h$	<b>Step length.</b>
$H'$	<b>Hardening parameter.</b>
$[J]$	<b>Jacobian matrix.</b>

$K_n$	Normal subgrade reaction of soil.
$[K]$	Stiffness matrix of the whole structure.
$[K_f]$	Soil stiffness matrix in local coordinates.
$[k]$	Stiffness matrix of an element in global coordinates.
$[k']$	Stiffness matrix of an element in local coordinates.
$L$	Length.
$[L]$	matrix of direction cosines.
$M_p$	Plastic moment.
$M'_p$	Changed plastic moment.
$N_p$	Squash load.
$P_i$	$i$ th pattern point.
$q$	Pressure at the base.
$\{R\}$	Vector of nodal forces for the whole structure.
$\{r'\}$	Vector of nodal forces for each element in local coordinate.
$t$	Thickness.
$t_f$	Floor thickness.
$t_l$	Thickness of wall in X-direction.
$t_r$	Roof thickness.
$t_w$	Thickness of wall in Y-direction.
$[T]$	Transformation matrix.
$[T]^T$	Transpose of the transformation matrix.
$U$	Strain energy.

$W$	Width.
$X,Y,Z$	Global Cartesian coordinate system.
$x,y,z$	Local Cartesian coordinate system.
$\{\Delta\}$	Vector of displacements for the whole structure.
$\{\delta\}$	Vector of displacements of an element in global coordinates
$\{\delta'\}$	Vector of displacements of an element in local coordinates.
$\varepsilon$	Axial strain.
$\varepsilon_1, \varepsilon_2, \varepsilon_3$	Principal strain.
$\{\varepsilon\}$	Vector of strains.
$\{\varepsilon^b\}$	Vector of axial strains due to bending action.
$\{\varepsilon^{pl}\}$	Vector of axial strains due to in-plane action.
$\varepsilon_x$	Axial strain in the local x-direction.
$\varepsilon_y$	Axial strain in the local y-direction.
$\gamma_{xy}$	Shear strain in the local x-y plane.
$\gamma_{yz}$	Shear strain in the local y-z plane.
$\gamma_{zx}$	Shear strain in the local z-x plane.
$\lambda$	Constant of proportionality.
$\nu$	Poisson's ratio.
$\{\sigma\}$	Vector of stresses.
$\sigma_1, \sigma_2, \sigma_3$	Principal stresses.
$\bar{\sigma}$	Effective stress.

$\sigma_Y$	Yield stress.
$\sigma_{Y_u}$	The upper yield point stress.
$\sigma_{u.t.s}$	Ultimate tensile stress.
$\tau$	Shear stress.
$\zeta, \eta$	Isoparametric coordinates

**Note: Any other notation may be explained where it appears.**

We certify that the preparation of this thesis was carried out under our supervision at the University of Babylon in partial fulfillment of the requirements for the degree of master of Science in Civil Engineering.

Signature :

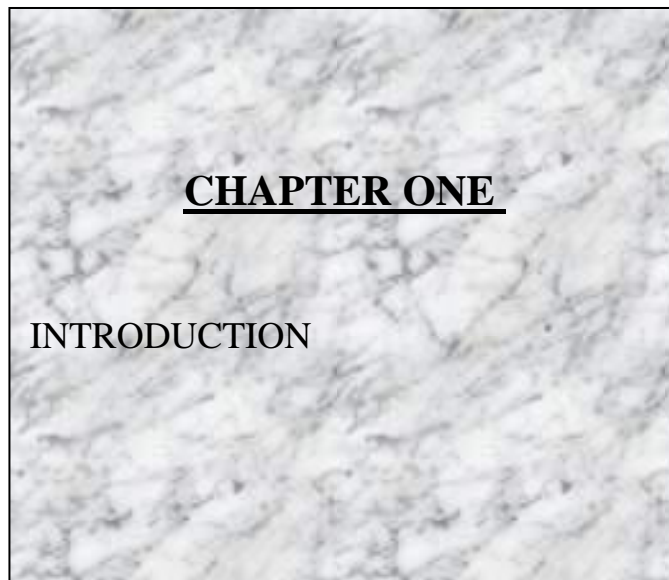
Name : N. A. Alwash

Date : / / ٢٠٠٦

Signature :

Name : M. B. Dawood

Date : / / ٢٠٠٦



**١.١ General :**

**Many structural design problems have numerous solutions and the purpose of optimization is to find the best possible solution among the many potential solutions satisfying the chosen criteria. Designers often base there**

**designs on minimum weight, especially in steel structures, or minimum cost as objectives, since they are seeking lighter and more economical design taking into account function, safety and serviceability.**

**With the increase of large computers and as a result of the important development in optimization techniques, many engineering researches, in the last few years, have been oriented to the field of obtaining optimum design by computers.**

**Consistent with the purpose of this thesis, this introduction makes basic reference to three aspects: the optimum design of rectangular tanks, non-linear analysis of rectangular tanks and non-linear behavior of soil.**

## **1.2 Structural optimization :**

**Since 1970, structural optimization has been the subject of intensive research and several different approaches for optimal design of structures have been advocated (10). The aim of optimization of structural system is to find out the best combination of design variables that minimize an objective function without sacrificing the functional and performance constraints. The simplest approach to design such structures is to perform analysis for all possible combinations of design variables. However, it is almost impossible to perform such analysis since a huge number of combinations has to be considered in actual cases.**

**Therefore, many kinds of structural optimization techniques have been proposed in the past years(13). Structural optimization problems are characterized by various objective and constraint functions that are generally non-linear functions of the design variables. The mathematical formulation of structural optimization**

problems with respect to the design variables, the objective and constraint functions depends on the type of application. However, all optimization problems can be expressed in standard mathematical terms as a non-linear programming problem, which in general form can be stated as follows:

$$\begin{aligned} & \min && f(x_1, x_2, x_3, \dots, x_n) \\ & \text{subject to} && g_i(x_1, x_2, x_3, \dots, x_n) \leq b_i \quad (i = 1, 2, \dots, m) \end{aligned}$$

where:

$(x_1, x_2, x_3, \dots, x_n)$  : vector of design variables

$f(x_1, x_2, x_3, \dots, x_n)$ : objective function to be minimized

$g_i(x_1, x_2, x_3, \dots, x_n)$ : behavioral constraints

$b_i$ : the bounds of the constraints.

$n$ : number of the design variables.

$m$ : number of the constraints.

1.3 Non-linear material analysis :

The study of non-linear behavior of a structure has been required increasingly in the last few years in order to insure the integrity of the structural design. The use of the finite element method with Newton-Raphson iteration technique, with the aid of computer facilities, make such study practically possible. The non-linear problems may be solved by taking a series of linear steps (19). In the present investigation a three level process has been used: subincrements, within iterations, within load increments.

The non-linear effects due to plastic deformation are treated based on von-Mises yield criterion and Prandtl-Reuss flow rule. The adopted approach to solve the present non-linear problem is the incremental finite element method in which the load is increased in small steps. The effect of material non-linearities is considered through updating the stiffness matrix at the beginning of

each load step and summing the results for all the preceding steps to give the overall effects at the end of that step ( $\epsilon$ ). This incremental approach is improved through the application of the modified Newton-Raphson iteration technique in each load step.

1.4 Non-linear behavior of soil :

Most phenomena in the soil mechanics are non-linear. In many applications, however, it is practical and convenient to use linear formulations for problems to obtain engineering solutions. On the other hand, some problems definitely require non-linear analysis if realistic results are to be obtained.

The stress-strain relation of any type of soil depends on a number of different factors including density, water content, structure of the soil, drainage conditions, strain condition (i.e. plane strain, triaxial), duration of loading, stress history and confining pressures ( $\sigma_3$ ).

It is commonly found (1.3) that the stress-strain curve for all soil is non-linear except in a very narrow region near the origin. Kondner (3.3) proposed that the stress-strain curve, which is shown in Figure (1.1), could be represented by a hyperbolic equation of the form :-

$$\sigma_1 - \sigma_3 = \frac{\epsilon}{a + b\epsilon} \quad \text{-----} \quad \text{-----(1.1)}$$

where

$\sigma_1$  and  $\sigma_3$  are the major principal stresses.

$\epsilon$  :is the axial strain in the direction of  $\sigma_1$  and (a) and (b) are constants which can be determined experimentally.



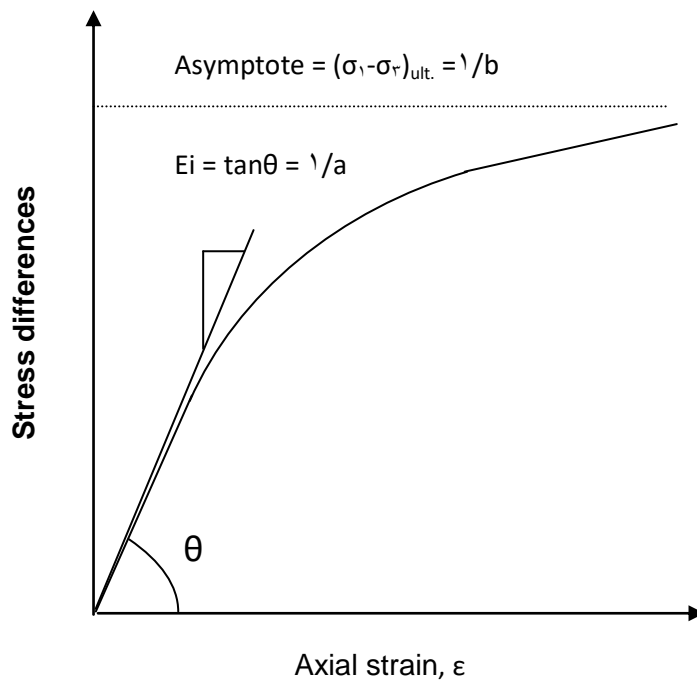


Figure (1.1): Proposed hyperbolic stress-strain curve of soil(۳۳).

#### ۱.۲ Aims and layout of the present study :

**The present work deals with the optimum design of rectangular tank on elastic foundation. The subject has a special importance because tanks are industrial structures with repetitive nature; therefore, any reduction in the cost whatever it is small will lead to high reduction in the total cost when a large number of tanks will be constructed.**

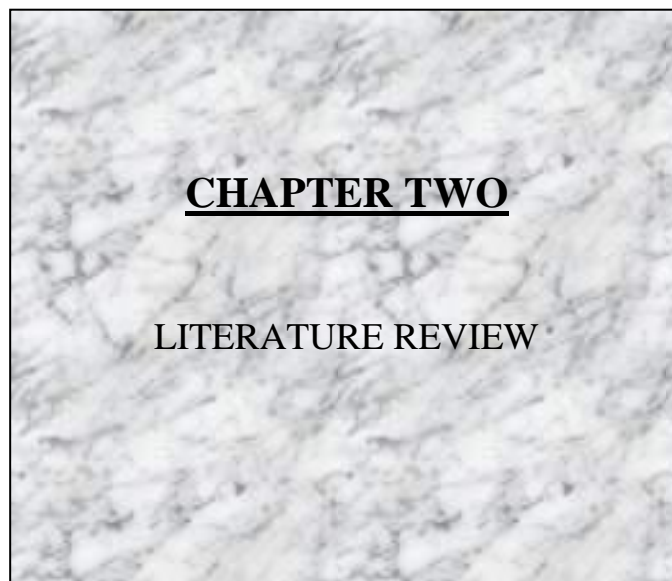
**The main aims of the present study are:**

- ۱- Studying the elastic-plastic analysis of rectangular tank structures by the incremental finite element method with iterations. The foundation is represented by a model ( either Winkler, or Kondner, or polynomial ) for normal subgrad reaction while the horizontal subgrad reaction is represented by Winkler model.**
- ۲- Performing an optimal design of the problem based on that non-linear analysis. To carry out the structural optimization, the modified Hooke and Jeeves method is**

used while the von-Mises yield criterion in terms of stresses resultant is used as a design technique.

The thesis consists of six chapters. The present introductory chapter is being the first. Chapter Two is concerned with the review of literature; outlines of some previous research work on optimal design and analysis of tanks are presented. The formulation of flat shell element, elasto-plastic constitutive relations and the non-linear behavior of elastic foundation are presented in Chapter Three.

Chapter Four is devoted to the optimal design formulation. In Chapter Five, several numerical examples are presented for both analysis and optimal design verified with previous analytical and experimental studies. Finally, Chapter Six gives the conclusions and suggestions for future studies.



**۲.۱ General :**

**This review covers two aspects. The first is the developments in the analysis of tank and the second is the developments in the optimal design of rectangular and circular tank resting on rigid or elastic media.**

**2.2 Analysis of tanks :**

**One of the tank problems is the interaction of the tank walls with roof or base. Specific work on tanks has endeavored to take this into account. The work on the tank problem, as it is a progression from the work on isolated plates, has been approached using directly analytical, numerical, and analogy methods. These methods of analysis have been surveyed in references (27, 28). Examples of directly analytical methods are direct integration, use of series, and energy methods. Finite difference and finite element are both numerical methods.**

**Analogy method includes such methods as grid-framework, plan-framework, and space-framework.**

**The cylindrical shape is structurally best suited for tank construction, but rectangular tanks are frequently preferred for specific purposes. Table (2.1) provides details of the types of tanks considered in various codes(29).**

<b>Codes</b>	<b>Type of tanks</b>
<b>ACI 308.1</b>	<ul style="list-style-type: none"> <li>● <b>Ground supported circular and rectangular concrete tanks with fixed and flexible base .</b></li> <li>● <b>Pedestal supported elevated tanks .</b></li> </ul>
<b>AWWAD- 100 &amp; D- 103</b>	<ul style="list-style-type: none"> <li>● <b>Ground supported steel tanks with fixed and flexible base .</b></li> <li>● <b>Elevated steel tanks with braced frame and pedestal type supporting tower .</b></li> </ul>
<b>AWWAD- 110 &amp; D-</b>	<ul style="list-style-type: none"> <li>● <b>Ground supported prestressed concrete tanks with fixed and flexible base .</b></li> </ul>

110	
API 650	<ul style="list-style-type: none"> <li>● Ground supported steel petroleum tanks ( Type of base support are not described )</li> </ul>
NZSEE Guidelines	<ul style="list-style-type: none"> <li>● Ground supported circular and rectangular tanks with fixed and flexible base .</li> <li>● Elevated tanks .</li> </ul>
Eurocode 8	<ul style="list-style-type: none"> <li>● Ground supported circular and rectangular tanks with fixed base .</li> <li>● Elevated tanks .</li> </ul>

Table (2.1): Types of tank considered in various codes(29).

**The following is a review of work specifically related to the tank problem.**

**In 1938, a paper by Buchi (12) described a simple approximate method of determining the maximum vertical and horizontal bending moments developed in the walls of open square tanks. He assumed complete fixity for the side and bottom edges. The Portland Cement Association published a booklet (21) containing tables of moment and shear values for rectangular tanks with walls in which the base joint is hinged or completely fixed.**

**The finite difference method, as applied to plates, was applied to tanks by Gali (22) in 1957. He found, however, that it was not a method readily amenable to programming for computer and it was difficult to express boundary conditions and various approximations have to be introduced to obtain numerical solutions.**

**One analogy method is that of the grid framework described by Lightfoot (30) in 1958. In that work, due to symmetry, the tank were developed into single flat plate, and the edge condition of that plate were taken as those**

that would occur in the tank. These plates were then treated as a grid framework. For analytical purposes, two systems were considered which were superimposed. The first one is the system of in-plane forces and the other includes bending moments and torques. These frame systems comprised rectangular frames, each with two diagonal members. The method took into account any value of Poisson's ratio. The linearly varying hydrostatic loads on the wall and the pressure on the base were treated as equivalent point loads acting at the nodes of the elements.

The rotation of the wall-base slab and wall-roof slab joints was taken into account by making use of a moment distribution method. This work was suggested by Ghali (٢٥) in ١٩٥٩. In this method the distribution factors are based on freely supported plates. In reality, this method is not accurate since the influence of subgrad reaction is not accounted in the calculation of the distribution factors in the base slab.

One of the most comprehensive texts on individual plates, used for tanks, was that of Timoshenko (٤٦) in ١٩٥٩, which contained extensive tables and charts for the elastic analysis of plates subjected to various loads including hydrostatic types of loading.

Davies (٢٠) in ١٩٦١ proposed a method for analyzing tanks resting on soil of various engineering properties making use of the moment distribution technique. The data required for the moment distribution is available in the form of tables and charts.

Davies (٢١) in ١٩٦٢ published another paper which describes a rapid method of predicting the elastic behavior of cylindrical tanks by assuming contact pressure distributions which are suitable for granular or cohesive

soils. Although, the contact pressure is not actual, the analysis by this approach had given a guide to the limits of the order of magnitude of bending moments to be considered in the design of tanks.

A second analogy method is called the space-frame method represented by Husain (۲۸) in ۱۹۶۴. The developed plate was considered as constituted of grid framework as previously explained. However, in the structural analysis of these analogous grid frameworks the in-plane forces and the bending moments and torques are not separated. The deformation of the analogous members was thus taken into account in the analysis. The method took into account any value of Poisson's ratio. He concluded that the advantages of the analogy method are:

- ۱- Its ability to be applied to any shape of tank.
- ۲- Its ability to take into account Poisson's ratio and deformations when necessary.
- ۳- Its amenability to computer programming.

He also, found that its principal disadvantage is that the analogy has its limitations predicting plate behavior when length to breadth ratio of plate exceeds ۳:۱.

The finite element method, as applied to plates, was applied to tanks by Cheung and Zienkiewicz (۱۶) in ۱۹۶۵.

The finite element method can deal with boundary conditions more easily than the finite difference method.

Indeed, it can deal with openings, interaction discontinuities, and point loads much more easily than the finite difference method. As the finite element method is a very powerful method used in conjunction with the digital computer, it has become popular for use in solving difficult analyses, including those involving discontinuities.

**It was therefore inevitable that it would be applied to tanks.**

**Cheung and Zienkiewicz (16) in 1960 applied the finite element method to the analysis of open square tanks on elastic foundation. They analyzed a square tank on spring of four different spring constants. The deflections and moments were compared with the experimental and theoretical work.**

**In 1967, Cheung and Davies (17) applied the finite element to the analysis of rectangular tanks on elastic foundation taking into account the interaction between wall-wall-base. The analysis gives a good agreement with experimental results.**

**Again, in 1967, Cheung and Davies (18) applied that work to the case of long-walled tanks, ignoring the interaction between wall-wall-base. They proved that horizontal bending moments were not negligible at and near the wall corners, as was previously assumed by many designers and recommended by various books.**

**Davies et al. (22) in 1970 extended that work by applying the finite element method to the analysis of long rectangular closed tanks. They proved that the one-dimensional bending action, often assumed by many designers, in a long walled tank was significantly modified due to the restraining action of the end cross walls.**

**In 1979, Gali (26) presented an approach based on the stiffness and flexibility methods of analysis to derive the relevant coefficients required for analysis. A set of design table in a dimensionless form is provided and their use is illustrated by examples. These tables are calculated assuming classical boundary conditions at the base i.e completely fixed, hinged, or free.**

Starzewski (22) in 1981 applied the fundamental theory to the analysis and design of some typical pressur vessels of non-circular cross-section, the most common of which are the rectangular section tanks. He designed an open top rectangular tank with continuous horizontal wall stiffeners.

Al-Mahaidi (23) in 1986 has advanced a treatment of circular storage tanks resting on a Winkler-type elastic media. He transformed the entire tank into a single equivalent one-dimension system having six degrees of freedom only. In this reference all components of the tank (top slab, bottom slab, and cylindrical shell ) are assumed to be prismatic.

Al-Sarrai (24) in 1988 presented a computer-based method for the analysis of non-prismatic circular cylindrical tanks resting on a Winkler-type elastic media. One-dimensional finite elements are used for this purpose. The study covered open or closed tanks, tanks with central columns, tanks with intermediate columns, and tanks with any number of concentric compartments.

In 1992, Kimence and Erguven (25) made a study of cylindrical tank on Vlasov model. The results have been compared to the Winkler model and elastic half-space. It was shown, that the Vlasov model and half-space solution were very close.

#### 2.3 Optimal design of tanks :

Meichoers and Rozvany (26) in 1970 studied the optimum design of reinforced concrete circular tanks. It was assumed that self weight of the tank is negligible, and that no axial ( longitudinal ) load was applied. Two cases were examined: (1) Free at the top and fixed at the base; and (2) Free at the top and hinged at the base. Only longitudinal bending and transverse tensile stresses were

**considered. The concrete was assumed to have zero tensile strength, then no interaction of behavior of the concrete in each direction would occur.**

**The steel reinforcing was assumed to take uniaxial stress only, its lateral strength was neglected. The design objective was the minimization of the reinforcing steel volume, subjected to the constraints of equilibrium. The geometry of the structure was taken as fixed with certain limits. Costs of labor and formwork were taken as fixed. No consideration was given to design parameters such as crack control, deflections and code provisions. For the problem being considered, it was shown that design based on lower bound analysis gave lower total steel volume than equivalent design based on elastic stress distribution, or on uniform isotropic yield-line analysis.**

**A more general formulation of the optimum design of reinforced concrete cylindrical tank by using constrained non-linear programming was developed by Adidam and Subramanyam (2), in 1982. The design was to conform to BS 5337:1976. The design procedure used was a combination of the limit state method and a numerical method of optimization. Cost of the tank consisting of the tank wall and floor, which included cost of concrete, reinforcement and formwork, was chosen as the objective function in the optimization problem formulation.**

**Thickness of the wall and its reinforcement were treated as the unknown of the design. The outer dimension and the thickness of the floor were taken as fixed. The objective function was subjected to the constraints of bending, hoop tension and crack width. No consideration was given to shear, shrinkage and temperature constraints. It had been found that optimization coupled**

**with limit state design results in significant reduction in the cost of the tank.**

**In 1980 Abdul Hussain (1) studied the optimum design of reinforced concrete under-ground rectangular water tanks. The design was to conform to BS 5337:1976. The provisions of this code formed the constraints on the design problem. The analysis was carried out by stiffness method. The variables of the problem included, the external dimensions, number of interior baffle walls, thickness of members and steel reinforcement area at six locations for each member. The problem with its variables and constraints was solved using Rosenbrock method for optimization after introducing the multilevel optimization approach. In that study, it was found that the external dimensions have significant influence on the optimal cost, with the square shape forming the best plan shape. The influence of the number of baffle walls was found to be rather insignificant.**

**In 1986, Therendran and Thambiratnam (2) made an optimum minimum weight, design of plane concrete cylindrical tank with piecewise linear variation of the thickness, assuming the shell is fixed at the bottom. A combination of the finite element analysis and numerical method of optimization was used in the design procedure.**

**The constraints of the problem were to conform to BS 5337:1976, and the design variable was only the variation of wall thickness. The internal radius and the height of the tank were assumed to be fixed. An optimization routine based on Rosenbrock's direct search method was used for optimization purposes.**

**Al-Ne'aimi and Al-Sabah (3) in 1988 made an optimum, minimum cost, design of tapered shell R/C cylindrical tank resting on Winkler type elastic medium.**

The analysis was performed according to the direct stiffness method. The radius, height of the tank, top and bottom thickness of the shell, floor thickness, and steel reinforcement area were treated as the design variables. The objective function was chosen as the cost of the tank consisting of the tank shell and floor which includes cost of concrete, reinforcement and formwork.

They devised the combined optimization approach to solve the non-linear programming problem. This approach is a combination of two techniques, the Lagrangian multipliers which optimized the radius and height of the tank for a specific storage capacity, and the sequential unconstrained minimization technique (SUMT) which optimized the tapered shell thickness, floor thickness, and steel reinforcement. The study showed the important influence of soil-structure interaction, wall tapering, and tank dimensions and resulted in significant reduction in the cost of the tank.

Again, in 1989, Al-Ne'aime and Al-Sabah (19) presented another study on an optimum, minimum cost, design of underground tapered shell cylindrical tank subjected to multiple load cases. The tank consists of circular top and bottom plates and the cylindrical shell. The soil structure interaction was taken into consideration by assuming that the bottom plate is resting on Winkler type elastic medium. The load cases considered in the problem are:

- 1- Stresses in the floor due to the shell fresh concrete weight.
- 2- Stresses in both floor and shell due to the roof weight.

- ۳- Stresses in both floor and shell due to leakage testing of tank before the earth was filled around it.
- ۴- Stresses in all parts due to earth pressure exerted by the surrounding earth.
- ۵- Stresses in all parts due to water and earth pressure.

It was found that the stresses constraints of the third and fourth load cases were proved to be critical.

Uraiby (۱۹۹۷) in ۱۹۹۷ studied an optimum design of reinforced concrete rectangular water tank on elastic foundation. A combination of the finite element analysis and numerical method of optimization was used in the design procedure. The constraints of the problem were to conform to BS 8007: ۱۹۸۷ for water retaining structures.

The objective function is chosen as the cost of tank consisting of the tank walls, roof and floor, which include cost of earth works, formworks, water proofing, reinforcement, and concrete.

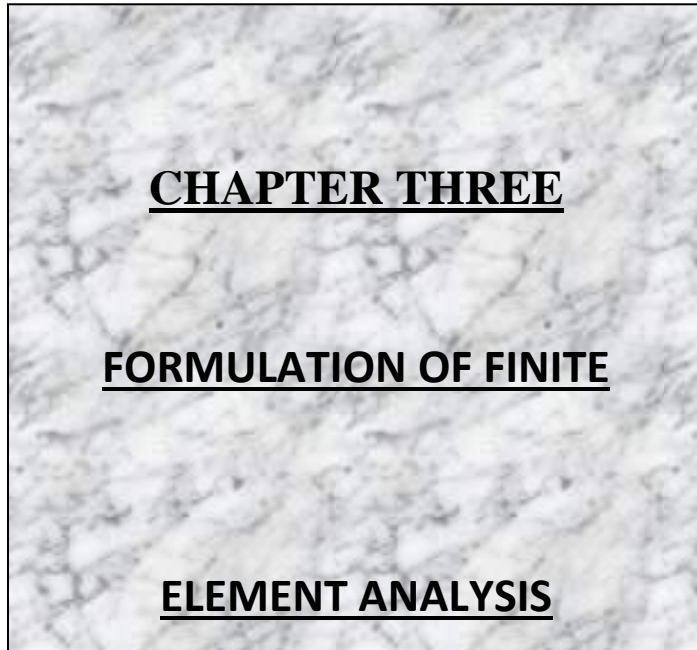
The width, length, height of the tank, plates thickness, and the steel reinforcement area are treated as design unknowns. An optimization process was formulated using the multilevel approach. The constraint non-linear programming of the problem was performed using a combination of two methods, the Lagrangian multipliers, and Constrained Rosenbrock method. The soil structure interaction was taken into consideration by assuming that the floor slab is resting on Winkler type elastic media.

In ۱۹۹۸, Hamdi (۲۷) presented an optimum design of reinforced concrete cylindrical tank resting on elastic

**media. The design procedure used was a combination of the direct stiffness method of analysis and a combined optimization technique, the constraints of the problem was to conform to BS 8007: 1987 for water retaining structures. The objective function is chosen as the cost of tank consisting of the tank wall, floor, which includes cost of concrete, reinforcement, and formwork. The radius, height of the tank, shell thickness, floor thickness and steel reinforcement area are treated as design unknown.**

**An optimization process was formulated using the multilevel approach. The constrained non-linear programming of the problem was performed using a combination of two method, the Lagrangian multiplier method, and the sequential unconstrained minimization technique (SUMT) method of Fiacco and McCormick. The soil structure interaction was taken into consideration by assuming that tank floor is resting on two types of elastic media ( Winker and Pasternak ).**

**Most of the methods of analysis described herein are based on a linearly elastic material, the foundation are represented by linear model. In the present study, an elastic-plastic behavior of metal tanks is studied. The foundation is represented by non-linear elastic model (Kondner, polynomial). For optimization, the modified Hooke and Jeeves method is employed by considering the volume of shells as the objective function and the dimensions as the design variables with geometrical constraints.**



**CHAPTER THREE**

**FORMULATION OF FINITE**

**ELEMENT ANALYSIS**

**۳.۱ General :**

In this chapter, an elastic–plastic analysis of rectangular tanks on elastic foundation subjected to static loading is presented using an incremental finite element method. In this analysis, the tank is subdivided into elements and within each element a displacement field is assumed. Flat shell element is adopted which is a combination of plane stress element and Mindlin plate bending element which takes into account the shear deformation. An isoparametric finite element formulation is presented. Derivation is presented for the basic equations relating to the incremental plasticity approach. An algorithm for the adopted method of analysis is also presented. The soil is represented by non-linear model (either Kondner, or polynomial) for normal subgrade reaction and represented by linear Winkler model for horizontal subgrade reaction.

## 3.2 Flat shell element :

A flat shell element is an element which is subjected simultaneously to in-plane and bending action as shown in Figure (3.1). The in-plane stretching and bending behavior within each element is completely uncoupled; the coupling only appears indirectly through the degree of freedom at the nodal points linking adjacent orthogonal elements. The resulting stresses are membrane in addition to shear and flexural. Therefore, the flat shell element is composed of two elements: plane stress element to resist the membrane forces and plate bending element to resist the bending moments and shear forces perpendicular to the plane of the element.

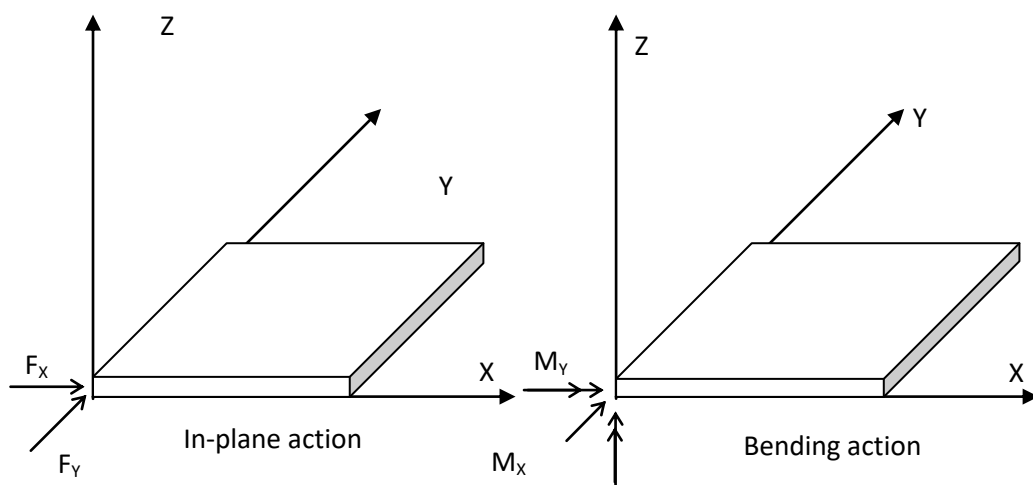


**Figure (3-1): Flat shell element subject to in-plane and bending action (3.1).**



$F_z$

**Plate bending element is based on Mindlin theory for thick plate which is in role is based on the following assumptions: -**

- 1-The deflection of the plate “w” is small.
- 2-Normals to the plate midsurface before deformation remain straight but do not necessarily remain normal to it after deformation.
- 3-Stresses normal to the midsurface are negligible.

**Problems involving small thickness as compared to the other dimensions with all applied loads in-plane of plate are classified as plane stress problems.**

**3.3 Formulation of element stiffness matrix :**

In the finite element analysis, the stiffness matrix of rectangular tank structure is considered to be built-up from the stiffness matrices of thick flat shell elements. The stiffness matrix for flat shell element will be a super position of plane stress matrix plus thick plate bending matrix (19).

The degrees of freedom per node of flat shell element considered in the present analysis are: -

- a- , w , transverse displacement.
- b- ,  $\theta_x$  , average rotation in x- direction.
- c- ,  $\theta_y$  , average rotation in y-direction.
- e- ,  $u_o$  , midsurface displacement in x-direction.
- f- ,  $v_o$  , midsurface displacement in y-direction.

**3.3.1 Strains :**

In the present analysis, the considered strains are the two direct strains ( $\epsilon_x, \epsilon_y$ ) and the in-plane shear strain ( $\gamma_{xy}$ ) and the two transverse shear strains ( $\gamma_{yz}, \gamma_{zx}$ ).

$$\{\epsilon\} = \begin{Bmatrix} \{\epsilon^b\} \\ \{\epsilon^{pl}\} \end{Bmatrix} \quad \text{-----}(\text{3.1})$$

where: -

$$\{\epsilon^b\} = [\epsilon_x^b \ \epsilon_y^b \ \gamma_{xy}^b \ \gamma_{yz}^b \ \gamma_{zx}^b]^T$$

$$\{\epsilon^{pl}\} = [\epsilon_x^{pl} \ \epsilon_y^{pl} \ \gamma_{xy}^{pl}]^T$$

$$u = -z\theta_x \quad \text{-----}(\text{3.2})$$

$$v = -z\theta_y \quad \text{-----}(\text{3.3})$$

The strain distribution corresponding to Eq.(3.2) and Eq.(3.3) is given by :-

$$\epsilon_x^b = \frac{\partial u}{\partial x} = -z \frac{\partial \theta_x}{\partial x} \quad \text{-----}(\text{3.4})$$

$$\epsilon_y^b = \frac{\partial v}{\partial y} = -z \frac{\partial \theta_y}{\partial y} \quad \text{-----}(\text{3.5})$$

$$\gamma_{xy}^b = \frac{\partial u}{\partial y} + \frac{\partial v}{\partial x} = -z \left( \frac{\partial \theta_x}{\partial y} + \frac{\partial \theta_y}{\partial x} \right) \quad \text{-----}(\text{3.6})$$

$$\gamma_{yz}^b = \frac{5}{6} \left[ \frac{3}{2} \left( \frac{\partial w}{\partial y} - \theta_y \right) \left( 1 - \left( \frac{z^2}{(0.5h)^2} \right) \right) \right] \quad \text{-----}(\text{3.7})$$

$$\gamma_{zx}^b = \frac{5}{6} \left[ \frac{3}{2} \left( \frac{\partial w}{\partial x} - \theta_x \right) \left( 1 - \left( \frac{z^2}{(0.5h)^2} \right) \right) \right] \quad \text{-----}(\text{3.8})$$

(5/6) : is the shear correction factor to allow for cross-sectional warping.

These modified expressions for  $\gamma_{yz}$  and  $\gamma_{zx}$  produce a parabolic distribution for the shear strains and their corresponding stresses  $\tau_{yz}$  and  $\tau_{zx}$  across the thickness of the plate. Such parabolic distribution seems to be more accurate and realistic, especially when these transverse shear stresses are to be included in the yield criterion.

For plane stress problem the general set of displacement are  $u_o$  and  $v_o$  in x and y directions, respectively. The strain distribution corresponding to the displacement above is given by :-

$$\epsilon_x^{pl} = \frac{\partial u_o}{\partial x} \quad \text{-----}(\text{3.9})$$

$$\epsilon_y^{pl} = \frac{\partial v_o}{\partial y} \quad \text{-----}(\text{3.10})$$

$$\gamma_{xy}^{pl} = \frac{\partial u_o}{\partial y} + \frac{\partial v_o}{\partial x} \quad \text{-----}(\text{3.11})$$

### 3.3.2 Stresses :

The stress – strain relationship is given by

$$\{\sigma\} = [E] \{\varepsilon\} \quad \text{-----}(3.12)$$

where

$$\{\sigma\} = [\sigma_x^b \ \sigma_y^b \ \tau_{xy}^b \ \tau_{yz}^b \ \tau_{zx}^b \ \sigma_x^{pl} \ \sigma_y^{pl} \ \tau_{xy}^{pl}]^T$$

$$[E] = \begin{bmatrix} [E^b] & 0 \\ 0 & [E^{pl}] \end{bmatrix} \quad \text{-----}(3.13)$$

$$[E^b] = \begin{bmatrix} \lambda & \lambda\nu & 0 & 0 & 0 \\ \lambda\nu & \lambda & 0 & 0 & 0 \\ 0 & 0 & G & 0 & 0 \\ 0 & 0 & 0 & G & 0 \\ 0 & 0 & 0 & 0 & G \end{bmatrix}$$

$$[E^{pl}] = \begin{bmatrix} \lambda & \lambda\nu & 0 \\ \lambda\nu & \lambda & 0 \\ 0 & 0 & G \end{bmatrix}$$

In which

$$\lambda = \frac{E}{(1-\nu^2)} \quad \text{and} \quad G = \frac{E}{2(1+\nu)}$$

**3.3.3 Isoparametric formulation :**

The finite element formulation of an eight-noded isoparametric element (serendipity element) is explained in this section; see Figure (3.2). The geometry of element, and the variation of displacements  $w$ ,  $u_o$ ,  $v_o$  and the rotations  $\theta_x$  and  $\theta_y$  are expressed by the shape function. Thus the geometry of the element is given by: -

$$X = \sum_{i=1}^{i=8} N_i x_i \quad \text{-----} (3.14)$$

$$Y = \sum_{i=1}^{i=8} N_i y_i \quad \text{-----} (3.15)$$

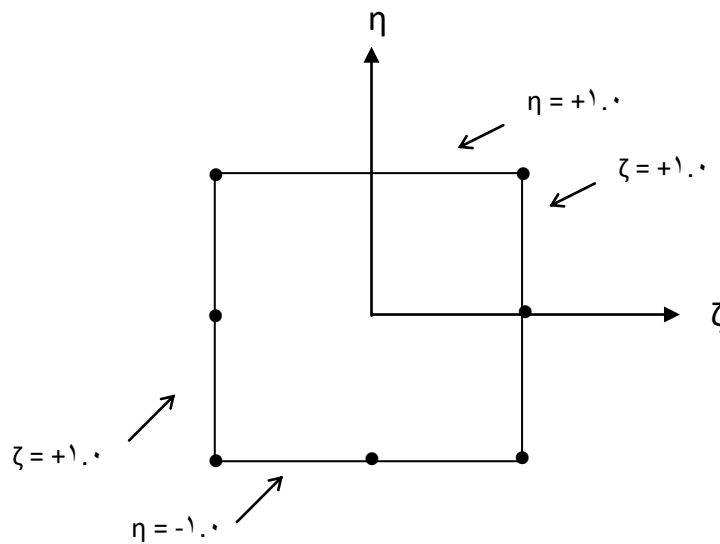


**Figure (3-2): Eight node quadrilateral in  $\zeta$ ,  $\eta$  space.**

The variation of displacements within an element is expressed in terms of the nodal values as :

$$w = \sum_{i=1}^{i=8} N_i w_i \quad \text{-----}(3.16)$$

$$\theta_x = \sum_{i=1}^{i=8} N_i \theta_{xi} \quad \text{-----}(3.17)$$

$$\theta_y = \sum_{i=1}^{i=8} N_i \theta_{yi} \quad \text{-----}(3.18)$$

$$u_o = \sum_{i=1}^{i=8} N_i u_{oi} \quad \text{-----}(3.19)$$

$$v_o = \sum_{i=1}^{i=8} N_i v_{oi} \quad \text{-----}(3.20)$$

$w_i, \theta_{xi}, \theta_{yi}, u_{oi}, v_{oi}$  are the values of  $w, \theta_x, \theta_y, u_o, v_o$  at node  $i$ .  $N_i$  is the shape function of  $\zeta$  and  $\eta$  ( isoparametric coordinates ) corresponding to node  $i$  and is given below :-

$$N_1 = -0.25(1 - \zeta)(1 - \eta)(1 + \zeta + \eta)$$

$$N_2 = -0.25(1 + \zeta)(1 - \eta)(1 - \zeta + \eta)$$

$$N_3 = -0.25(1 + \zeta)(1 + \eta)(1 - \zeta - \eta)$$

$$N_4 = -0.25(1-\zeta)(1+\eta)(1+\zeta-\eta) \quad \text{-----}(3.21)$$

$$N_5 = 0.5(1-\zeta^2)(1-\eta)$$

$$N_6 = 0.5(1-\eta^2)(1+\zeta)$$

$$N_7 = 0.5(1-\zeta^2)(1+\eta)$$

$$N_8 = 0.5(1-\eta^2)(1-\zeta)$$

The strain-displacement matrix [B] is derived in the following steps(11):

Rewriting Eq.(3.4) to (3-8) and (3-9) to (3-11) in a matrix form :-

$$\{\varepsilon\} = [H]\{C\} \quad \text{-----}(3.22)$$

where

$$[H] = \begin{bmatrix} [H^b] & 0 \\ 0 & [H^{pl}] \end{bmatrix} \quad \text{-----}(3.23)$$

$$[H^b] = \begin{bmatrix} 1 & 0 & 0 & 0 & 0 & 0 & 0 & 0 & 0 \\ 0 & 0 & 0 & 0 & 1 & 0 & 0 & 0 & 0 \\ 0 & 1 & 0 & 1 & 0 & 0 & 0 & 0 & 0 \\ 0 & 0 & 0 & 0 & 0 & b_1 & 0 & b_1 & 0 \\ 0 & 0 & b_1 & 0 & 0 & 0 & b_1 & 0 & 0 \end{bmatrix}$$

$$b_1 = \frac{5}{6} \left( \frac{3}{2} \left( 1 - \frac{z^2}{(0.5h)^2} \right) \right)$$

$$[H^{pl}] = \begin{bmatrix} 1 & 0 & 0 & 0 & 0 & 0 \\ 0 & 0 & 0 & 0 & 1 & 0 \\ 0 & 1 & 0 & 1 & 0 & 0 \end{bmatrix}$$

$$\{C\} = [ \{C^b\} \{C^{pl}\} ]^T \quad \text{-----}(\text{3.24})$$

$$\{C^b\} = [u, x, u, y, u, z, v, x, v, y, v, z, w, x, w, y, w, z]^T$$

$$\{C^{pl}\} = [u_o, x, u_o, y, u_o, z, v_o, x, v_o, y, v_o, z]^T$$

Transformation from (x, y) coordinates to isoparametric coordinates (ζ, η) may be given as:

$$\{C\}_{in(x,y)} = [Γ] \{C\}_{in(ζ,η)} \quad \text{-----}(\text{3.25})$$

$$[Γ] = \begin{bmatrix} [J]^{-1} & 0 & 0 & 0 & 0 \\ 0 & [J]^{-1} & 0 & 0 & 0 \\ 0 & 0 & [J]^{-1} & 0 & 0 \\ 0 & 0 & 0 & [J]^{-1} & 0 \\ 0 & 0 & 0 & 0 & [J]^{-1} \end{bmatrix}$$

**where the jacobian matrix is:**

$$[J] = \begin{bmatrix} x, \zeta & y, \zeta & 0 \\ x, \eta & y, \eta & 0 \\ 0 & 0 & 1 \end{bmatrix}$$

Substituting form Eqs.(3.16) to (3.20) in Eqs.(3.2) and (3.3) and differentiating with respect to (ζ, η, z) give in a matrix form :-

$$\{C\} = [N] \{\delta\} \quad \text{-----}(\text{3.26a})$$

$$\begin{Bmatrix} u, \zeta \\ u, \eta \\ u, z \\ v, \zeta \\ v, \eta \\ v, z \\ w, \zeta \\ w, \eta \\ w, z \\ u_o, \zeta \\ u_o, \eta \\ u_o, z \\ v_o, \zeta \\ v_o, \eta \\ v_o, z \end{Bmatrix} = \sum_{i=1}^{i=8} \begin{bmatrix} 0 & -zN_{i, \zeta} & 0 & 0 & 0 \\ 0 & -zN_{i, \eta} & 0 & 0 & 0 \\ 0 & -N_i & 0 & 0 & 0 \\ 0 & 0 & -zN_{i, \zeta} & 0 & 0 \\ 0 & 0 & -zN_{i, \eta} & 0 & 0 \\ 0 & 0 & -N_i & 0 & 0 \\ N_{i, \zeta} & 0 & 0 & 0 & 0 \\ N_{i, \eta} & 0 & 0 & 0 & 0 \\ 0 & 0 & 0 & 0 & 0 \\ 0 & 0 & 0 & N_{i, \zeta} & 0 \\ 0 & 0 & 0 & N_{i, \eta} & 0 \\ 0 & 0 & 0 & 0 & 0 \\ 0 & 0 & 0 & 0 & N_{i, \zeta} \\ 0 & 0 & 0 & 0 & N_{i, \eta} \\ 0 & 0 & 0 & 0 & 0 \end{bmatrix} \begin{Bmatrix} w_i \\ \theta_{xi} \\ \theta_{yi} \\ u_{oi} \\ v_{oi} \end{Bmatrix} \quad \text{-----} (3.26b)$$

Substituting from Eqs.(3.25) and (3.26) in Eqs.(3.22) leads to

:-

$$\{\varepsilon\} = [B] \{\delta\} \quad \text{-----} (3.27)$$

$$\{\varepsilon\} = \{\delta\} [B]^T \quad \text{-----} (3.28)$$

**where:**

$$[B] = [H][\Gamma][N] \quad \text{-----}$$

--(3.29)

Then, the stiffness matrix at element level could be derived from strain energy :

$$U = \frac{1}{2} \int_V [\sigma]^T \{\varepsilon\} dv \quad \text{-----} (3.30)$$

**Substitute from Eq.(3.12), Eq.(3.27) and Eq.(3.28) in Eq.(3.30) to get :-**

$$U = \frac{1}{2} [\delta]^T \left( \int_v [B]^T [E] [B] dv \right) \{\delta\} \quad \text{-----}$$

(3.31)

The element stiffness matrix  $[k']$  in x-y plane is given by :

$$[k'] = \int_v [B]^T [E] [B] dv \quad \text{-----}(3.32)$$

The expression above in natural coordinates is written as :

$$[k'] = \int_{-1}^{+1} \int_{-1}^{+1} \int_{-\frac{h}{2}}^{\frac{h}{2}} [B]^T [E] [B] |J| dz d\eta d\zeta \quad \text{-----}(3.33)$$

Where  $|J|$  is the determinant of the jacobian matrix .

Using the expression of  $[E]$  from Eq.(3.13) and for  $[B]$  from Eq.(3.29), the expression  $[k']$  can be written as :

$$[k'] = \begin{bmatrix} [k_{11}] & [k_{12}] & & [k_{18}] \\ [k_{21}] & [k_{22}] & & [k_{28}] \\ & & \dots & \\ [k_{81}] & [k_{82}] & & [k_{88}] \end{bmatrix}$$

The expression  $[K_U]$  in x-y plane will be in the form :

$$[k_{ij}] = \begin{bmatrix} S_{11} & S_{12} & S_{13} & 0 & 0 \\ S_{21} & S_{22} & S_{23} & 0 & 0 \\ S_{31} & S_{32} & S_{33} & 0 & 0 \\ 0 & 0 & 0 & S_{44} & S_{45} \\ 0 & 0 & 0 & S_{54} & S_{55} \end{bmatrix}$$

**According to the stiffness matrix above the displacements prescribed for in-plane forces do not affect the bending deformations and vice versa.**

Because the elements do not lie in one plane, a new degree of freedom ( $\theta_z$ ) must be introduced. See Figure (3.3). ( $\theta_z$ ) does not enter as parameter into the definitions of deformations in x y plane. In this case one needs to consider this rotation and add it to the displacements.

( $\theta_z$ ) can be defined by inserting an appropriate number of zeros into the stiffness matrix .

Redefining the combined nodal displacements as:

$$\{\delta\} = [w \ \theta_x \ \theta_y \ u_o \ v_o \ \theta_z]^T$$

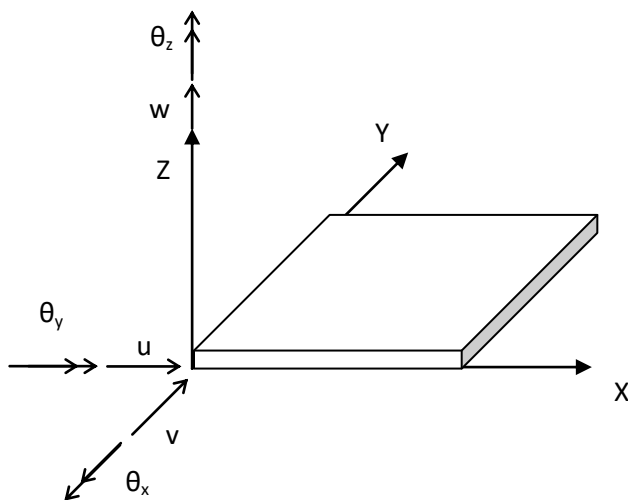


Figure (3-3): Flat shell displacements in global direction.

The stiffness matrix for flat shell element lying in x-y plane will be in the form :

$$[k_{ij}] = \begin{bmatrix} S_{11} & S_{12} & S_{13} & 0 & 0 & 0 \\ S_{21} & S_{22} & S_{23} & 0 & 0 & 0 \\ S_{31} & S_{32} & S_{33} & 0 & 0 & 0 \\ 0 & 0 & 0 & S_{44} & S_{45} & 0 \\ 0 & 0 & 0 & S_{54} & S_{55} & 0 \\ 0 & 0 & 0 & 0 & 0 & 0 \end{bmatrix} \quad \text{-----}(\text{3.34})$$

### **3.3.4 Numerical integration :**

In finding the stiffness matrix  $[K']$  from Eq.(3.33), the integration with respect to  $(\zeta, \eta)$  is carried out numerically by selective integration, in which case different strain terms are integrated with different orders of integration. In the selective integration technique(3.9), bending and membrane energies are integrated using the normal rule, the shear terms are computed using the reduced integration rule in Figure(3.4). After transforming z-coordinate to isoparametric coordinate a 2-point Gauss rule is applied to integrate numerically in the thickness direction .

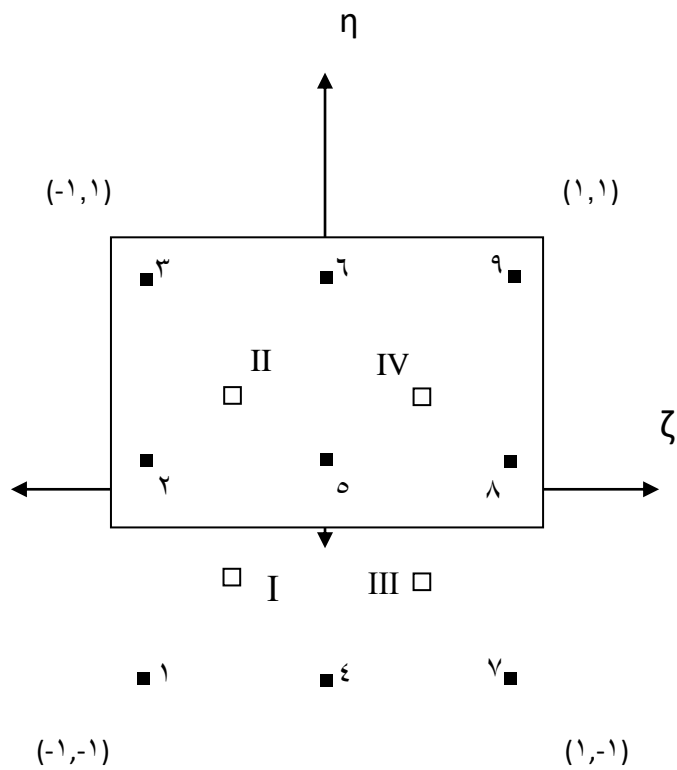


Figure (3-ε): Four and nine gauss point positions for selective integration.

**3.3.0 Elastic foundation :**

**For foundation represented by compressional and frictional resistance the stiffness matrix is :**

$$[K_f] = \begin{bmatrix} [k_f] & 0 & 0 & 0 & 0 \\ & [k_f] & 0 & 0 & 0 \\ 0 & 0 & [k_f] & 0 & 0 \\ 0 & 0 & 0 & \ddots & 0 \\ 0 & 0 & 0 & 0 & [k_f] \end{bmatrix}_{48 \times 48} \quad \text{-----}(3.30)$$

$$[k_f] = \begin{bmatrix} k_{f1} & 0 & 0 & 0 & 0 & 0 \\ 0 & 0 & 0 & 0 & 0 & 0 \\ 0 & 0 & 0 & 0 & 0 & 0 \\ 0 & 0 & 0 & k_{f2} & 0 & 0 \\ 0 & 0 & 0 & 0 & k_{f3} & 0 \\ 0 & 0 & 0 & 0 & 0 & 0 \end{bmatrix}$$

### In which

$[K_f]$  : is a (  $6 \times 6$  ) soil stiffness matrix in local coordinates.

$k_{f1}$  : is the normal spring constant in z direction

$k_{f2}$  : is the tangential nodal spring constant in x direction.

$k_{f3}$  : is the tangential nodal spring constant in y direction.

$$k_{fi} = \alpha a_f b_f k_i \quad i = 1,2,3$$

where

$k_1$  : is the normal subgrade reaction modulus.

$k_2$  : is the tangential subgrade reaction modulus in x-direction.

$k_3$  : is the tangential subgrade reaction modulus in y-direction.

$a_f, b_f$  : is the finite element mesh dimension.

$\alpha$  : is a coefficient which take a value of (1/4) at corner node and (1/2) at side node.

### 3.4 Transformation of the coordinates :

The stiffness matrix is computed for each element in local coordinate system ( x, y, z ). Then, because the element does not lie in one plane, a transformation element stiffness matrix from x-y plane to other planes ( x-z and y-z ) will be necessary to assemble the appropriate equilibrium equations in global form :

$$[k] \{\delta\} = \{r\} \quad \text{-----}(3.36)$$

The stiffness matrix of a node  $[K_{ij}]$  given in local system (xy) transform to the global system by matrix  $[L]$  where  $[L]$  a six by six matrix of direction cosines of angles formed between the two sets of axes (local and global)(47). By the rules, of the orthogonal transformation the stiffness matrix of an element in the global coordinates becomes

$$[k] = [T]^T [k'] [T] \quad \text{-----}(3.37)$$

where :

$[k]$  : Global stiffness matrix .

$[k']$ : Local stiffness matrix .

$[T]$  : Transformation matrix

$[T]^T$  : Transpose of the transformation matrix .

The transformation matrix  $[T]$  is given by :

$$[T] = \begin{bmatrix} [L]_{6 \times 6} & 0 & 0 & 0 \\ 0 & [L] & 0 & 0 \\ 0 & 0 & [L] & 0 \\ & & & \ddots \\ 0 & 0 & 0 & [L]_{48 \times 48} \end{bmatrix} \quad \text{-----}(3.38)$$

The transformation matrix  $[L]$  to transform the stiffness matrix of a node  $[K_{ij}]$  given in x-y plane to the x-y plane in global system is given by:(39)

$$[L] = \begin{bmatrix} 1 & 0 & 0 & 0 & 0 & 0 \\ 0 & 1 & 0 & 0 & 0 & 0 \\ 0 & 0 & 1 & 0 & 0 & 0 \\ 0 & 0 & 0 & 1 & 0 & 0 \\ 0 & 0 & 0 & 0 & 1 & 0 \\ 0 & 0 & 0 & 0 & 0 & 1 \end{bmatrix} \quad \text{-----}(3.39)$$

The transformation matrix  $[L]$  to transform the stiffness matrix of a node  $[K_{ij}]$  given in x-y plane to the x-z plane in global system is given by:

$$[L] = \begin{bmatrix} 0 & 0 & 0 & 0 & -1 & 0 \\ 0 & 0 & 0 & 0 & 0 & -1 \\ 0 & 0 & 1 & 0 & 0 & 0 \\ 0 & 0 & 0 & 1 & 0 & 0 \\ 1 & 0 & 0 & 0 & 0 & 0 \\ 0 & 1 & 0 & 0 & 0 & 0 \end{bmatrix} \quad \text{-----}(3.40)$$

The transformation matrix  $[L]$  to transform the stiffness matrix of a node  $[K_{ij}]$  given in x-y plane to the y-z plane in global system is given by:

$$[L] = \begin{bmatrix} 0 & 0 & 0 & -1 & 0 & 0 \\ 0 & 1 & 0 & 0 & 0 & 0 \\ 0 & 0 & 0 & 0 & 0 & 1 \\ 1 & 0 & 0 & 0 & 0 & 0 \\ 0 & 0 & 0 & 0 & 1 & 0 \\ 0 & 0 & -1 & 0 & 0 & 0 \end{bmatrix} \quad \text{-----}(\text{3.41})$$

### **3.9 Formulation of the basic elastic-plastic equations:**

The stress-strain relationship which is assumed to be elastic-perfectly plastic and von Mises' yield criterion and Prandtl-Reuss flow rule are adopted to consider the non-linear effect due to the plasticity, for the more extensively used yield criterion see (Appendix A). According to this criterion, yielding begins under any state of stress when the effective stress ( $\bar{\sigma}$ ) exceeds the yield strength in uniaxial tension or compression ( $\sigma_y$ ):

$$\bar{\sigma} = \frac{\sqrt{2}}{2} \left[ (\sigma_x - \sigma_y)^2 + (\sigma_y - \sigma_z)^2 + (\sigma_z - \sigma_x)^2 + 6(\tau_{xy}^2 + \tau_{yz}^2 + \tau_{zx}^2) \right]^{1/2} \quad \text{---}(\text{3.42})$$

Through neglecting the transverse direct stress ( $\sigma_z$ ) and squaring both sides of Eq.(3.42), von Mises' yield criterion can be rewritten as follows

$$\bar{\sigma}^2 = \frac{1}{2} \left[ (\sigma_x - \sigma_y)^2 + \sigma_y^2 + \sigma_x^2 + 6(\tau_{xy}^2 + \tau_{yz}^2 + \tau_{zx}^2) \right] \quad \text{-----}(\text{3.43a})$$

The effective stress ( $\bar{\sigma}$ ) may be expressed in terms of principal stresses ( $\sigma_1, \sigma_2, \sigma_3$ ) as follows:

$$\bar{\sigma}^2 = \frac{1}{2} \left[ (\sigma_1 - \sigma_2)^2 + (\sigma_2 - \sigma_3)^2 + (\sigma_3 - \sigma_1)^2 \right] \quad \text{-----}(\text{3.43b})$$

By differentiating Eq.(3.4a), one gets

$$d\bar{\sigma} = [Q]^T \{d\sigma\} \quad \text{-----}(3.4a)$$

where

$$[Q] = \frac{3}{\bar{\sigma}} \left[ \frac{\bar{\sigma}_x}{2} \quad \frac{\bar{\sigma}_y}{2} \quad \bar{\tau}_{xy} \quad \bar{\tau}_{yz} \quad \bar{\tau}_{zx} \right] \quad \text{-----}(3.4b)$$

$$\{d\sigma\} = [d\sigma_x \quad d\sigma_y \quad d\tau_{xy} \quad d\tau_{yz} \quad d\tau_{zx}]^T$$

in which

$$\bar{\sigma}_x = \sigma_x - \sigma_a$$

$$\bar{\sigma}_y = \sigma_y - \sigma_a$$

$$\sigma_a = \frac{\sigma_x + \sigma_y}{3}$$

$$\bar{\tau}_{xy} = \tau_{xy} ; \bar{\tau}_{yz} = \tau_{yz} ; \bar{\tau}_{zx} = \tau_{zx}$$

According to von Mises' theory, the effective plastic strain increment ( $d\bar{\epsilon}^p$ ) is defined as follows (neglecting  $\epsilon_z$ ) (19),(30).

$$d\bar{\epsilon}^p = \frac{\sqrt{2}}{3} \left[ (d\epsilon_x^p - d\epsilon_y^p)^2 + (d\epsilon_y^p)^2 + (d\epsilon_x^p)^2 + \frac{3}{2} [(d\gamma_{xy}^p)^2 + (d\gamma_{yz}^p)^2 + (d\gamma_{zx}^p)^2] \right]^{1/2}$$

$$\text{-----}(3.4a)$$

and in terms of principal plastic strain increments ( $d\epsilon_1^p, d\epsilon_2^p, d\epsilon_3^p$ )

$$d\bar{\epsilon}^p = \frac{\sqrt{2}}{3} \left[ (d\epsilon_1^p - d\epsilon_2^p)^2 + (d\epsilon_2^p - d\epsilon_3^p)^2 + (d\epsilon_3^p - d\epsilon_1^p)^2 \right]^{1/2} \quad \text{-----}(3.4b)$$

The stress-strain relations for an elastic–perfectly plastic material were first proposed by Prandtl. The mathematical form of flow rule (Prandtl-Reuss relation ) is (3.4)

$$\frac{d\varepsilon_x^p}{\bar{\sigma}_x} = \frac{d\varepsilon_y^p}{\bar{\sigma}_y} = \frac{d\gamma_{xy}^p}{2\bar{\tau}_{xy}} = \frac{d\gamma_{yz}^p}{2\bar{\tau}_{yz}} = \frac{d\gamma_{zx}^p}{2\bar{\tau}_{zx}} = d\lambda \quad \text{-----}(3.46)$$

where

$d\lambda$ : is an instantaneous non-negative constant of proportionality.

Rewriting Eq.(3.46) considering principal stress direction

$$\frac{d\varepsilon_1^p - d\varepsilon_2^p}{\sigma_1 - \sigma_2} = \frac{d\varepsilon_2^p - d\varepsilon_3^p}{\sigma_2 - \sigma_3} = \frac{d\varepsilon_3^p - d\varepsilon_1^p}{\sigma_3 - \sigma_1} = d\lambda \quad \text{-----}(3.47)$$

or in other form :

$$d\lambda \sqrt{(\sigma_1 - \sigma_2)^2 + (\sigma_2 - \sigma_3)^2 + (\sigma_3 - \sigma_1)^2} = \sqrt{(d\varepsilon_1^p - d\varepsilon_2^p)^2 + (d\varepsilon_2^p - d\varepsilon_3^p)^2 + (d\varepsilon_3^p - d\varepsilon_1^p)^2} \quad \text{-----}(3.48)$$

Hence, from Eq.(3.47b), Eq.(3.48), and Eq.(3.48), one gets

$$d\lambda = \frac{3}{2} \frac{d\bar{\varepsilon}^p}{\bar{\sigma}} \quad \text{-----}(3.49)$$

By substituting Eq.(3.49) into Eq.(3.46), the following relation is obtained

$$\frac{d\varepsilon_x^p}{\bar{\sigma}_x} = \frac{d\varepsilon_y^p}{\bar{\sigma}_y} = \frac{d\gamma_{xy}^p}{2\bar{\tau}_{xy}} = \frac{d\gamma_{yz}^p}{2\bar{\tau}_{yz}} = \frac{d\gamma_{zx}^p}{2\bar{\tau}_{zx}} = \frac{3}{2} \frac{d\bar{\varepsilon}^p}{\bar{\sigma}} \quad \text{-----}(3.50)$$

In a matrix form

$$\{d\varepsilon^p\} = \{Q\} d\bar{\varepsilon}^p \quad \text{-----}(3.51)$$

where

$$\{d\varepsilon^p\} = \{d\varepsilon_x^p \quad d\varepsilon_y^p \quad d\gamma_{xy}^p \quad d\gamma_{yz}^p \quad d\gamma_{zx}^p\}$$

In the elastic range (referring to Figure (3.6)) the stress increments  $\{d\sigma\}$  can be expressed in terms of strain increments  $\{d\varepsilon^e\}$  as follows :

$$\{d\sigma\} = [E] \{d\varepsilon^e\} \quad \text{-----}(3.52)$$

or in the elastic-plastic range

$$\{d\sigma\} = [E] [\{d\varepsilon^{ep}\} - \{d\varepsilon^p\}] \quad \text{-----}(3.53)$$

where

$\{d\varepsilon^e\}$  : vector of elastic strain increments

$\{d\varepsilon^p\}$  : vector of plastic strain increments

$\{d\varepsilon^{ep}\}$  : vector of total strain increments

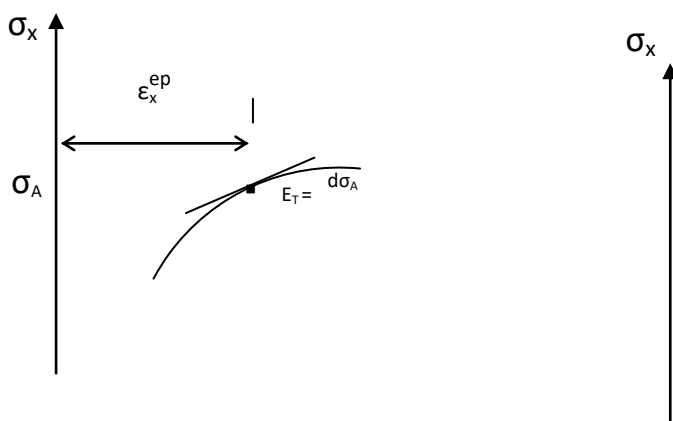
Premultiplying both sides of Eq.(3.53) by  $\{Q\}$  and substituting from Eq.(3.44) and Eq.(3.51) in the resulting equation give

$$d\bar{\sigma} = \{Q\}^T [E] [\{d\varepsilon^{ep}\} - \{Q\} d\bar{\varepsilon}^p] \quad \text{-----}(3.54)$$

**But from figure(3.5)**

$$d\bar{\sigma} = H' d\bar{\varepsilon}^p \quad \text{-----}$$

$$\text{---}(3.55)$$



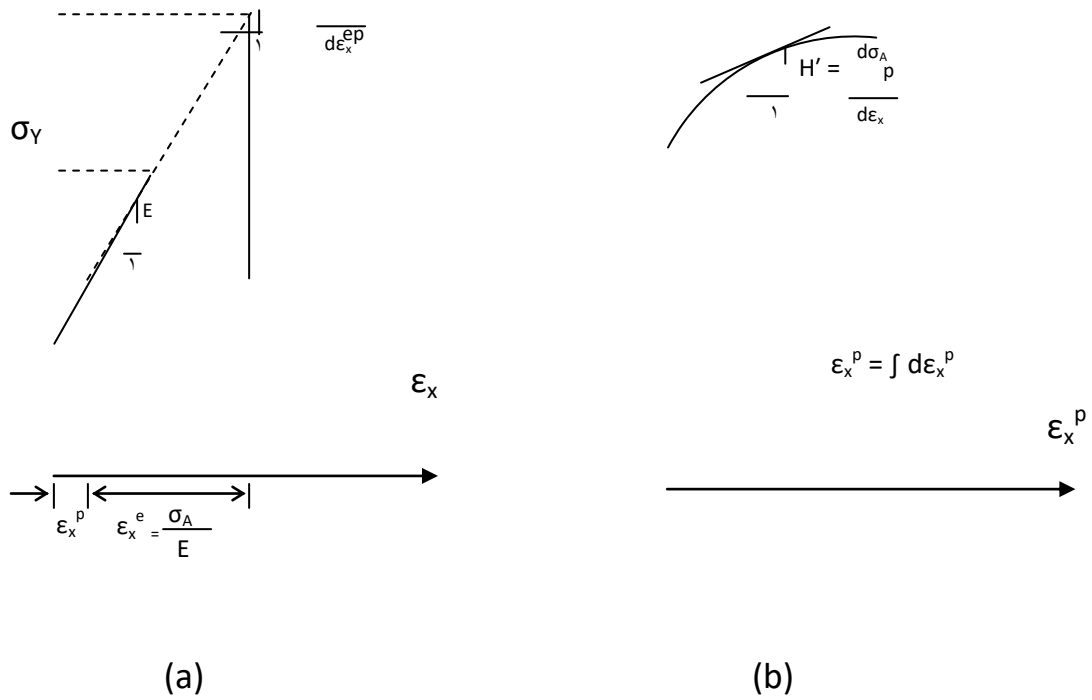


**Figure (3.5): Stress strain relation in uniaxial tension(3.5).**

a- elastic modulus (E) and tangent modulus (E<sub>T</sub>).

**From Eq.(3.54) and Eq.(3.55), the following equation is obtained**

$$d\bar{\epsilon}^p = [W] \{d\epsilon^{ep}\} \quad \text{-----}(3.56)$$

where

$$[W] = \frac{\{Q\}^T [E]}{H' + \{Q\}^T [E] \{Q\}} \quad \text{-----}(3.57)$$

$H' = \cdot$  (for elastic-perfectly plastic material)

Then, to find the elastic-plastic stress-strain matrix  $[E^{ep}]$ , the stress increments  $\{d\sigma\}$  could be expressed in terms of total strain increments  $\{d\epsilon^{ep}\}$  as follows:

$$\{\mathbf{d}\sigma\} = [\mathbf{E}^{\text{ep}}] \{\mathbf{d}\varepsilon^{\text{ep}}\} \quad \text{-----}(\text{3.58})$$

But from Eq.(3.51) and Eq.(3.56), the relation between the plastic strain increments  $\{\mathbf{d}\varepsilon^{\text{p}}\}$  with the total strain increments  $\{\mathbf{d}\varepsilon^{\text{ep}}\}$  can be obtained by the following equation

$$\{\mathbf{d}\varepsilon^{\text{p}}\} = \{\mathbf{Q}\} [\mathbf{W}] \{\mathbf{d}\varepsilon^{\text{ep}}\} \quad \text{-----}(\text{3.59})$$

Then, substituting Eq.(3.59) in Eq.(3.53) gives

$$\{\mathbf{d}\sigma\} = [[\mathbf{E}] - [\mathbf{E}]\{\mathbf{Q}\}[\mathbf{W}]] \{\mathbf{d}\varepsilon^{\text{ep}}\} \quad \text{-----}(\text{3.60})$$

By comparing Eq.(3.58) with Eq.(3.60), one concludes that

$$[\mathbf{E}^{\text{ep}}] = [\mathbf{E}] - [\mathbf{E}]\{\mathbf{Q}\}[\mathbf{W}] \quad \text{-----}(\text{3.61})$$

The prescribed equations relating the stresses with strains within plastic range are the same for both plane stress problem (if one neglects terms of transverse shear stress and strain) and plate bending problem.

### **3.6 An algorithm for the present incremental finite**

#### **element analysis :**

The solution algorithm which takes into account the nonlinearity in the material follows a three level process: subincrements within iterations within

load increments. Effectively, the problem is treated as a sequence of linearly elastic problems. Each step of the sequence is represented by a load increment based on material properties appropriate to that step. In other words, the stiffness matrix of the structure is updated at the beginning of each load increment. The solution has been achieved by using modified Newton-Raphson iterations technique as shown in Figure(۳.۶).

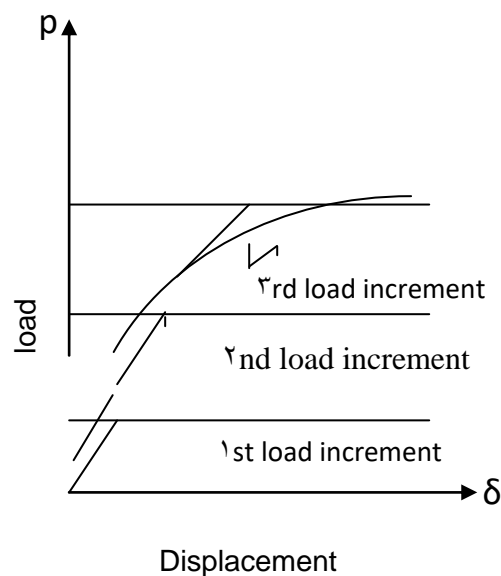


Figure (۳-۶): Incremental technique with modified Newton-Raphson iteration for single degree of freedom.

The steps of analysis could be given as follows :

- ۱- Construct the vector of nodal forces  $\{r'_i\}$  for each element in the local coordinate system. Then, transform it to the global coordinate system. Then,

assemble the vectors of nodal forces for all elements to find the total vector of nodal forces for the whole structure  $\{R_i\}$ .

In the first step, the structure is considered as linear elastic structure. Find the elastic stiffness matrix for each element in the local coordinate system from Eq.(3.34). Now, transform the stiffness matrix for each element from local to global coordinate system by using Eq.(3.35), i.e.

$$[k] = [T]^T [k'] [T]$$

Then, assemble the stiffness matrices to find the total stiffness matrix, where

$$[K] = \sum [k]$$

3- Apply load vector  $\{R_i\}$ .

4- Find the nodal displacements vector  $\{\Delta_i\}$  corresponding to the applied load vector  $\{R_i\}$ .

5- Extract each element displacement vector  $\{\delta_i\}$  from  $\{\Delta_i\}$  and transform it to find the element displacement vector  $\{\delta'_i\}$  in the local coordinate system. Then, compute the resulting strain increments at each Gauss-point in the natural coordinate system.

$$\{\varepsilon_i\} = [B] \{\delta'_i\}$$

Then, find the corresponding elastic stresses.

$$\{\sigma_i\} = [E] \{\varepsilon_i\}$$

6- Find the effective stresses  $\bar{\sigma}_i$  at each Gauss-point in each element corresponding to the applied load vector. Then, select the maximum one from them  $\bar{\sigma}_{max}$ . The first yield load factor “ $P_{fy}$ ” is found from

$$P_{fy} = \sigma_y / \bar{\sigma}_{max}$$

7- Select the value of load increment “ $\Delta P_i$ ” to be

$$\Delta P = 0.05 \times P_{fy}$$

$$P_{Ti} = P_{fy}$$

$$P_{Ti} = P_{Ti-1} + \Delta P$$

$$\{dR_i\} = \{R_i\} \times \Delta P$$

where

$P_{Ti}$  = Accumulated total load factor up to step i

^ - At ith load increment; find  $[E_i^{ep}]$  using Eq.(3.11) at each Gauss point in each element, corresponding to stress history  $\{\sigma_{i-1}\}$  of that point. For Gauss-points have effective stress not exceeding the yield limit ( $\sigma_y$ ), the matrix  $[E_i^{ep}]$  being replaced by  $[E_i]$ . Then, find the total stiffness matrix of the structure in the global coordinate system.

$$[k] = [T]^T [k'] [T]$$

$$[K_i] = \sum [k_i]$$

Such updated total stiffness matrix  $[K_i]$  at the beginning of each load increment will be used in all iterations in that load increment.

^ - At ith load increment, use

a-if  $j=1$  where ( $j$ = iteration number), apply the load step  $\Delta P_i$  for  $\{dR_j\}$

b-if  $j>1$ , apply the residual forces from the previous iteration to be  $\{dR_j\}$

$$\{dIr'_j\} = \{dIr'_j\} + \int [B]^T \{\sigma\} dv$$

$$\{dIr_j\} = [T] \{dIr'_j\}$$

$$\{dIR_j\} = \sum \{dIr_j\}$$

$$\{dR_j\} = \{R_i\} \times P_{Ti} - \{dIR_j\}$$

where

$\{dIr'_j\}$  = vector of internal forces for each element in the local coordinate system

$\{\sigma\}$  = vector of total stresses upto the jth iteration

$\{d\mathbf{I}r_j\}$  = vector of internal forces for each element in the global coordinate system

$\{d\mathbf{R}_j\}$  = vector of residual forces for the whole structure calculated from the previous iteration

$\{d\mathbf{I}R_j\}$  = vector of internal forces for the whole structure .

Then, find the corresponding  $\{d\Delta_j\}$  from the equilibrium equation

$$\{d\mathbf{R}_j\} = [\mathbf{K}_i] \{d\Delta_j\}$$

10- Extract the element displacement vector  $\{d\delta_j\}$  from  $\{d\Delta_j\}$  and transform it to the local coordinate system to find  $\{d\delta'_j\}$  and compute the resulting strain increments at each Gauss-point.

$$\{d\epsilon_j^{ep}\} = [\mathbf{B}] \{d\delta'_j\}$$

After that, find the effective elastic-plastic strain increment  $d\bar{\epsilon}_j^{ep}$  from Eq.(3.40a) putting the subscript (ep) instead of (p) in all terms of that equation. Then, subdivide such strain increments into subincrements, where for each subincrement (m):

$$\{d\epsilon_m^{ep}\} = \{d\epsilon_j^{ep}\} / (d\bar{\epsilon}_j^{ep} / 0.0002)$$

The factor 0.0002 is suitable for ductile metals (19)

11- In each subincrement (m) at a certain Gauss-point in an element from the structure, find the effective plastic strain increment  $d\bar{\epsilon}_m^p$  from Eq.(3.46). Then find the plastic strain increments  $\{d\epsilon_m^p\}$  from Eq.(3.47). The stress increments are found from Eq.(3.48) to be added to the total stress vector from the previous subincrement (or iteration)  $\{\sigma_{m-1}\}$  to find  $\{\sigma_m\}$  at the end of subincrement (m). Then, compute the effective stress ( $\bar{\sigma}_m$ ) from Eq.(3.49a). The subscript (m) is put in each term of the preceding indicated equations in this step.

A finite size stress increments produced from each subincrements within iteration within load increment may depart the yield surface as shown in Figure (3.7). This discrepancy is particularly eliminated since the subincrements in each iteration are sufficiently small. However, the point of final stress can be reduced to the yield surface simply by scaling the stress vector  $\{\sigma_m\}$  as given in Figure (3.7).

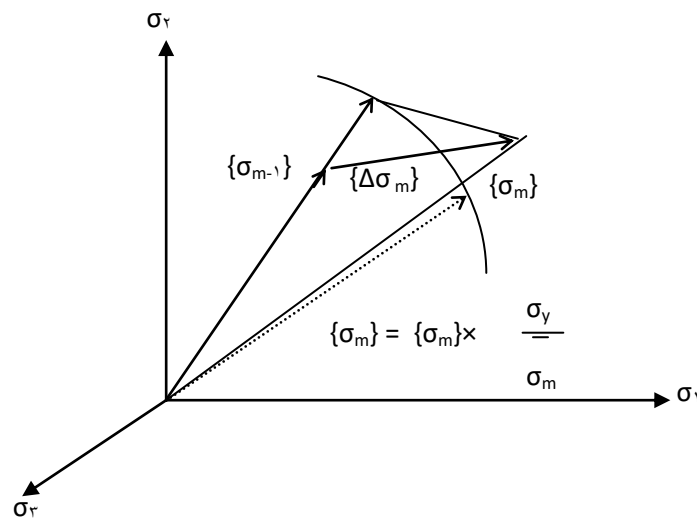


Figure (3.7): Scaling the stresses vector  $\{\sigma_m\}$  at the end of subincrement (m) so as to satisfy the yield criterion.

At the end of subincrement (m), update  $\{Q_{m+1}\}$  and  $[W_{m+1}]$  as given in Eq.(3.44b) and (3-67) respectively utilizing the stress history  $(\sigma_m)$  for the considered Gauss-point.

12- If subincrements have not completed for a Gauss point, then go to the next subincrement step (11) for subincrement (m+1). Otherwise go to the next Gauss point and repeat the subincrement process (steps: 10 and 11) in the same iteration.

13- If subincrements are completed for all Gauss points in the structure within iteration (j), find the residual forces in the whole structure  $\{dR_{j+1}\}$  as given in step (9-b) to be used in the next iteration(j+1).

14- Find the normality (norm) of residual forces at the end iteration (j) as follows :

$$\text{norm}_j = \left( \frac{\sqrt{\sum \{dR_{j+1}\}^2}}{\sqrt{\sum \{R_j\}^2}} \right) \times 100$$

then

a-If  $\text{norm}_j \leq \text{norm}_{j-1}$  and  $\text{norm}_j \leq 0.1$ , print the total applied load factor  $p_{Ti}$ , then go to step (8) with next load increment  $(i+1)$ .

b-If  $\text{norm}_j \leq \text{norm}_{j-1}$  and  $\text{norm}_j > 0.1$  go to step (9) for next iteration  $(j+1)$

c-Otherwise (i.e  $\text{norm}_j > \text{norm}_{j-1}$ ), the solution has diverged indicating the collapse state. Print the collapse load factor to be  $P_{Ti-1}$ , and stop the analysis process.

### 3.7 Computer program for analysis:

A computer program presented by Alwash[1989](11) for elastic-plastic analysis of thick plates by incremental finite element method was developed by Karkush[1998](31) to deal with non-linear behavior of folded plates structure by incremental finite strip method. It is developed in the present study to deal with elastic-plastic behavior of rectangular tank resting on nonlinear elastic foundation by incremental finite element method. The flow chart of the developed computer program is given in Figure(3.8).

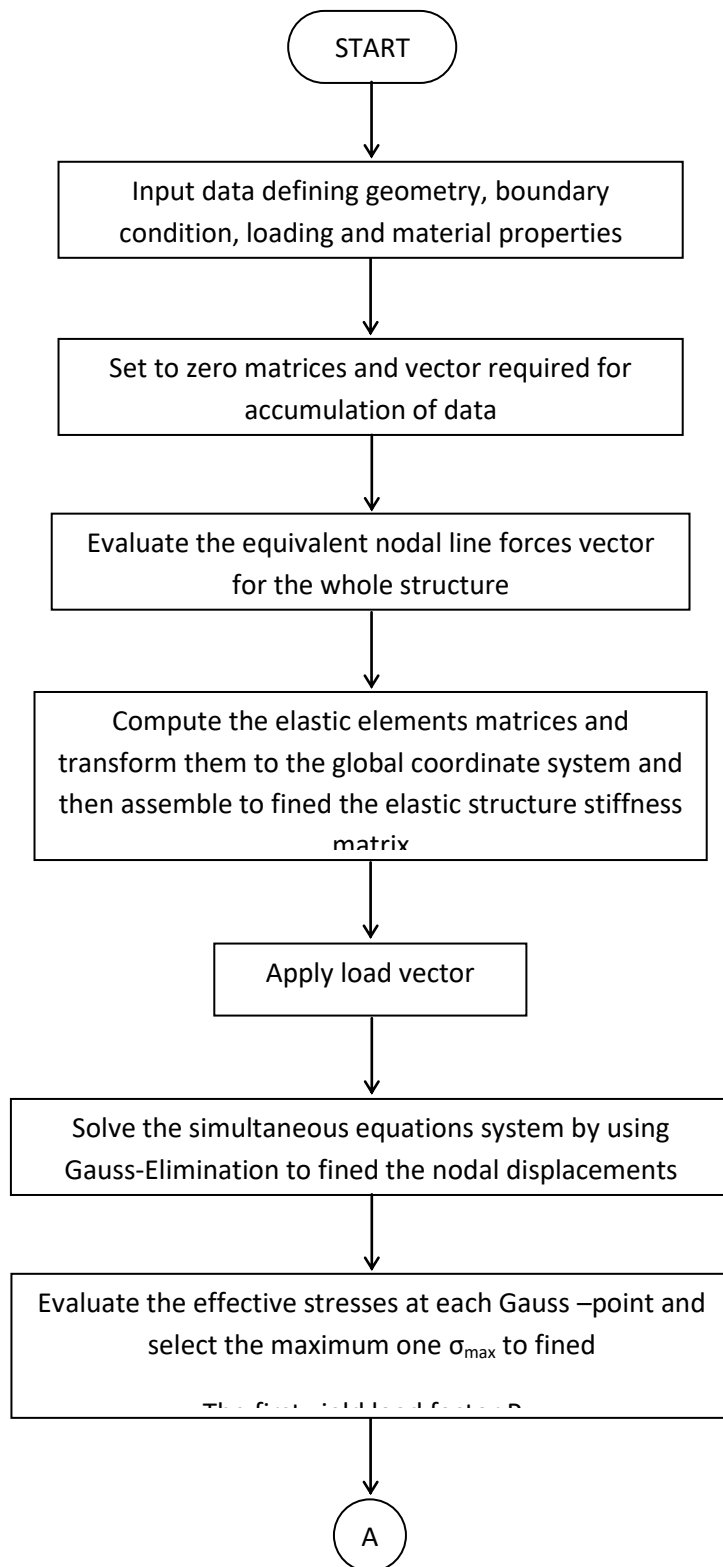


Figure (3.8): Flow chart of the developed program.

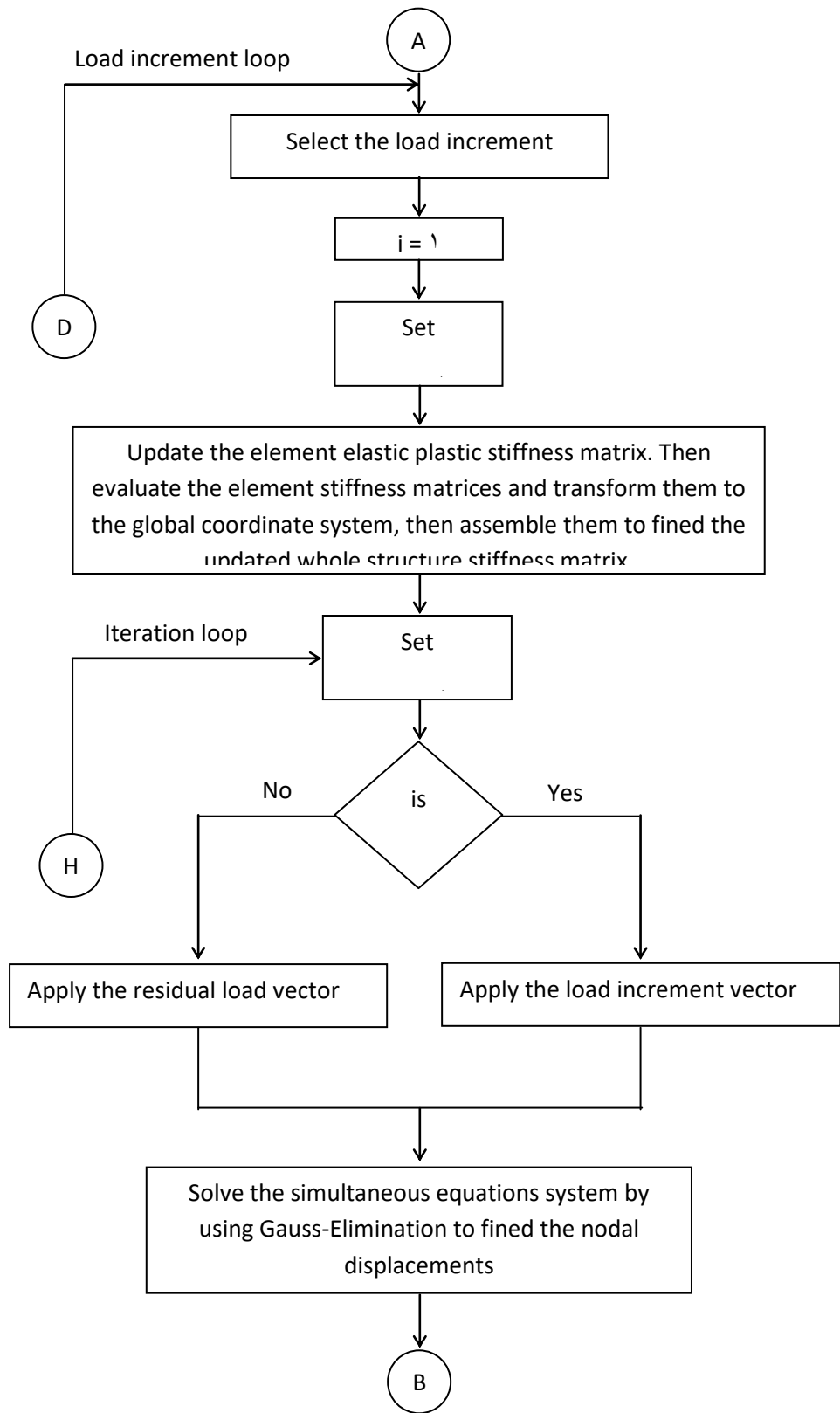


Figure (3.4): Continued.

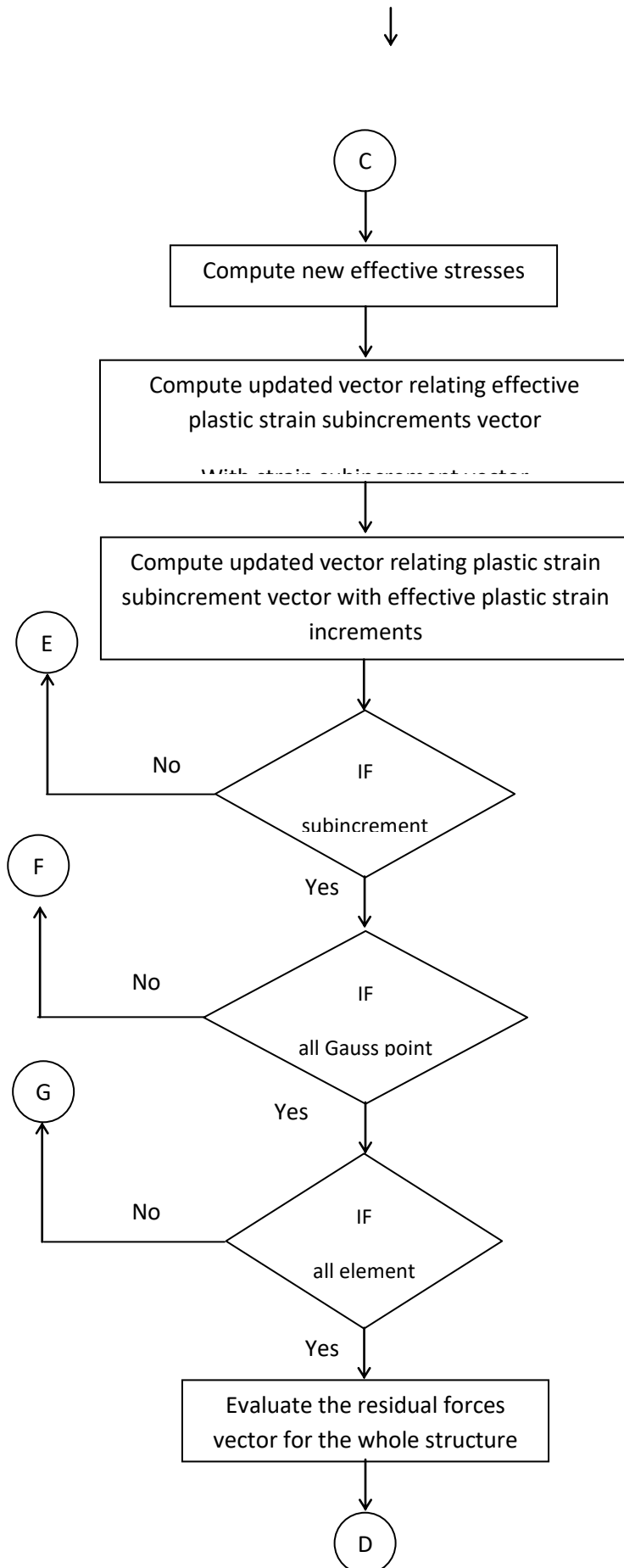


Figure (3.8): Continued.

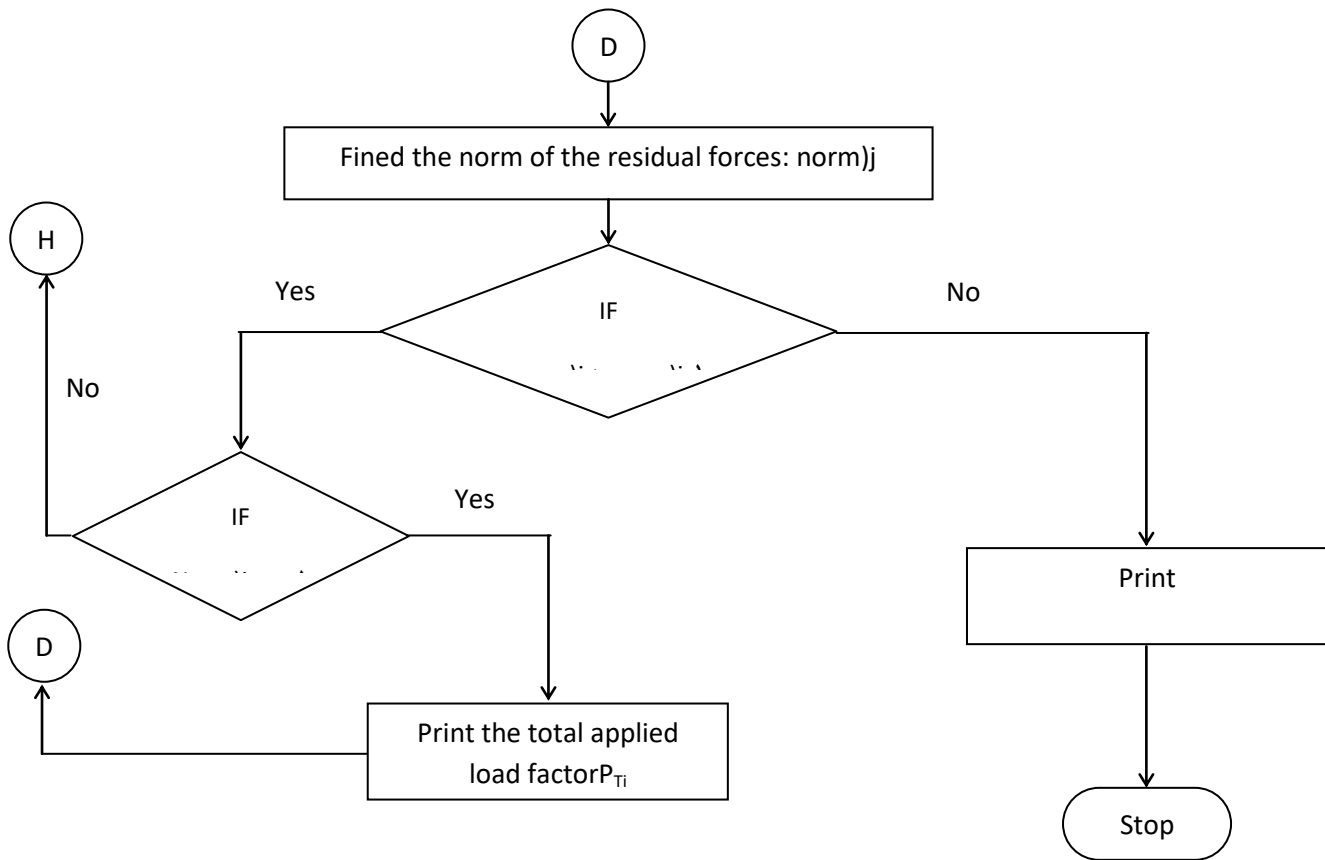


Figure (3.8): Continued.

### **3.8 Non-linear behavior of soil :**

Before the development of computers, it was not feasible to perform analysis of load in soil masses for other than assumed linear elastic soil behavior.

Now, due to the availability of high speed computers and powerful numerical analytical techniques, it is possible to approximate non-linear soil behavior in analysis. In order to perform non-linear analysis of soil, however, it is necessary to be able to describe the load-deflection behavior of the soil quantitatively, and to develop techniques for incorporating this behavior in the analysis.

### **३.८.१ Soil characterization :**

The stress-strain curve of any type of soil depends on a number of different factors including density, water content, structures, drainage condition, strain condition (i.e. plane strain, triaxial ...etc ), duration of loading, stress history and confining pressure (३५) .

In many cases it may be possible to take account of these factors by selecting soil specimens and testing condition which simulate the corresponding field condition. When this can be done accurately, it would be expected that the strains resulting from given stress changes in laboratory would be representative for the same stress changes.

Among many theories established to study different material properties, the following theories are widely used in studying soil characteristics, especially stress-strain relation under different stress changes :

- १- Classical linear elastic theory.
- २- Plastic theory.
- ३- Elasto-plastic theory.
- ४- Visco- elastic theory.
- ०- Non-linear elasticity theory.

It is commonly found that the soil behavior over a wide range of stresses is non-linear, inelastic, and dependent upon the magnitude of the confining pressures employed in the test.

### **३.८.२ Modeling of stress-strain curve of soil :**

The stress-strain curve for all soils is non-linear except in a very narrow region near the origin (१३). In this section, two models can be used to model the stress-strain response of soils :

- १-Hyperbolic stress-strain model.
- २-Polynomial model.

3.8.2.1 Hyperbolic stress-strain model :

In this model, the stress-strain curve could be represented by a hyperbolic curve. Kondener (33) proposed a hyperbolic equation of the form :

$$\sigma_1 - \sigma_3 = \frac{\varepsilon}{a + b\varepsilon} \quad \text{-----}(3.62)$$

where

$\sigma_1$  and  $\sigma_3$  are the major principal stresses.

$\varepsilon$  is the axial strain.

(a) and (b) are constant whose values may be determined experimentally.

The ultimate value of principal stresses difference  $(\sigma_1 - \sigma_3)_{ult.}$  can be obtained by taking the limit of Eq.(3.62) as  $(\varepsilon)$  becomes very large , or

$$(\sigma_1 - \sigma_3)_{ult.} = \lim_{\varepsilon \rightarrow \infty} (\sigma_1 - \sigma_3) = \frac{1}{b} \quad \text{-----}(3.63)$$

Differentiating Eq.(3.62) with respect to the strain and evaluating the derivative at  $(\varepsilon)$  equal to zero yields :

$$\left( \frac{d(\sigma_1 - \sigma_3)}{d\varepsilon} \right) = \frac{1}{a} \quad \text{-----}(3.64)$$

Thus, both of these constants (a) and (b) have a visualized physical meaning, referring to Figure(3.9), (a) is the reciprocal of the initial tangent modulus,  $E_i$  , and (b) is the reciprocal of the asymptotic value of stress difference which the stress-strain curve approaches at infinite strain  $(\sigma_1 - \sigma_3)_{ult.}$

In order to develop a realistic model in soil mechanics, such a model must use a combination of :

- 1- Observations of the material behavior, and
- 2- Laboratory experiments that will measure the physical parameters that are needed to transfer the model into usable mathematical equations.

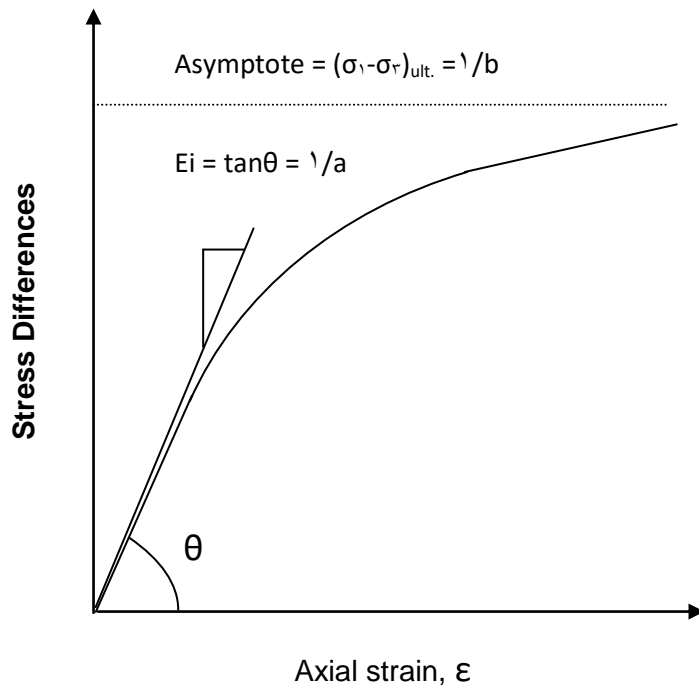
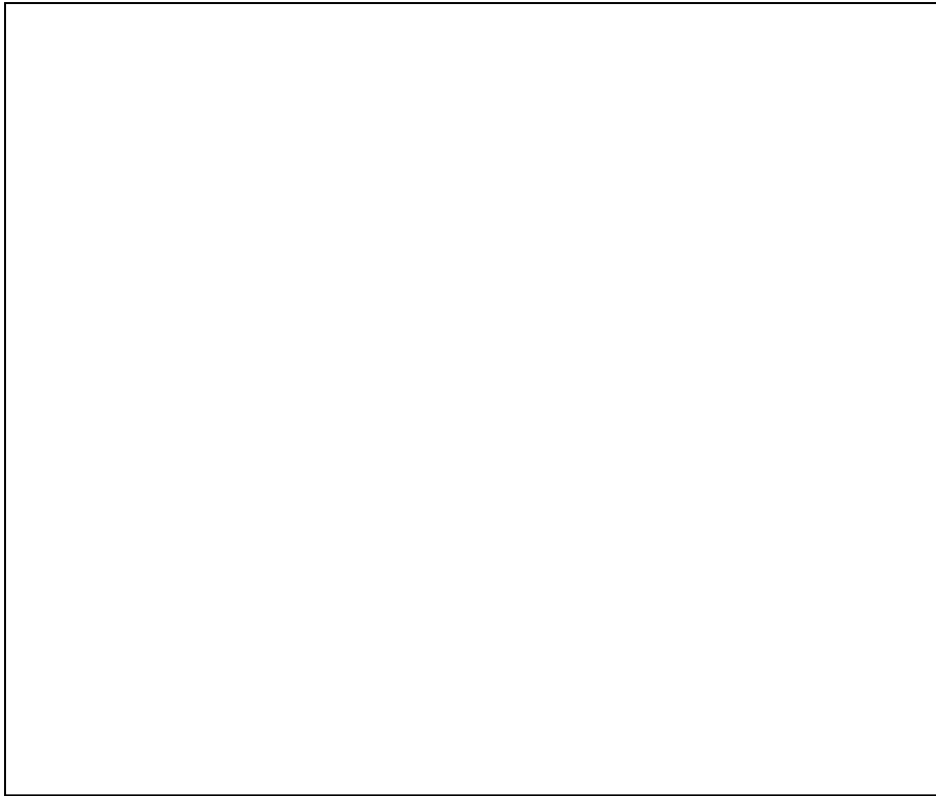


Figure (3.9): Proposed hyperbolic stress-strain curve of soil(33).

The behavior of soil under compressive loading is non-linear as verified by the results of plate-load test. Considering the load-settlement curve of a plate-load test in the field, the soil response can approximately be modeled using the two-constant hyperbolic stress-strain equation which now takes the following form:

$$P = \frac{\delta}{a + b\delta} \quad \text{-----}(3.65)$$

Eq.(3.65) was used firstly by Al-Rubai (1970), to represent the non-linear behavior of soil. Figure(3.10) shows the hyperbolic load-settlement curve of plate-load test.

Differentiating Eq.(3.65) with respect to the settlement ( $\delta$ ), yields:

$$K_n = \frac{a}{(a + b\delta)^2} \quad \text{-----}(3.66)$$

where

$P$  : is the transverse load on shell element that is concentrated at the node.

$\delta$  : is the transverse displacement of the node.

$K_n$  : is the normal subgrade reaction of soil.

(a) and (b) are the physical parameter required for the hyperbolic equation which can be obtained from the load settlement curve of the plate-load test.

The value of the coefficients (a) and (b) may be determined most readily if the load-settlement data are plotted on transformed axes as shown in Figure (3.11) when Eq.(3.65) is written in the following form :

$$\frac{\delta}{P} = a + b\delta$$

----- (3.67)

where, (a) and (b) are the intercept and the slope of the resulting straight line shown in Figure (3.11), respectively.

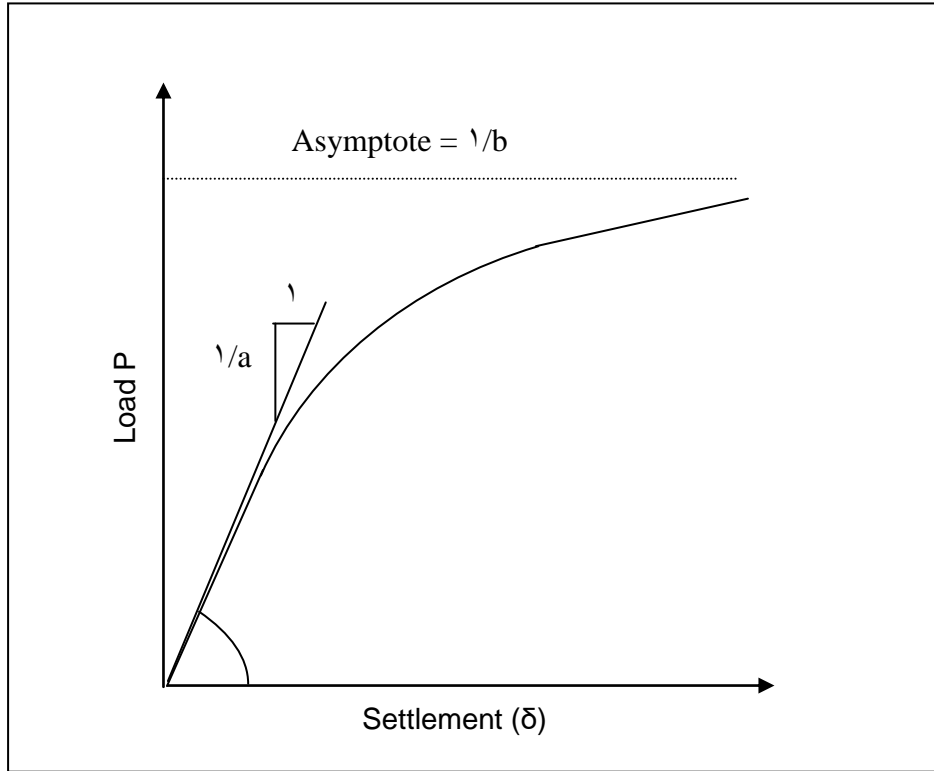


Figure (3-10): Hyperbolic load-settlement curve.



Figure (3-11): Transformed hyperbolic load-settlement curve.

3.8.2.2 Polynomial model :

In this model, the non-linear behavior of soil can be represented by a polynomial equation which takes the following form(4):

$$P = a_0 + a_1\delta + a_2\delta^2 + a_3\delta^3 + a_4\delta^4 \dots \text{-----}(3.78)$$

Where:

$a_0, a_1, a_2, a_3$  and  $a_4$  are the coefficients of the polynomial equation.

The values of the coefficients  $a_1, a_2, a_3 \dots$  may be determined by making curve fitting for the experimental load-settlement data.

Differentiating Eq.(3.78) with respect to settlement ( $\delta$ ) yields:

$$K_n = a_1 + 2a_2\delta + 3a_3\delta^2 + 4a_4\delta^3 + \dots \text{-----}(3.79)$$

where

$\delta$  : is the transverse displacement of node.

$K_n$  : is the normal subgrade reaction of soil.

CHAPTER FOUR  
**OPTIMAL DESIGN**  
**FORMULATION**

ξ.1 Optimization :

ξ.1.1 General :

**Optimization is defined as finding the optimum value (maximum or minimum) of a function called the objective function  $f(x_1, x_2, x_3, \dots, x_n)$  of  $n$  real variables called the design variables. The optimization is constrained when certain limitations are imposed on the design variables, while the optimization is non-linear when the mathematical expressions relating the design variables in constraints or in the objective function are of a non-linear nature.**

If for example, the function refers to the profit obtained by producing quantities  $x_i$  of products  $p_i$ , it may well be that the desire is to maximize the function. If, on the other hand, it refers to costs involved in an operation or volume of materials, it should be probably to minimize the function. From the mathematical point of view, there is no real difference in considering both maximization and minimization, since maximizing  $f$  is equivalent to minimizing  $-f$ . It is normal to confine the problem to minimization. In the present work, the nonlinear constrained optimization by the modified Hooke and Jeeves method will be implemented.

### 4.1.2 Direct search methods:

The general optimization problem is minimize:  $f(x_1, x_2, x_3, \dots, x_n)$ , of  $n$  real variables subject to the constraints:  $g_i(x_1, x_2, x_3, \dots, x_n) \leq b_i$  ( $i = 1, 2, \dots, m$ ). There is of course no loss of generality in assuming that all constraints are of less than or equal to variety. (The constraint  $g(x) \geq c$  can be written as  $-g(x) \leq -c$ ). Much effort has been devoted to devising direct search methods to locate the minimum of a function of  $n$  real variables. A direct search method is one that uses function values only. A number of methods have been suggested (23). A function of two variables will be considered. Its contour lines are shown in Figure (4.1), its minimum is at  $(x_1^*, x_2^*)$ . The crudest search method is the alternating variable search method. One starts at some point A and search in the direction of  $x_1$  axis for a minimum in this direction and thus find B at which the tangent to the contour line is parallel to the  $x_1$  direction. From B one then search in the direction of  $x_2$  - axis and so proceeds to C and then to D by searching parallel to  $x_1$  - axis... etc. In this way, one proceeds to the optimum point. It is clearly possible to extend the idea to the function of  $n$  variables. One of the direct search methods is Hooke and Jeeves method which is adopted in this study.

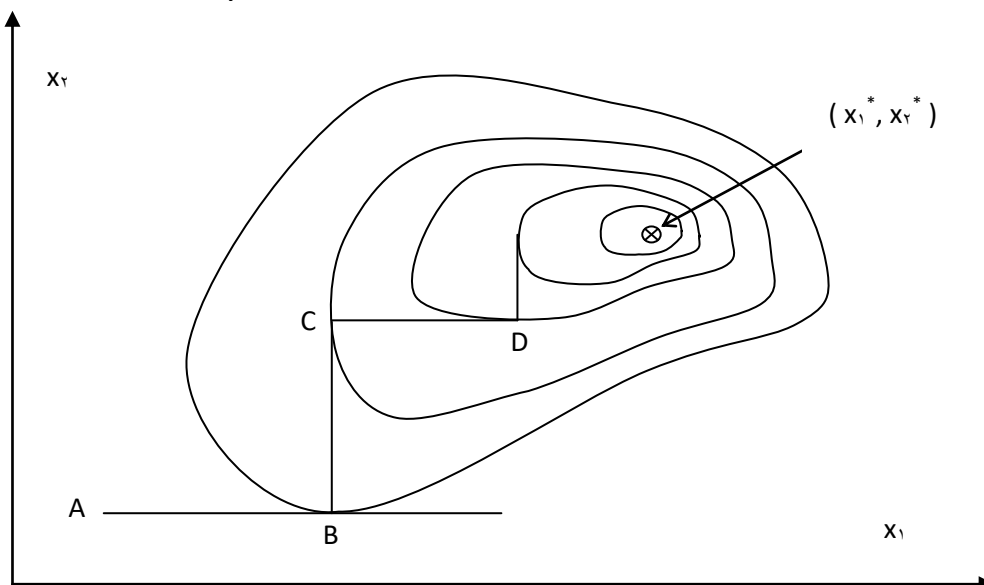


Figure (4.1): Contour lines for function of two variables(10).

### ξ.1.3 Hooke and Jeeves method :

In this method the search consists of a sequence of exploration steps about a base point which if successful are followed by pattern moves. The procedure is as follows: (10)

(A) Choose an initial base point  $b_0$  and a step length  $h_j$  for each variable  $x_j$ ;  $j=1, 2, \dots, n$ . The program written in this work uses a fixed step  $h$  for each variable

(B) Carry out an exploration about  $b_0$ . The purpose of this is to acquire knowledge about the local behavior of the function. This knowledge is used to find a likely direction for the pattern move by which it is hoped to obtain an even greater reduction in the value of the function. The exploration about  $b_0$  proceeds as indicated.

(i) Evaluate  $f(b_0)$ .

(ii) Each variable is now changed in turn, by adding the step length. Thus one evaluates  $f(b_0 + h_1 e_1)$  where  $e_1$  is a unit vector in the direction of the  $x_1$ -axis. If this reduces the function, replace  $b_0$  by  $b_0 + h_1 e_1$ . If not, find  $f(b_0 - h_1 e_1)$  and replace  $b_0$  by  $b_0 - h_1 e_1$  if the function is reduced. If neither step gives a reduction leave  $b_0$  unchanged and consider changes in  $x_2$ , i.e. find  $f(b_0 + h_2 e_2)$  etc. When one has considered all  $n$  variables, it is possible to have a new base point  $b_1$ .

(iii) If  $b_r = b$ , i.e. no function reduction has been achieved, the exploration is repeated about the same base point  $b$ , but with a reduced step length. In the present work, in which a structural optimization is performed using this method, it was found that reducing the step length to one half of its former value is satisfactory.

(iv) If  $b_r \neq b$ , one makes a pattern move.

(C) Pattern moves utilizing the information acquired by exploration, and accomplish the function of the minimization by moving in the direction of the established "pattern". The procedure is as follows:

(i) It seems sensible to move further from the base point  $b_r$  in the direction  $b_r - b$ , since that move has already led to a reduction in the function value. So one can evaluate the function at the next pattern point.

$$P_1 = b_r + \gamma (b_r - b) \quad \text{-----} \quad (\xi.1)$$

In general

$$P_i = b_i + \gamma (b_{i+1} - b_i) \quad \text{-----} \quad (\xi.2) \quad \text{(ii) Then}$$

continue with exploratory moves about  $P_1$  ( $P_i$ ).

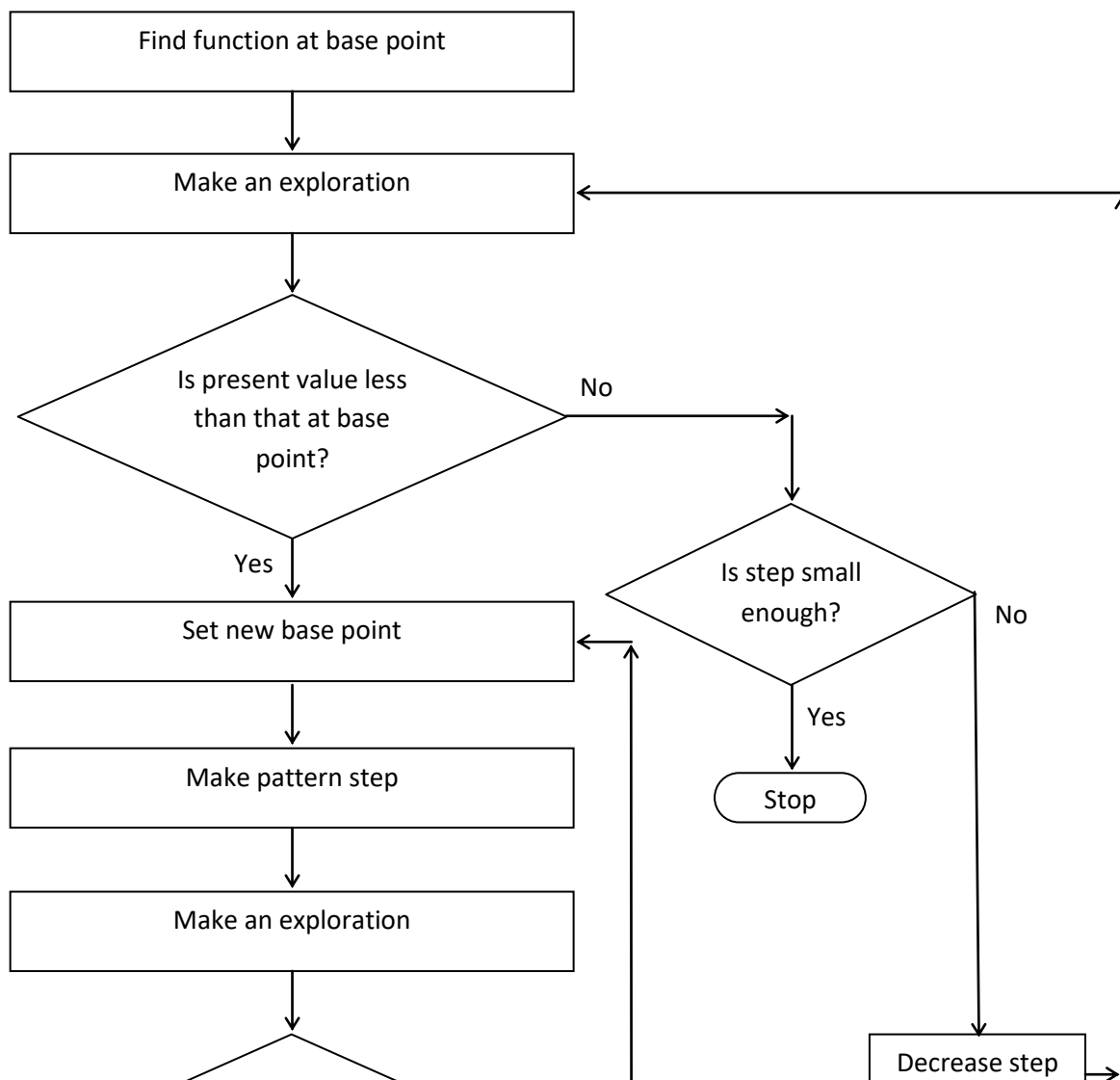
(iii) If the lowest value at step C(ii) is less than the base point  $b_r$  ( $b_{i+1}$  in general) then, a new base point  $b_r$  ( $b_{i+1}$ ) has been reached. In this case repeat C(i). Otherwise abandon the pattern move from  $b_r$  ( $b_{i+1}$ ) and continue with an exploration about  $b_r$  ( $b_{i+1}$ ).

(D) Terminate the process when the step length has been reduced to a predetermined small value. The presentation of this method as a flow chart is shown in Figure ( $\xi.2$ ) and Figure ( $\xi.3$ ).

**$\xi.1.4$  Dealing with constraints :**

When applying the method of Hooke and Jeeves to the constrained optimization problem, one might suppose that it could be modified to take account of constraints. So, in the modified Hooke and Jeeves method it has been suggested that merely giving the objective function a very large value (in a minimization problem) will suffice whenever the constraints are violated. Certainly this idea has an intuitive appeal and is easy to program.

**For each trial point one checks whether it lies within the constrained region or not. If so one evaluates the objective function in the normal way. If not, one gives the objective function a very large value. In this way, the search method will be directed back into the feasible region and hence towards the minimum point within the feasible region.**



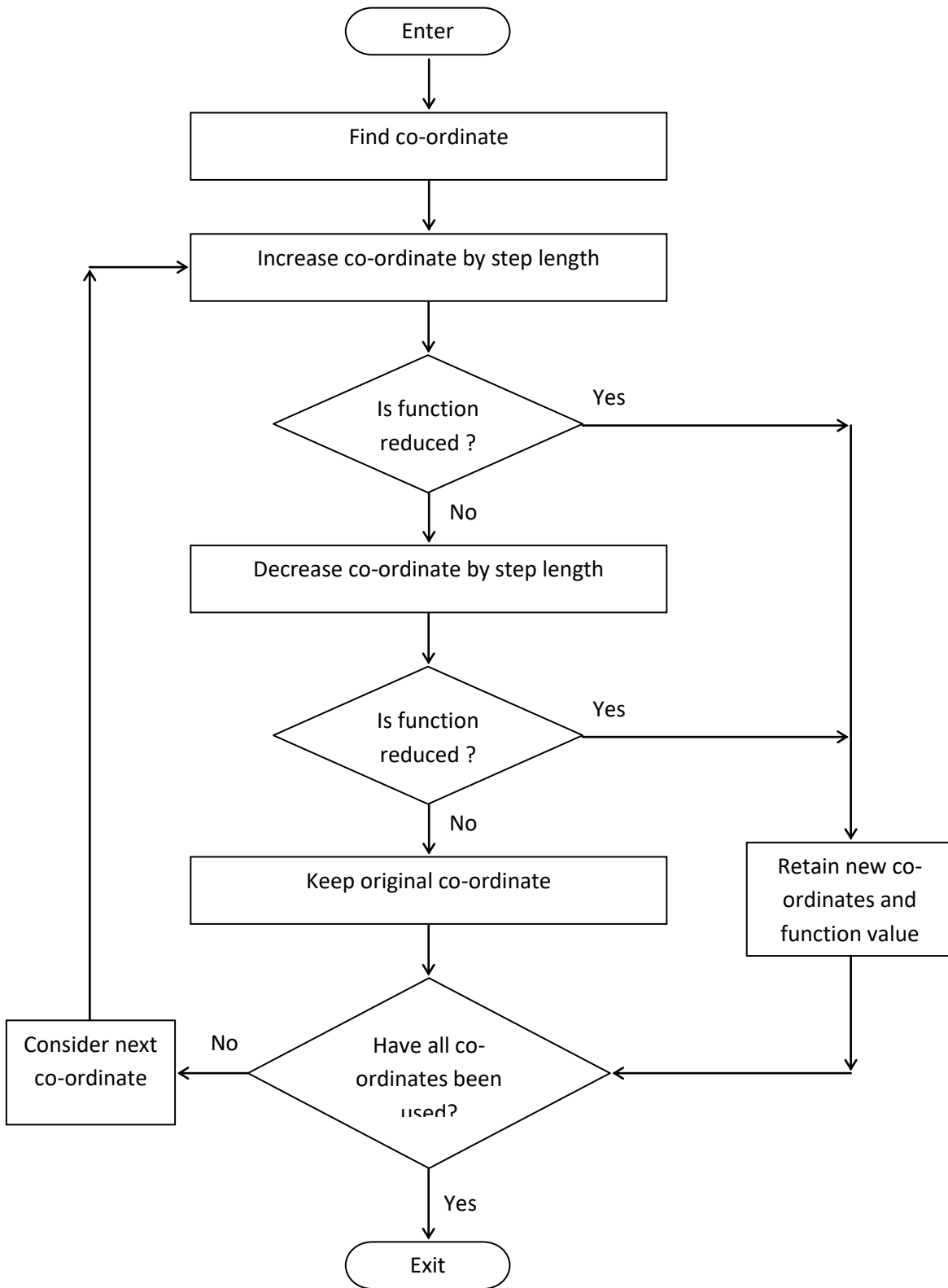


Figure (4.3): Flowchart for an exploration(10).

## **ξ.۲ Plastic design :**

### **ξ.۲.۱ General :**

In the structural analysis and design, the classical approach is based on the assumption that the stresses in the structure caused by the applied loads are within the elastic limit of the material used and thus deflections are small. The approach is, of course, widely used.

However, an alternative approach has gained increasing support recently(۳۷). It is obvious that any structure can be made to fall down (collapse) by applying loading of sufficient magnitude. The purpose of the new analysis is to find that magnitude. It requires knowledge of what happens at collapse and how structures behave when the stresses in the material exceed the elastic limit. This philosophy is embodied in the plastic methods of analysis and design. It is informative to examine the behavior of structures from zero load to failure because it is possible to show clearly the ideas behind the plastic methods.

### **ξ.۲.۲ Elastic-plastic behavior :**

Mild steel will be taken here as an example of elastic-plastic behavior of materials.

To achieve an understanding of the relation between stresses and strains in both elastic and plastic ranges, laboratory tests must be accomplished.

The simplest mechanical test is to apply a controlled tensile force to a long bar of material Figure (ξ.ξ). In the middle of the bar, remote from the clamps at each end, a state of pure uniaxial tension exists.

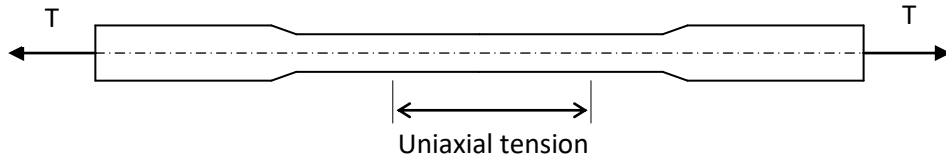


**Figure (1.1): Uniaxial tensile specimen.**

If the extension of a mild steel specimen is measured (as strain) in this region and plotted against the applied force (expressed as a stress) the typical stress-strain curve shown in Figure (1.2) is obtained. At small strains, stress is directly proportional to strain (region OU). The material is elastic, and the slope,  $E$ , is the Young's modulus.

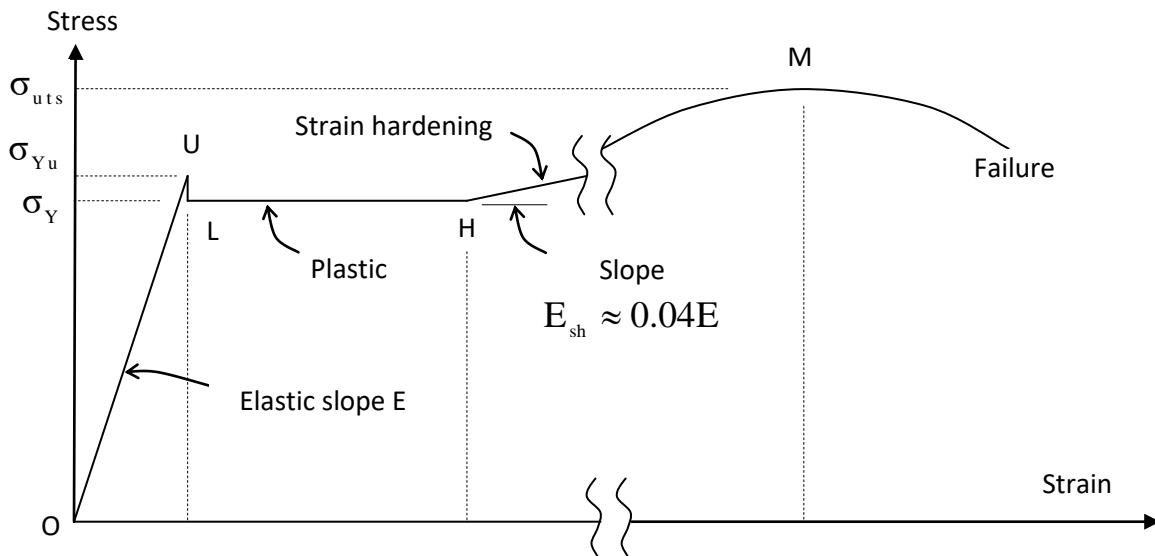


**Figure (1.2): Stress-strain diagram (1.2).**

On average,  $E$  is about  $200 \text{ kN/mm}^2$  (37). The point U is the limit of proportionality between stress and strain. When this limit is reached there is a rapid drop in stress to the point L. U is called the upper yield point with a corresponding stress  $\sigma_{Yu}$ . The magnitude of  $\sigma_{Yu}$  depends on the cross-sectional shape of the specimen and the type of equipment used to carry out the test. In many of the common structural steel sections which are hot rolled into shape, the residual stresses from the rolling process effectively remove point U. Hence the upper yield point is of no practical significance. The stress corresponding to point L is the yield stress  $\sigma_Y$  with a typical magnitude for mild steel of  $200 \text{ N/mm}^2$  (37).

The strain at the yield stress is about  $0.002$ . When the strain is increased above this value, it is found that no corresponding stress increase is required. The behavior in the region LH of the graph is called plastic (increase in strain without change in stress is called plastic flow). The end of plateau H is somewhat variable but a typical strain is  $0.015$ . The strain in the plateau is thus at least ten times the strain at the yield point.

After H, an increase in strain requires an increase in stress, but the relation is now non-linear. This is called strain hardening. The initial slope  $E_{sh}$  of this region is about 5 percent of Young's modulus,  $E$ . At a strain of at least  $0.05$ , a 20 percent increase in the length of the specimen, the stress reaches its maximum value (point M). This stress is called the ultimate tensile strength  $\sigma_{uts}$  and is about  $410 \text{ N/mm}^2$  for mild steel. Further increase in strain produces necking and eventually a cup and a cone fracture.

Careful tests have shown that the stress-strain curve for mild steel in compression is in fact identical to the one in tension up to the point of maximum stress. The complete graph is as in Figure (4.6). If the specimen is

loaded to, say, point X and the load then removed, initially the change in strain is elastic (slope E) as shown by the solid line XY. Ideal behavior will follow the solid line with compressive plastic flow occurring when the stress reaches  $\sigma_Y$  in the compressive sense. The actual behavior follows the broken line XY' indicating an apparently reduced yield stress in compression. The divergence from the ideal path is called the Bauschinger effect.

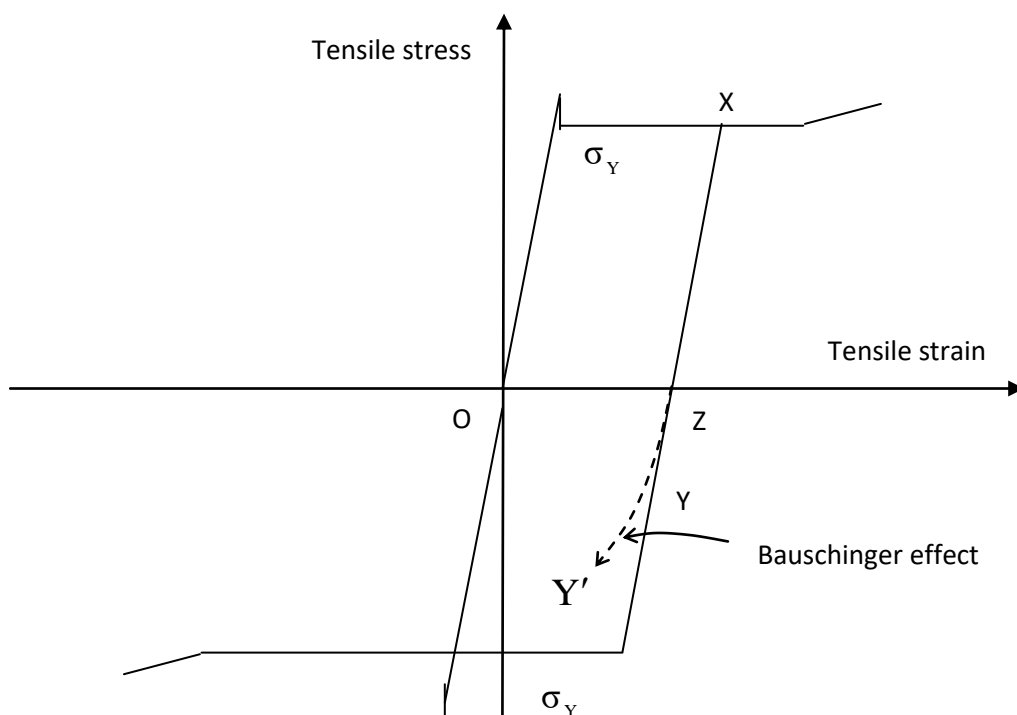


**Figure (4.6) Bauschinger**

Perfect elastic-plastic behavior is shown in Figure (4.5). Mild steel can be made to fit this by (4.5)

(1) Ignoring the upper yield point. This causes no problems; many structural members do not show it anyway.

(v) Ignoring strain hardening. This introduces some errors because many structures will have areas in the strain hardening region at collapse. However, the errors are small because of the small slope ( $E_{sh}$ ) and are on the safe side since strain hardening represents an increase in strength.

(vi) Ignoring the Bauschinger effect. This causes errors but usually they are small. Figure (4.6) shows that when the stress is reduced to zero (point Z) there is little difference in the curves. In structures where full stress reversal is possible the errors can be significant(vii). In the present optimal design formulation, the nature of the load is taken to be static and constant, i.e. there are no unloading cycles, and accordingly, Bauschinger phenomenon has no significant effect.

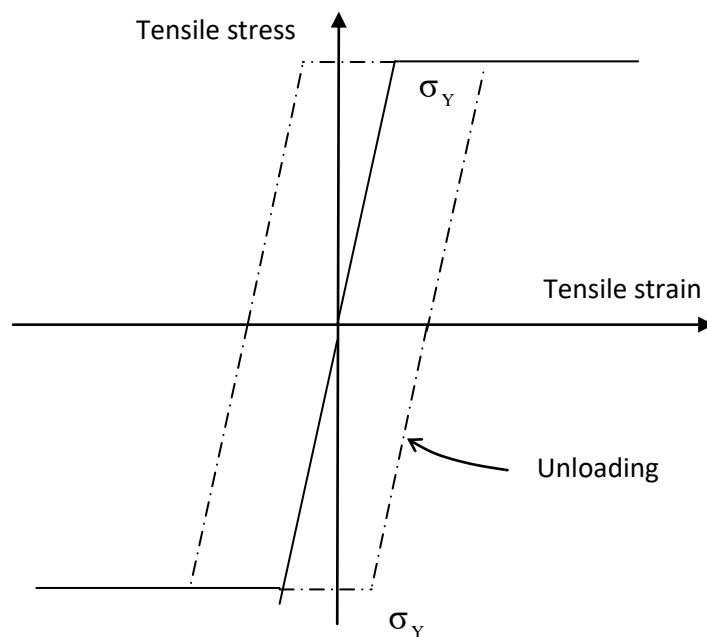


**Figure (4.6): Perfect elastic-plastic**

Mild steel is not the only structural steel, various higher strength grades are in common use. Higher strengths are achieved at the expense of ductility as shown in Figure (4.7). In general, plastic analysis can be applied, with care, to

structures made from these steels. The plastic design of rectangular tanks made of elastic-plastic material will be discussed in this chapter.

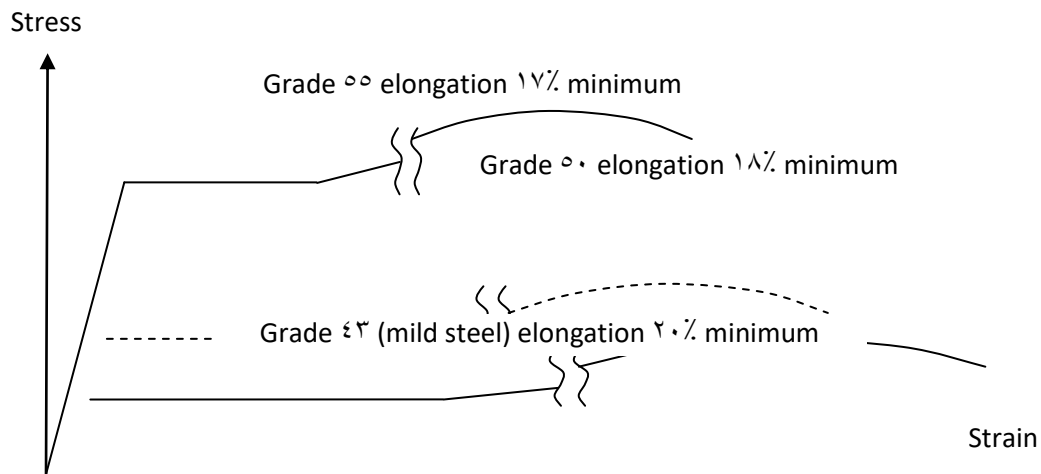


**Figure (4.1): Stress-strain curves for different →**

**4.2.3 Plastic bending :**

Simple bending theory (based on elastic behavior) gives the following information about a general section under bending. If there is no yield in the material, there are straight line relationships for stress and strain over the

whole depth of the section, as in Figure (ξ.9). The level at which the stress and strain are zero is the axis of zero strain. Stress and strain are proportional to distance (z) from this axis and for sagging there is maximum compression at the top and tension at the bottom. The maximum stress is given by

$$\sigma_{\max} = \frac{M}{S}$$

where M = bending moment and S = elastic section modulus (minimum). (Notice that for unsymmetric section, as in Figure (ξ.9) with bending about the y axis, there are two possible values of the section modulus.)

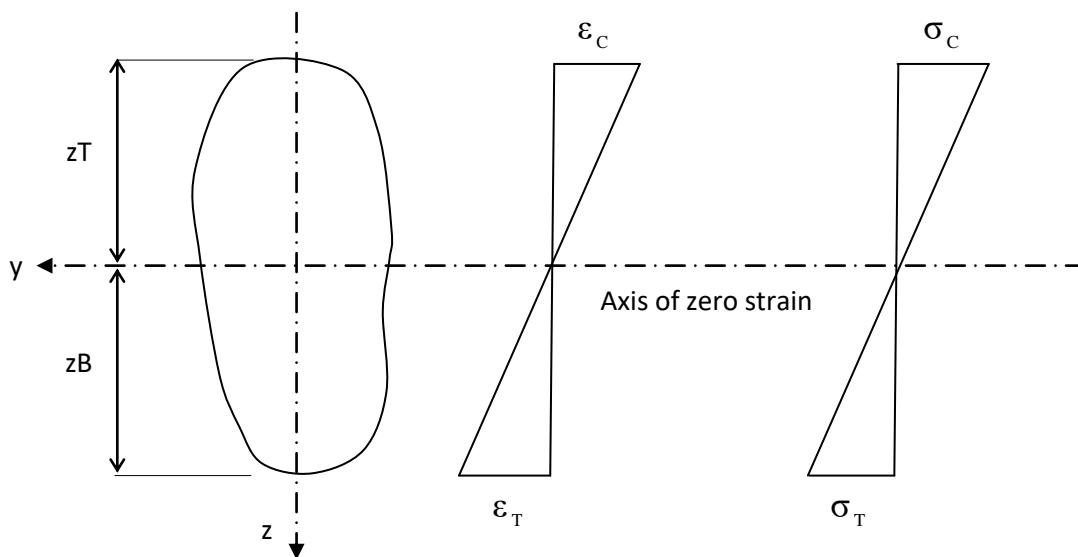


**Figure (ξ.9): Elastic stress and strain.**

$S_T = I/z_T$  and  $S_B = I/z_B$  where I is the second moment of area of the section about the y-axis. There will be different intensities of stress and strain at the top and bottom.

There will be elastic behavior until the maximum stress reaches the yield point. At this stage, of course, only material at the outside edge of the section yields. It has been shown in tests that the distribution of strains stays linear over the depth of the section after yield ( $\sigma_y$ ). The simple bending theory assumption of plane sections remaining plane is still valid. It is possible to find the stress at any position from the stress-strain curves as shown in Figures (ε.10) and (ε.11). As the bending moment is increased, yielding spreads towards the axis of zero strain. The stress distribution shows two constant regions where yield has occurred (the stress is limited to the yield stress, but strain can be increased by plastic flow), joined by a linear (elastic) stress distribution.

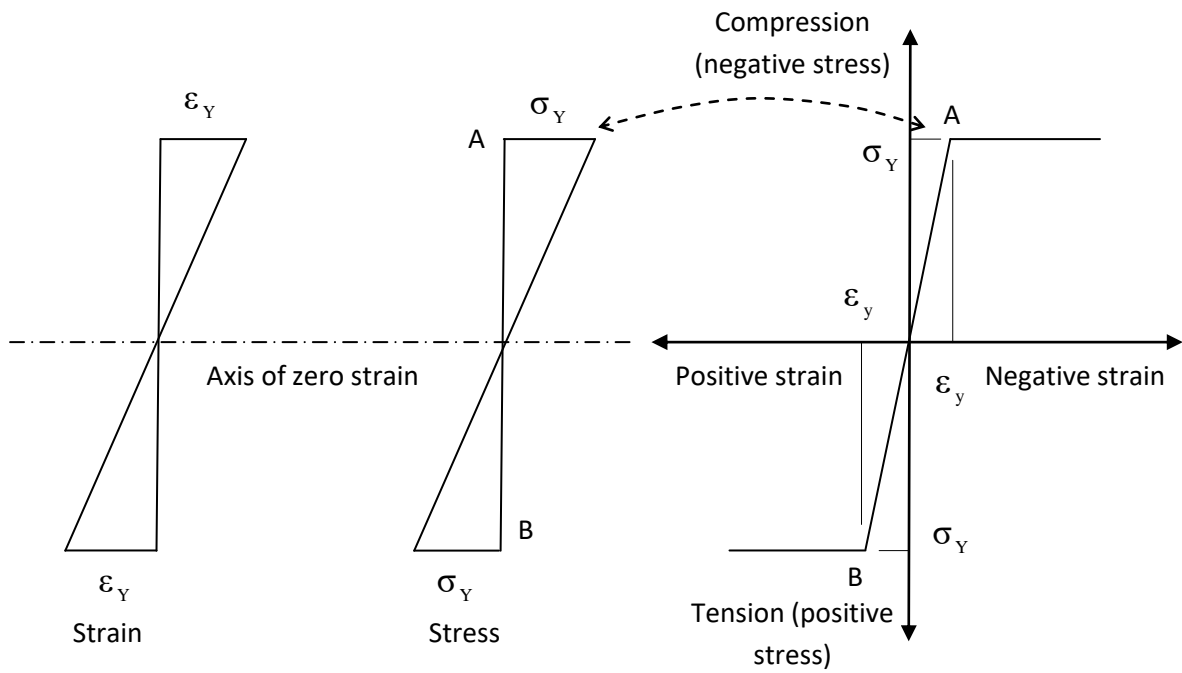


Figure (ε.1.0): Stress distribution at yield.

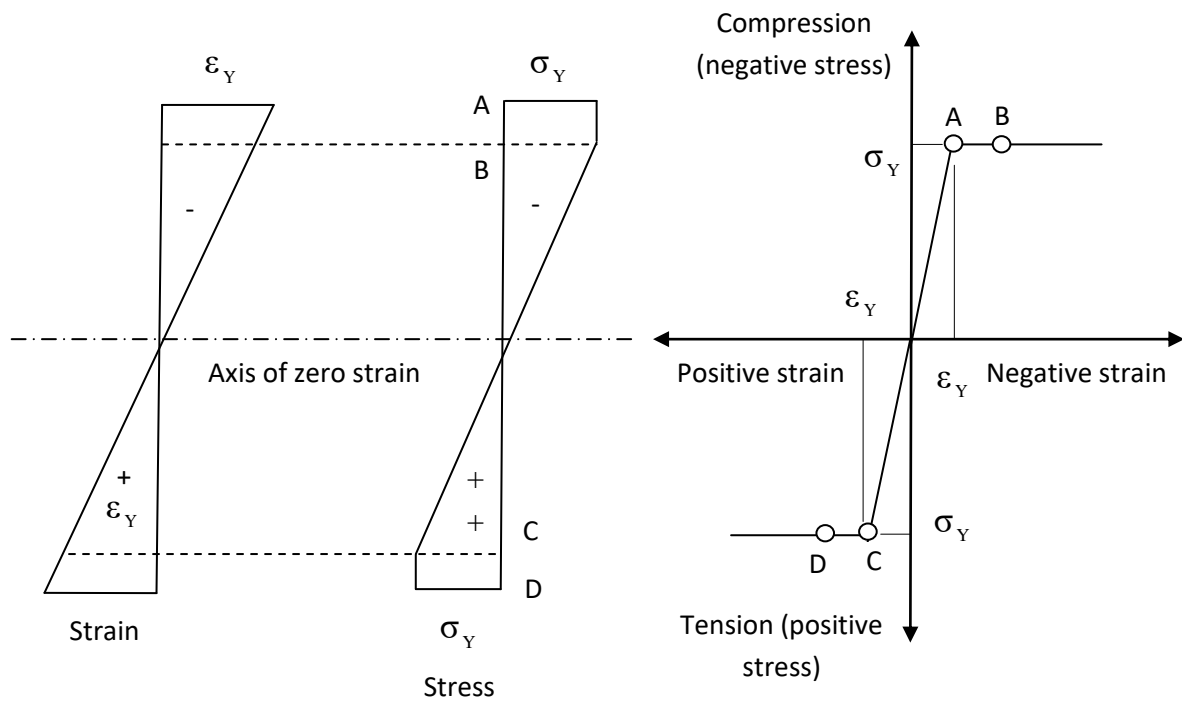
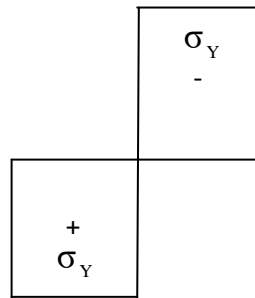


Figure (ε.1.1): Stress distribution after yield.

The logical conclusion is shown in Figure (ε.12) with constant stress to the axis of zero strain. With all the material yielding (in compression above and in tension below the axis of zero strain) the section behaves like a hinge because the strain can increase everywhere in the section without any change in stress.



**Figure (ε.12): Constant yield stress at**

This hinge action is illustrated in Figure (ε.13). The section has become a plastic hinge. The plastic hinge is formed at a bending moment equal to the plastic moment of resistance of the section, which is the largest bending moment the section can carry. It is usually shortened to plastic moment and given the symbol  $M_p$ .

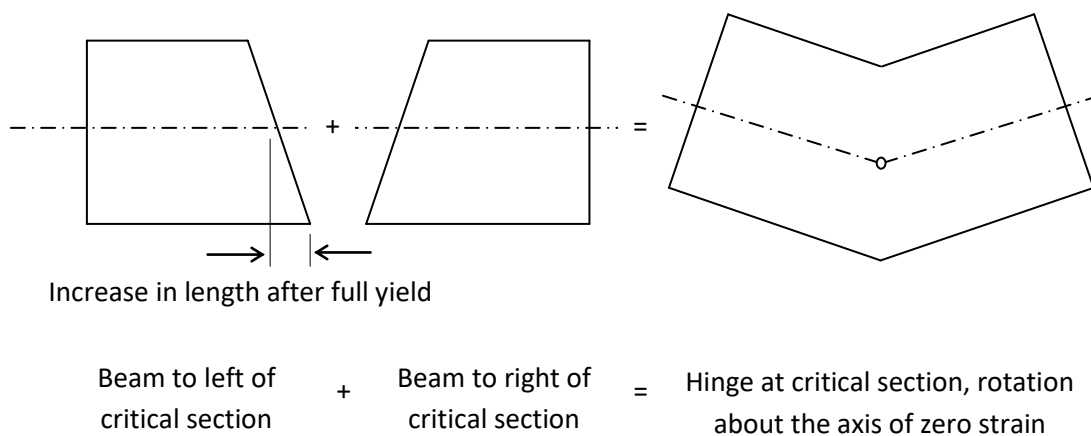


**Figure (ε.13): Formation of plastic hinge.**

### 4.2.4 Calculation of the plastic moment :

#### 4.2.4.1 General :

The load capacity of beams, frames, and plates is generally calculated according to plastic limit analysis. A general cross-section is shown in Figure (4.14). The stress distribution due to the formation of a plastic hinge by bending about the y-axis is also shown. Since the hinge has been formed by bending only, horizontal equilibrium of the section requires that  $C = T$ , where  $C$  is the compressive force due to compressive yield above the axis of zero strain and  $T$  is the tensile force due to tensile yield below the axis.

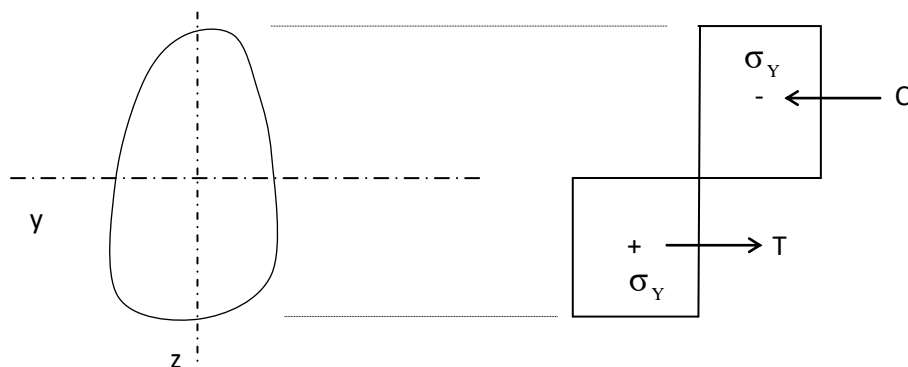


Figure (4.14): Constant stress distribution.

The area of section in compression is equal to the area of section in tension. Hence the axis of zero strain, when a plastic hinge forms, bisects the cross sectional area. This axis only coincides with the centroid of the section when the section is symmetric about the axis of zero strain.

#### 4.2.4.2 Rectangular section :

In a rectangular section Figure (4.15) bending about the y-axis, where the axis of zero strain is  $d/2$  from the top of the section,

$$C = T = \frac{bd}{2} \sigma_Y \quad \text{----- (1.3)}$$

Since these forces are caused by a bending moment equal to  $M_p$ , taking moments about the axis of zero strain gives:

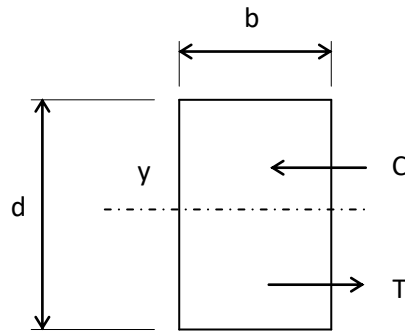


Figure (1.4): Rectangular section.  
Figure (1.4): Rectangular section.

$$M_p = C \times \frac{d}{4} + T \times \frac{d}{4} = 2 \times \frac{bd}{2} \sigma_Y \times \frac{d}{4}$$

that is

$$M_p = \frac{bd^2}{4} \sigma_Y \quad \text{----- (1.4) This is}$$

usually written:

$$M_p = Z \sigma_Y \quad \text{----- (1.5)}$$

where  $Z$  is called the plastic modulus of the section (differs from the section modulus  $S$ ). Both the plastic and elastic moduli are geometric properties of the cross-section. The ratio of the plastic section modulus to the elastic section modulus is the shape factor of the section:

$$\text{shape factor} = \frac{Z}{S} \quad \text{----- (1.6)}$$

For the rectangular section  $S = bd^2/6$  so that:

$$\text{shape factor} = \frac{bd^2}{4} / \frac{bd^2}{6} = 1.5$$

### ξ.γ.ξ.γ Axial force :

In shell and plate structures, cross sections may be exposed to high axial force and this will alter the plastic moment. The axial force, P, moves the axis of zero strain as in Figure (ξ.γ). To simplify the mathematics the stresses have been replaced by two equivalent distributions. (γγ) The stresses in A are assumed wholly due to the axial force, that is

$$P = bz\sigma_Y \quad \text{----- (ξ.γ)}$$

The stresses in M are caused by the changed plastic moment  $M'_p$

$$\begin{aligned} M'_p &= 2 \frac{(d-z)}{2} \times b \times \sigma_Y \left( \frac{d-z}{4} + \frac{z}{2} \right) \\ &= (d-z) \times b \times \sigma_Y \left( \frac{d+z}{4} \right) \\ &= \left( \frac{d^2 - z^2}{4} \right) b \sigma_Y \\ &= \frac{bd^2}{4} \sigma_Y \left[ 1 - \left( \frac{z}{d} \right)^2 \right] \end{aligned}$$

From (ξ.ξ),  $bd^2 \sigma_Y / 4$  is the plastic moment  $M_p$  of the rectangular section, so that

$$\frac{M'_p}{M_p} = 1 - \left( \frac{z}{d} \right)^2 \quad \text{----- (ξ.λ)}$$

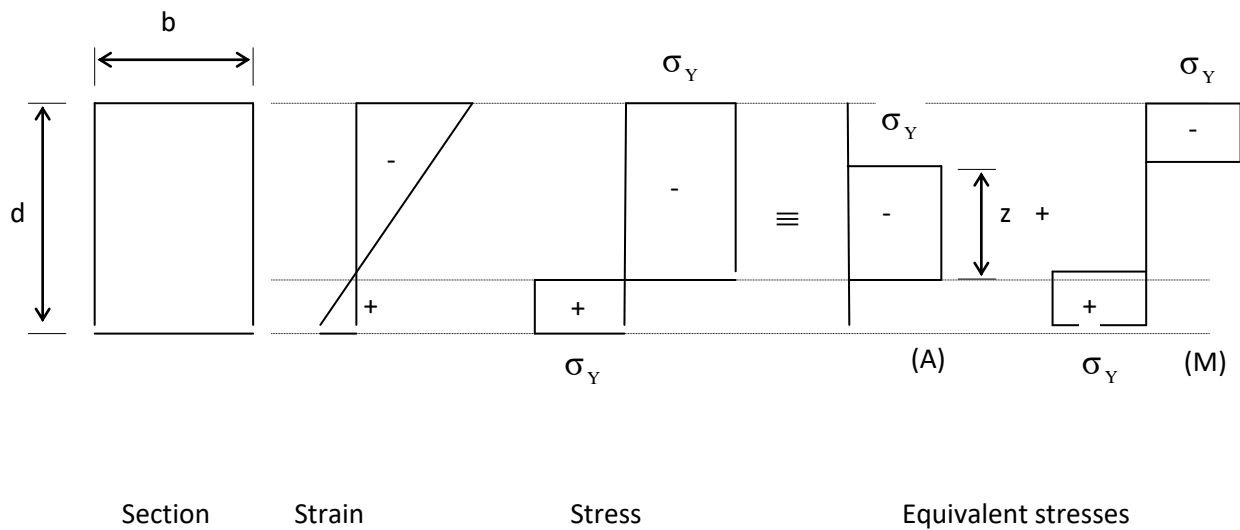


**Figure (4.16): The equivalent**

The maximum axial force  $N_p$ , where the section can carry ignoring buckling, is called the squash load (4.17) and is given by:

$$N_p = bd\sigma_Y \quad \text{----- (4.9)}$$

so that

$$\frac{P}{N_p} = \frac{z}{d}$$

and

$$\frac{M'_p}{M_p} + \left( \frac{P}{N_p} \right)^2 = 1 \quad \text{----- (2.10)}$$

Equation (2.10) shows that both tensile and compressive forces reduce the plastic moment because the reduction term is  $(P/N_p)^2$ . Equation (2.10) is represented in Figure (2.11)

Shells and plates frequently have a large slenderness ratio (span-to-thickness ratio); the conservation of material normal to the median surface is well verified. Shear forces cause smaller reductions in plastic moment than axial forces, and need only be considered in the rare cases when they are exceptionally large. (21)

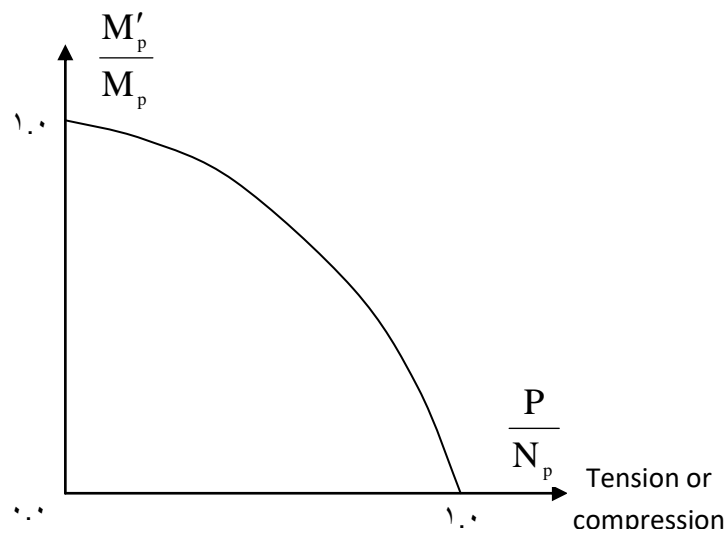


Figure (2.11): Diagram for equation (2.10)

Figure (4.17): Diagram for equation(4.16).

#### 4.2.6 Design technique :

To formulate a reliable design technique, a yield criterion must be derived in terms of general, multi-axial stress resultants state. The yield criteria is given in terms of stress components. When the state of stress is uniaxial tension or compression, the yield condition for most metals is:

$$\sigma = \pm \sigma_Y \quad \text{----- (4.11) In a}$$

multiaxial state of stress, yielding will occur when a certain physical condition related to the state of stress will be satisfied, as in the more extensively used yield criteria of von-Mises. The equation of this surface is:

$$\sigma_1^2 + \sigma_2^2 + \sigma_3^2 - \sigma_1 \sigma_2 - \sigma_2 \sigma_3 - \sigma_3 \sigma_1 = \sigma_Y^2 \quad \text{----- (4.12)}$$

For a state of plane stress as the case in the flat shell element ( $\sigma_3 = 0$ ), condition (4.12) is represented by :

$$\sigma_1^2 + \sigma_2^2 - \sigma_1 \sigma_2 = \sigma_Y^2 \quad \text{----- (4.13) and}$$

since:

$$\sigma_1 = \frac{\sigma_x + \sigma_y}{2} + \sqrt{\frac{1}{4}(\sigma_x - \sigma_y)^2 + \tau_{xy}^2} \quad \text{----- (4.14)}$$

$$\sigma_2 = \frac{\sigma_x + \sigma_y}{2} - \sqrt{\frac{1}{4}(\sigma_x - \sigma_y)^2 + \tau_{xy}^2} \quad \text{----- (4.15) the}$$

following relation could be obtained:

$$\sigma_x^2 + \sigma_y^2 - \sigma_x \sigma_y + 3\tau_{xy}^2 = \sigma_Y^2$$

or

$$\left(\frac{\sigma_x}{\sigma_y}\right)^2 + \left(\frac{\sigma_y}{\sigma_Y}\right)^2 - \left(\frac{\sigma_x}{\sigma_Y}\right)\left(\frac{\sigma_y}{\sigma_Y}\right) + 3\left(\frac{\tau_{xy}}{\sigma_Y}\right)^2 = 1 \quad \text{----- (1.16)}$$

The formula (1.16) does not account for the stress component  $\tau_{xz}$  and  $\tau_{yz}$  which are small in magnitude and can be neglected, while the normal stress component  $\sigma_z$  is already ignored.

Because moments are seen to be proportional to the stress components, the yield surface in the space of moments will have the same form as in the space of stress components. (1) (1.17) i.e.

$$\left(\frac{M_x}{M_p}\right)^2 + \left(\frac{M_y}{M_p}\right)^2 - \left(\frac{M_x}{M_p}\right)\left(\frac{M_y}{M_p}\right) + 3\left(\frac{M_{xy}}{M_p}\right)^2 = 1 \quad \text{----- (1.17)}$$

By combining (1.16) and (1.17) and using the notations  $N_x$ ,  $N_y$  and  $N_{xy}$  for the axial stress resultant, one can obtain the following criterion of yielding:

$$\left(\frac{M_x}{M_p} + \left(\frac{N_x}{N_p}\right)^2\right)^2 + \left(\frac{M_y}{M_p} + \left(\frac{N_y}{N_p}\right)^2\right)^2 - \left(\frac{M_x}{M_p} + \left(\frac{N_x}{N_p}\right)^2\right)\left(\frac{M_y}{M_p} + \left(\frac{N_y}{N_p}\right)^2\right) + 3\left(\frac{M_{xy}}{M_p} + \left(\frac{N_{xy}}{N_p}\right)^2\right)^2 = 1 \quad \text{----- (1.18)}$$

For a section with unit width and thickness t:

$$\left(\frac{4M_x}{\sigma_Y t^2} + \left(\frac{N_x}{\sigma_Y t}\right)^2\right)^2 + \left(\frac{4M_y}{\sigma_Y t^2} + \left(\frac{N_y}{\sigma_Y t}\right)^2\right)^2 - \left(\frac{4M_x}{\sigma_Y t^2} + \left(\frac{N_x}{\sigma_Y t}\right)^2\right) \times$$

$$\left(\frac{4M_y}{\sigma_Y t^2} + \left(\frac{N_y}{\sigma_Y t}\right)^2\right) + 3\left(\frac{4M_{xy}}{\sigma_Y t^2} + \left(\frac{N_{xy}}{\sigma_Y t}\right)^2\right)^2 = 1$$

or

$$t = \left[ \left(\frac{4M_x}{\sigma_Y} + \left(\frac{N_x}{\sigma_Y}\right)^2\right)^2 + \left(\frac{4M_y}{\sigma_Y} + \left(\frac{N_y}{\sigma_Y}\right)^2\right)^2 - \left(\frac{4M_x}{\sigma_Y} + \left(\frac{N_x}{\sigma_Y}\right)^2\right) \times \right. \\ \left. - \left(\frac{4M_y}{\sigma_Y} + \left(\frac{N_y}{\sigma_Y}\right)^2\right) + 3\left(\frac{4M_{xy}}{\sigma_Y} + \left(\frac{N_{xy}}{\sigma_Y}\right)^2\right)^2 \right]^{(1/4)} \quad \text{----- (4.19)}$$

#### 4.2.1 Computer program for optimization :

A computer program is written in FORTRAN for optimal design of rectangular tank on elastic foundation following the modified Hooke and Jeeves method. In the present work, at each exploration, an elastic-plastic analysis, in which the thickness is constrained by equation (4.19), is performed. The process is continued as described in article (4.1.3) until the optimum (minimum volume of material) is reached.

#### 4.3 Load factor :

The objective of any design based on plastic theory must produce a structure with a specified load factor against collapse. The value of the load

factor to be used is in itself a complex object and is always an issue of debate. It is worthwhile presenting the existing and proposed load factors.

The current British Standard, BS 449 (1969), allows design by plastic methods without stating explicitly the required load factor. BS 449 is based mainly on elastic theory and it can be shown that the load factor for a single-span beam resulting from the elastic requirements varies with the end support conditions and type of loading. The minimum value is 1.70 for a simply supported (I-beam). It was argued (37) that this value could be adopted for any structure. BS 449 recognizes that it is highly unlikely that maximum wind load and maximum imposed load will occur simultaneously so that the load factor for such a load combination could be reduced. Consequently the commonly accepted load factors for design to BS 449 are:

Imposed and dead load 1.70

Wind and imposed and dead load 1.4

**The American specification for structural steel adopts a similar but more detailed approach than BS 449. It allows plastic methods of design and requires a collapse load factor of 1.7 on live and dead load, and a reduced factor of 1.3 when these loads act in conjunction with wind or earthquake loads.**

## **CHAPTER FIVE**

### **APPLICATIONS**

### **AND**

### **DISCUSSION**

#### **٥.١ General :**

In this chapter, some numerical examples are worked out to compare the results obtained by the present finite element analysis to those obtained from available experimental and numerical solutions. A number of examples have been analyzed by the developed program. The examples also serve as means to check the validity of the elastic-plastic representation of the material and to demonstrate the applicability and efficiency of the present analysis method to a variety of two-dimensional problems of rectangular tanks. From the practical point of view, it is necessary to indicate that some approximations are involved in this method. These approximations are mainly due to:(٣)

- ١- Approximations included in the material modeling.
- ٢- Approximations in the finite element modeling technique.
- ٣- Approximations introduced due to the type of procedure used in dealing with the non-linear problem.

## ٥.٢ Applications for testing the program :

This section contains the following examples analyzed using program OPTANK.

- ١- A uniformly loaded square plate with simply supported edges.
- ٢- A rectangular wall loaded by hydrostatic pressure with three edges built-in and the fourth edge is free.
- ٣- A simply supported box beam which was loaded with uniformly distributed load.
- ٤- An open-topped rectangular tank filled with water with fully clamped bottom edges.
- ٥- An open-topped rectangular tank filled with water supported on dwarf walls around the edges.
- ٦- A closed square tank filled with water on elastic foundation.

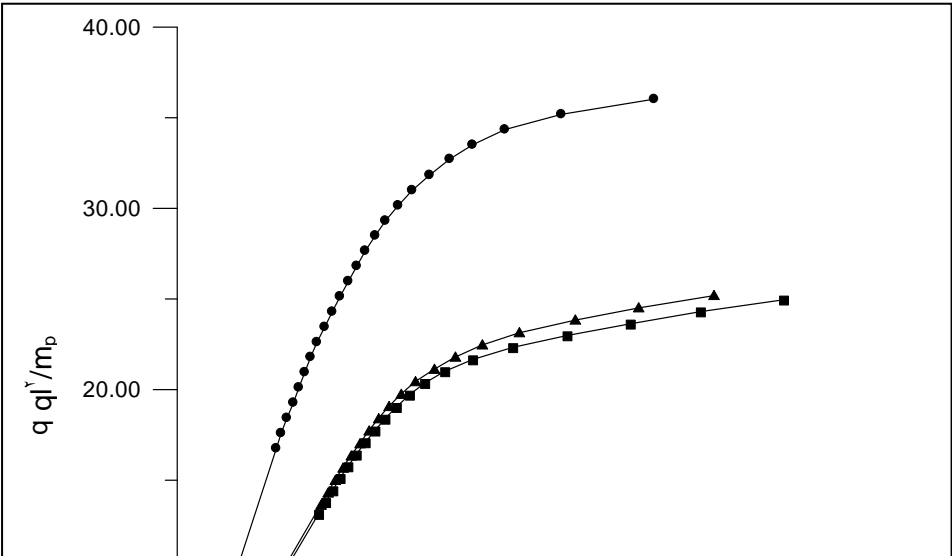
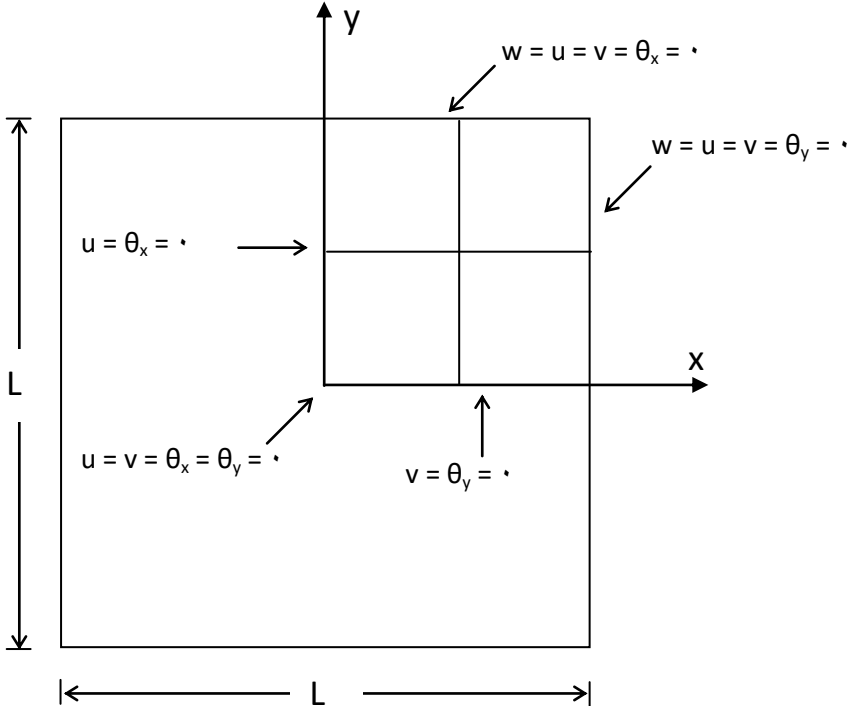
A convergence study is carried out in this application in order to select the suitable mesh with minimum number of elements that indicates a convergence in results.

### ٥.٢.١ Example No.١ :

A simply supported square plate subjected to an increasing uniform load as described in Figure (٥.١) was

analyzed by Hinton (199) a plate bending with 8-node finite element were assumed. Due to symmetry of loading, geometry and boundary condition, only one quarter of the plate is analyzed. From Figure (10.2) it can be noticed that the quarter plate needs (4) elements as a suitable mesh with minimum number of elements that indicated a convergence in results. The adopted load increment after the first yield load factor was (first yield load factor/20). The thickness of the plate is  $t = 0.01$  m and span length is  $L = 1.0$  m. The following properties of the plate material are used:

$$E = 10.92 \text{ MN/m}^2, \quad \nu = 0.3, \quad \sigma_Y = 1600 \text{ MN/m}^2$$

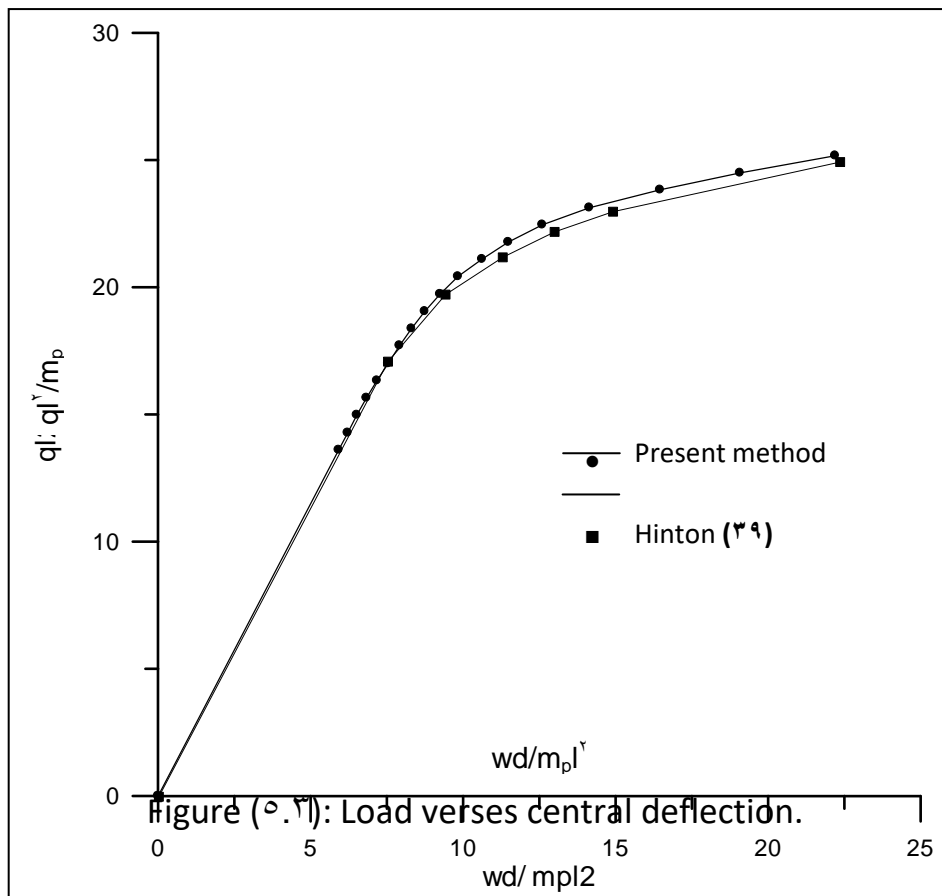


- Element
- ▲ Elements
- Elements

$$wd/m_p l^2$$

Figure (5.2): Load verses central deflection for different

The results of the deflection at the plate center versus uniformly distributed load are plotted in Figure (5.3). The percentage differences in the failure load and corresponding vertical displacement were about 1.17% and -1.63% respectively. There is a good agreement between the present results and those obtained by Hinton.



The second problem to be considered is a rectangular wall loaded by hydrostatic pressure, as shown in Figure

(0.4), with three built-in edges and the fourth edge is free. Half of the wall is discretised by  $8 \times 8$  finite elements. The following properties are chosen for the wall:

Length = 6.0 m

Width = 1.0 m

Pressure at the base = 60.0 KN/m<sup>2</sup>

Young's modulus =  $2 \times 10^7$  KN/m<sup>2</sup>

Poisson's ratio = 1/6, Thickness = 0.2 m

The finite element results are compared with those of Timoshenko (26) and Uraiby (27). The results are presented in Table (0.1). The average percentage differences in the bending moment of Timoshenko and the present study and Uraiby with this study were about 4.9% and 4.3% respectively. The use of 8-node flat shell element in the present study and 9-node element in Uraiby study may be the reason of the reduce in the percentage differences.

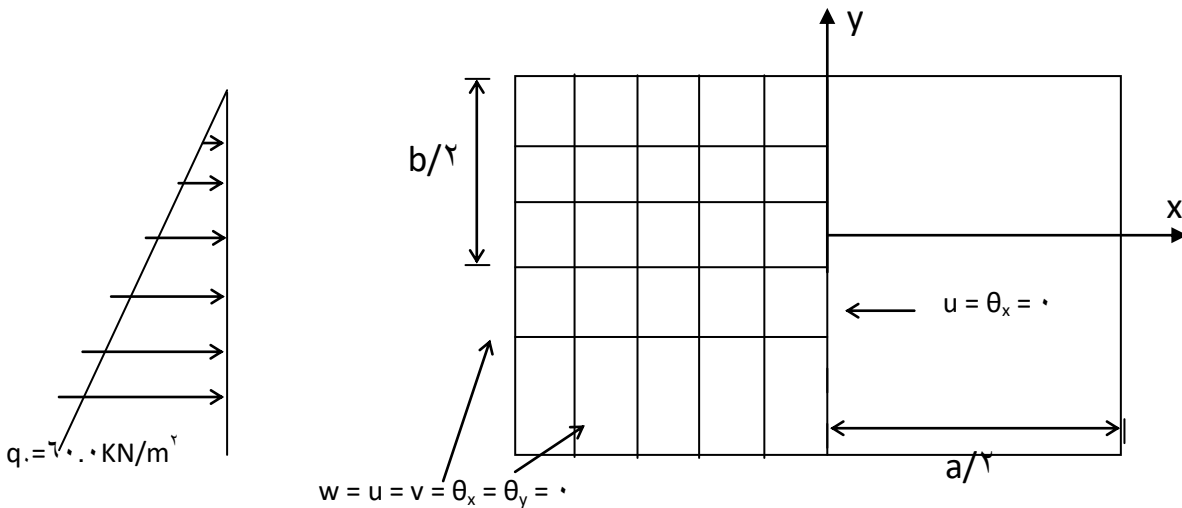


Figure (0.4): Rectangular wall with hydrostatic pressure.

Method	$M_x$ $x=0, y=b/2$	$M_x$ $x=a/2, y=b/2$	$M_y$ $x=0, y=-b/2$
Timoshenko	03.4	-10.7.7	-140.2
Uraiby	01.9	-10.3.4	-140.4
Present	47.3	-10.1.1	-139.0

<b>study</b>			
--------------	--	--	--

Table (0.1): Bending moments in a rectangular wall loaded by hydrostatic pressure.

**0.2.3 Example No.3 :**

Another example analyzed in the present work was a simply supported box beam, considered by Ng. et al. in 1991 (38), which was loaded with a uniformly distributed load upon the top plate and has the dimensions ( $L = 6.0$  m) as shown in Figure (0.0). The material properties of the adopted box beam are: modulus of elasticity  $E = 210$  GPa, yield stress  $\sigma_y = 235$  MPa, and Poisson's ratio  $\nu = 0.3$ . One quarter of the box beam is discretised by 4 finite elements.

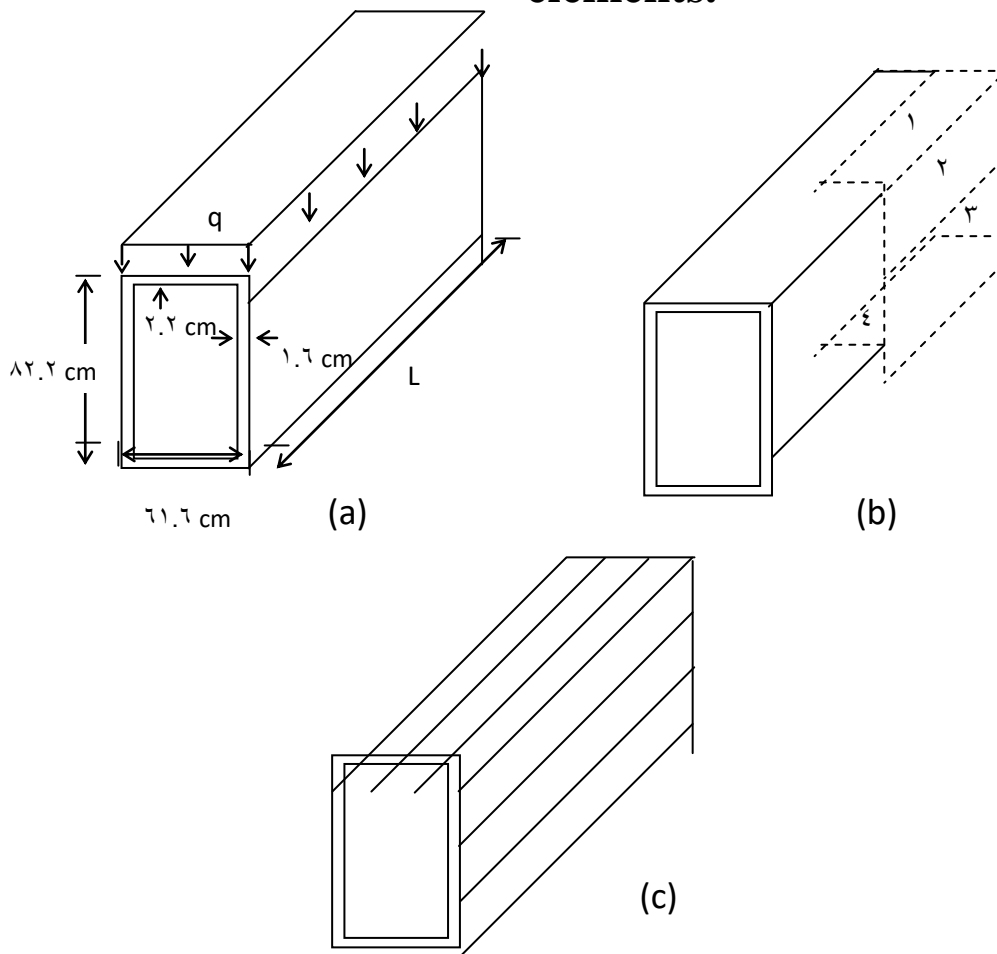
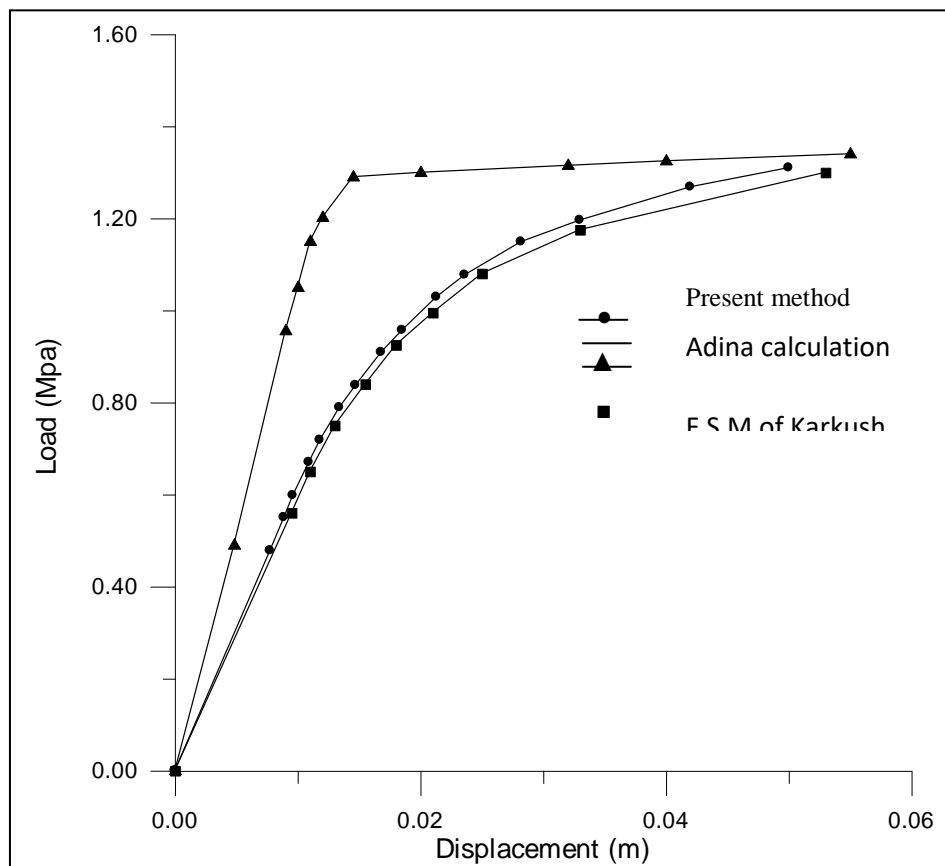


Figure (0.0): Structure considered by Ng et al.(38).

a- Dimension and loading condition.

b- Finite element method idealization in the present study.

Karkush (31) divided the structure into twelve strips as shown in Figure (5.5.c). The relation between the vertical displacement at mid span, at the center, of the top plate and the applied load as obtained by the present incremental finite element method is compared with that calculated by Adina (38) and Karkush(31) by elastic perfectly plastic incremental finite strip method as illustrated in Figure (5.6). The percentage differences in the failure load and the corresponding vertical displacement between Adina with this work were about 2.29% and 10.0% respectively, and between Karkush and this work were about 0.76% and 6.0% respectively. i.e. the results of the present study is closer to that of Karkush.



topped rectangular tank filled with water with fully clamped bottom edges. The open-topped rectangular tank having

length : width : depth proportions of 2 : 1 : 1. One quadrant of the tank is analyzed due to symmetry in geometry and in loading. The following properties are chosen for the tank:

Length = 1.22 m

Width = 0.61 m

Depth = 0.61 m

Wall thickness = 1.27 cm

Floor thickness = 1.09 cm

Young's modulus =  $2 \times 10^8$  KN/m<sup>2</sup>, Poisson's ratio = 0.375

The intensities and distributions of the applied load due to the contained liquid ( hydrostatic on the walls and uniform on the floor ) are shown in Figure (0.7).

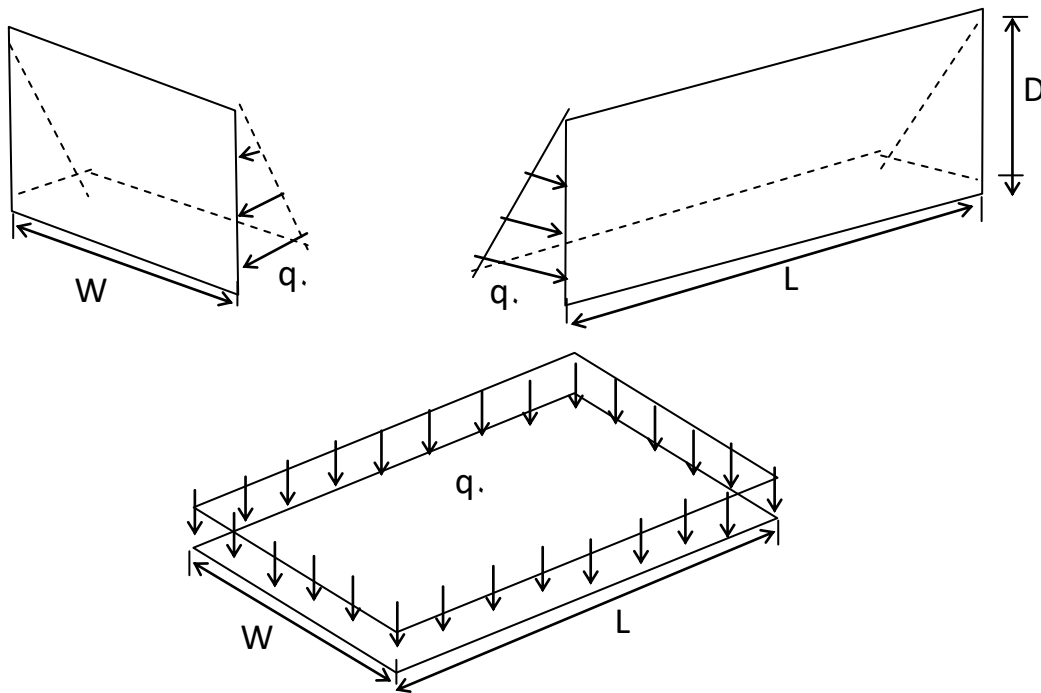


Figure (0.7): Applied load on wall panel and floor. The open-topped rectangular tank is discretised by 22 finite elements. The results of the analysis are compared with finite element results for the same example obtained by Cheung and Davies (19) and Uraiby (29). In Cheung and Davies model, the tank slabs to be analyzed are divided into a number of rectangular elements, which are

then jointed together at a discrete number of nodal points where continuity and equilibrium conditions are established; the resulting set of algebraic equations is then solved to obtain the deformations, and subsequently the moments in all the elements can be obtained by simple matrix multiplication, the twisting couples, shears and direct forces, are assumed to have a negligible effect on the general structural behavior. They compared these results with measurements made on a Prespex model tank and they were show that, in general, there is a good correlation between the theoretical and experimental values. Uraiby used linear elastic Langrangian elements in his analysis.

Figure (0.8) shows the bending moments obtained by Cheung and Davies , Uraiby and the present work.

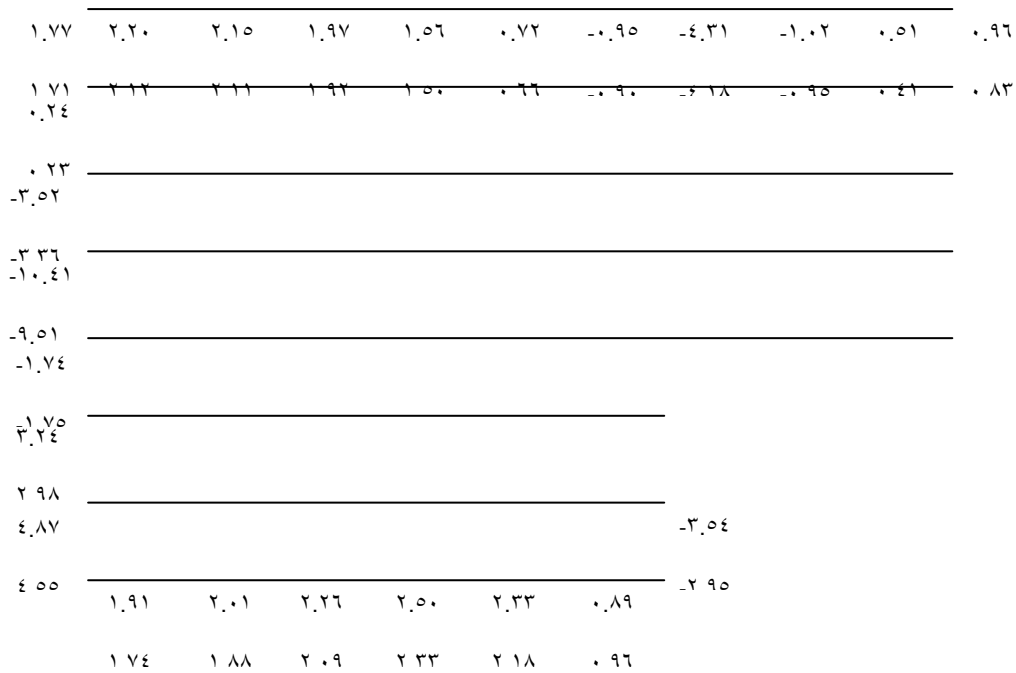
Neglecting the effect of the twisting couples, shears and in plane forces in the study of Cheung and Davies (14) make the percentage of differences in the bending moment between those and present study more than the percentage difference between the Uraiby (15) study and the present study. The average percentage differences in the bending moment between Cheung and Davies with this work and Uraiby with this work are about 14.8% and 8.9%, respectively.

#### 0.2.0 Example No.0 :

The same open rectangular tank considered in example number four is considered here, except that the tank is supported on dwarf walls around the edges.

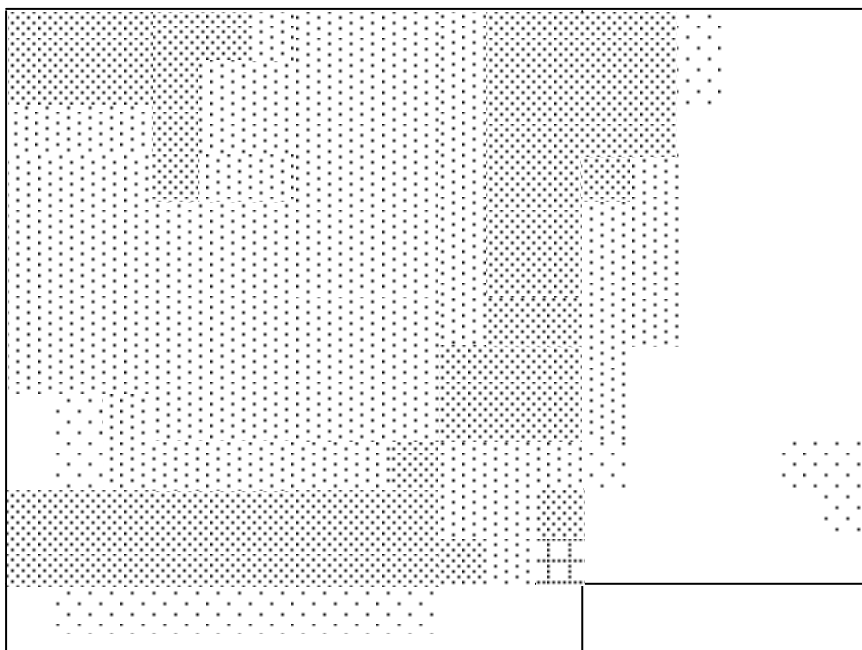
Experimentally, the support condition was realized by placing the tank on four bright mild-steel bars located under the walls. Again the results obtained from this study are compared with Cheung and Davies (14) and Uraiby (15) . Figure (0.9) shows the bending moments obtained by Cheung and Davies, Uraiby and the present work. The





**Bending moments in N-m/m units**  
**Positive moments cause tension on outside face**  
**Upper figures : Cheung and Davies**  
**Medium figures : Uraiby**  
**Lower figures : Present work**

Figure (9.9): Bending moments obtained by finite element solution for rectangular tank filled with water when the bottom edge of the tank is supported on dwarf walls around the edges (Example 9)



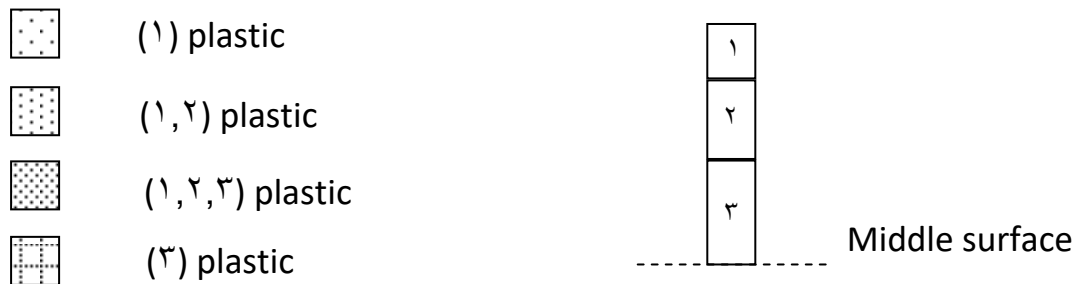


Figure (0.10) Distribution of plastic zones of an open-topped rectangular tank at failure stage.

### 0.2.6 Example No.6 :

**The sixth problem to be considered is closed square tank within elastic analysis filled with water of  $1000 \text{ m}^3$  storage capacity resting on Winkler elastic foundation. One quadrant of the tank is analyzed due to symmetry in geometry and in loading. Each of roof slab, walls and floor slab is discretised by (20) finite elements. The following properties are chosen for the tank:**

**Length =  $12.8 \text{ m}$**

**Width =  $12.8 \text{ m}$**

**Depth =  $6.1 \text{ m}$**

**Roof thickness =  $0.10 \text{ m}$**

**Wall thickness =  $0.23 \text{ m}$**

**Floor thickness =  $0.23 \text{ m}$**

Young modules =  $2.8 \times 10^4$  Mpa

Poissons ratio =  $1/6$

Winkler foundation modules =  $12000$  Kn/m<sup>2</sup>

Uraiby (1984) decided to consider a given group of element as shown in Figure (2.11) (a-b)). He derived a flat shell element resting on linear Winkler foundation using the principle of minimum potential energy. The present results of the analysis are shown in Table (2.2), with the finite element results for the same example obtained by Uraiby. There is a good agreement between the present study and these obtained by Uraiby (1984) study. The average percentage differences in the bending moment were about 2.89%.

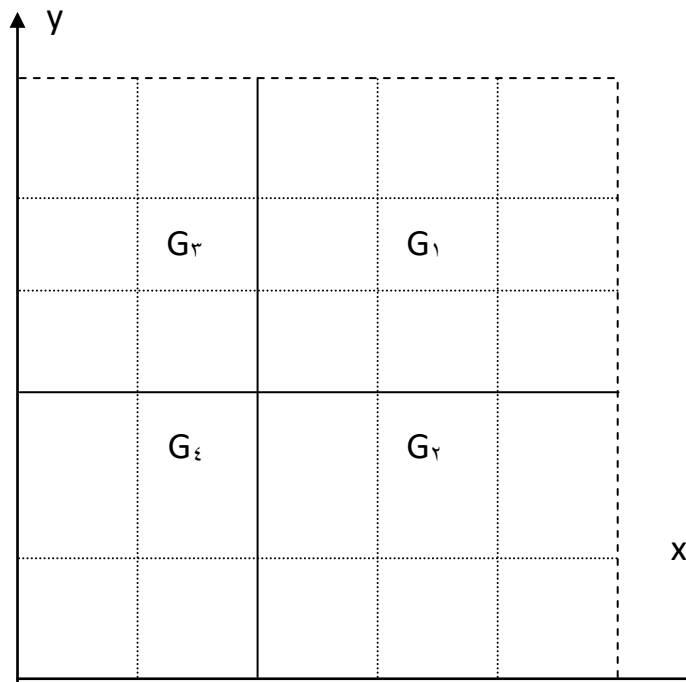
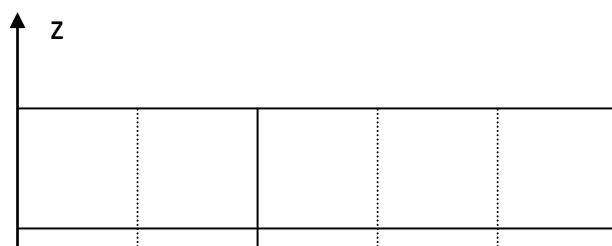


Figure (2.11).a): Finite elements groups for roof slab.



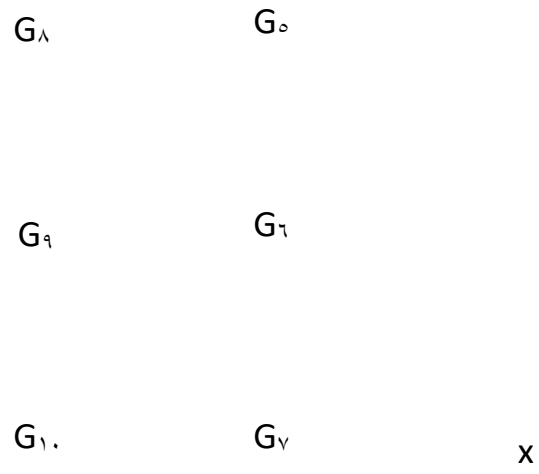


Figure (9.11).b): Finite elements groups for wall in x-direction.

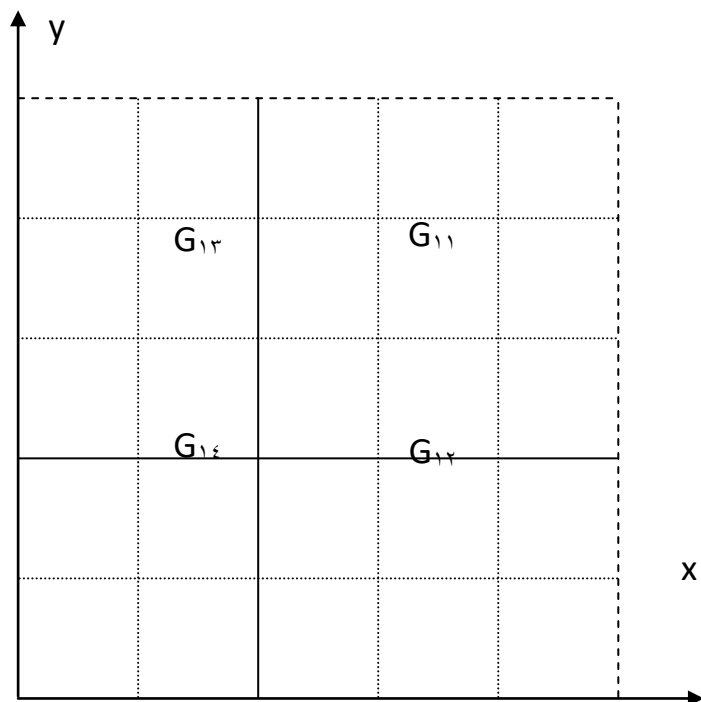
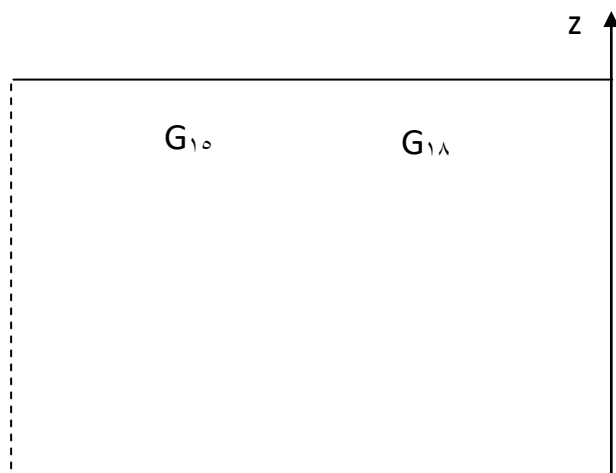


Figure (9.11).c): Finite elements groups for floor slab.



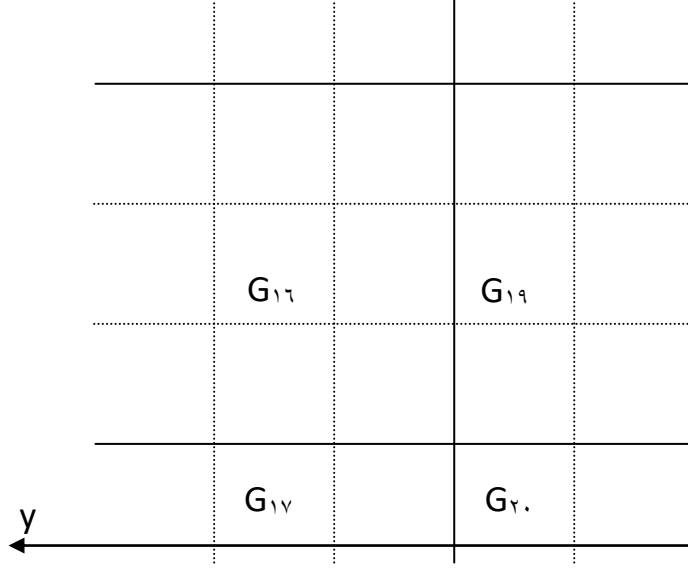


Figure (٥.١١.d): Finite elements groups for wall in y-direction.

Group No.	Uraiby ( $\epsilon\gamma$ )		Present study	
	Mx (kN.m)	My (kN.m)	Mx (kN.m)	My (Kn.m)
١	٥٩.٩٣	٦٠.٤٠	٥٧.٤٢	٥٨.١٨
٢	٣١.١٠	٩٦.٠٧	٣٠.٦٧	٩٣.٣٥
٣	٩٥.٧٣	٣١.٤١	٩٣.١٨	٣٠.٨٢
٤	٥١.٩١	٥١.٢٠	٤٩.٨٣	٥٠.٤٧
٥	٢٨.٤٧	٩٧.٤١	٢٧.٣١	٩٥.٨١
٦	٤٨.٤٣	١١٠.٠	٤٧.٤٢	١٠٥.٩٨
٧	٣٢.٨٤	٨٤.٠٨	٣٢.١٧	٨٢.٦٧
٨	٨٥.٥٠	٥١.٧٦	٨٤.٨٤	٥٠.٩٣
٩	١٥٢.٦٠	٥٧.٩٠	١٤٦.٤٦	٥٦.٥٥
١٠	١١٩.٤٠	٦٣.٧٣	١١٤.٧٩	٦٠.٨٩
١١	٣٦.٨٦	٣٧.٠١	٣٥.٢٤	٣٥.٤٢
١٢	٣٣.٧٦	٨٤.٤٩	٣٢.١٣	٨١.٩٧
١٣	٨٣.٤٨	٣٣.٩٣	٨١.٩٠	٣٢.٣٨
١٤	٦٢.٨٤	٦٣.٠٩	٦٠.٨٣	٦١.٢٥
١٥	٩٧.١١	٢٨.٥٩	٩٥.٧٣	٢٧.٤٦
١٦	١٠٩.٦	٤٨.٦٠	١٠٥.٨٢	٤٧.٧٣
١٧	٨٤.١٣	٣٢.٩٢	٨٢.٤٤	٣٢.٢٨
١٨	٥١.٤٩	٨٥.٥٥	٥٠.٨٦	٨٤.٩٩
١٩	٥٧.٤٩	١٥٢.٧٠	٥٦.٣٨	١٤٦.٧٣
٢٠	٦٣.٥٣	١١٩.٥٠	٦٠.٧٥	١١٤.٨٥

Table (٥.٢): Maximum absolute service bending moments in groups.

٥.٣ Optimal design application :

٥.٣.١ Open topped rectangular tank :

The optimal design of open-topped rectangular tank, with storage capacity of (  $١٠٠ \text{ m}^3$  ) on elastic foundation shown in Figure (٥.١٢) is investigated. The tank is filled with liquid having density of  $١٠ \text{ kN/m}^3$  (water). One quarter of the tank is analyzed due to symmetry in geometry and in loading. From Figure (٥.١٣) it can be noticed that the quarter tank needs ( ٢٧ ) elements in order to be a suitable mesh with minimum number of elements that indicates a convergence in results. Thus, each of walls and floor slab is discretised by ( ٩ ) finite elements.

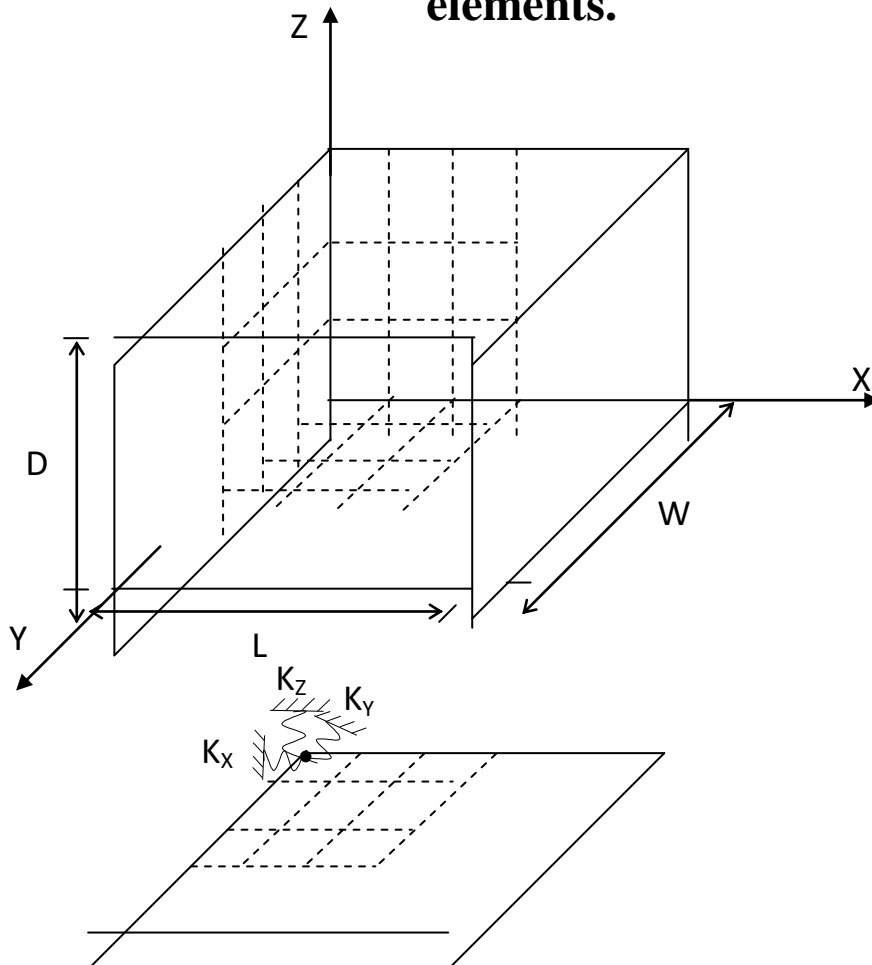


Figure (٥.١٢): Tank on elastic foundation.

The design variables are Length L, Width W, Depth D, Thickness of floor slab  $t_f$ , Thickness of wall in X-direction  $t_l$  and thickness of wall in Y-direction  $t_w$ . Volume of shell =  $(L \times W \times t_f) + 2 \times (L \times H \times t_l) + 2 \times (W \times H \times t_w)$ , the step length = 0.2.

To test the stability of the optimum solution obtained, the problem has been solved with different starting values of dimensions, as in Table (5.3). The constraints are:  $L > 0$ ,  $W > 0$ ,  $H > 3.5$ . The following material properties are used:

$$E = 200000 \text{ MN/m}^2, \quad \nu = 0.3, \quad \sigma_Y = 400 \text{ MN/m}^2$$

Initial dimensions in the optimal design process				
Case No.	Length (m)	Width (m)	Depth (m)	$t_f, t_l, t_w$ (mm)
1	3.6	3.6	7.71	30
2	4.6	4.6	4.72	20

Table (5.3): Initial values of dimensions.

For Winkler model, the values of horizontal subgrade reaction is  $(0.002069 \text{ kN/mm}^2)$ , for Kondner model the value of  $(a=483.48 \text{ mm}^2/\text{kN})$  and  $(b=0.167 \text{ mm}^2/\text{kN})$ . The search direction and consequently the optimal results are not the same in the case of linear and non-linear analysis as shown in Figure (5.14), the reason is that the structural behavior of the tank differs in case of non-linear analysis due to redistribution of stresses in the plastic range. The results have been shown to be quite satisfactory and have thus demonstrated the stability of the program as shown in Figure (5.15), Table (5.4) and Table (5.5); in the two cases the optimal results are volume of shell =  $1.98 \text{ m}^3$ ,  $L=0.42 \text{ m}$ ,  $W=0.42 \text{ m}$ ,  $D=3.55 \text{ m}$ ,  $t_f=19.8 \text{ mm}$ ,  $t_l = t_w = 19.1 \text{ mm}$ .

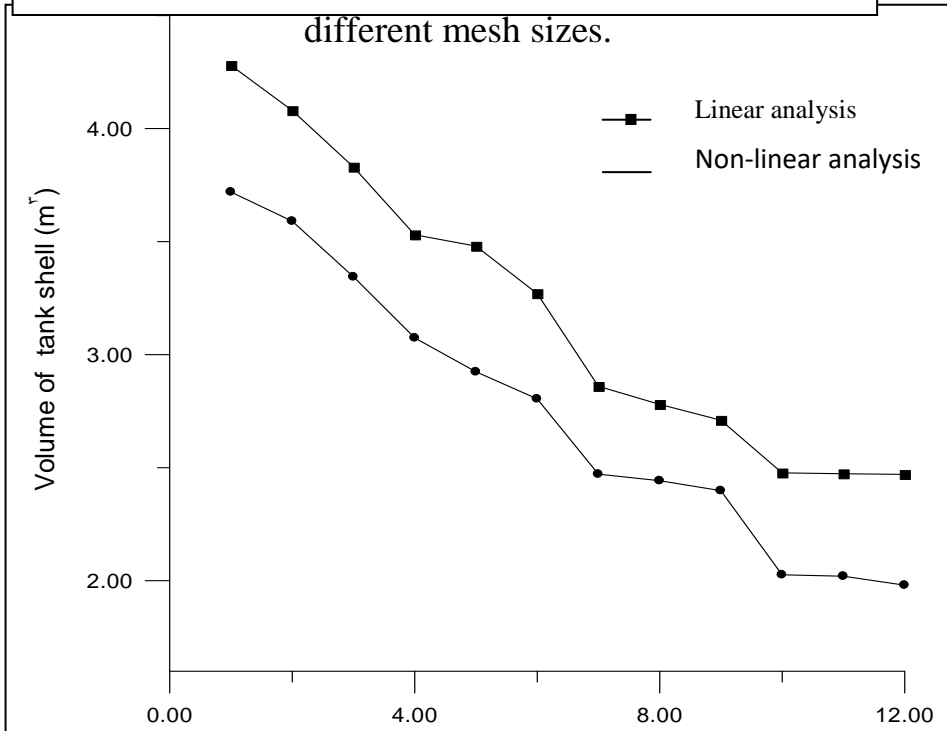
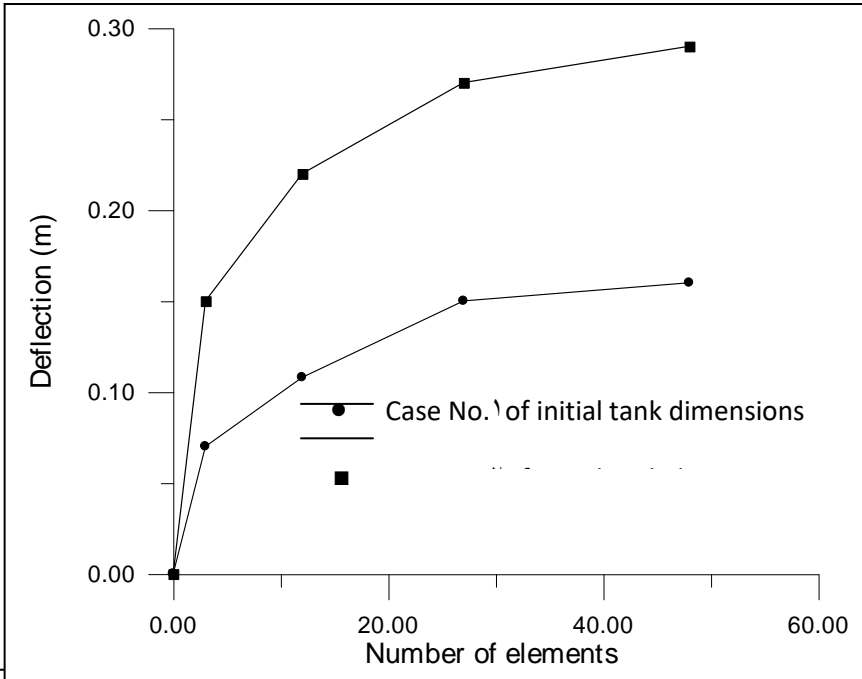


Figure (9.14): Volume of shell versus number of cycles for case No. 1

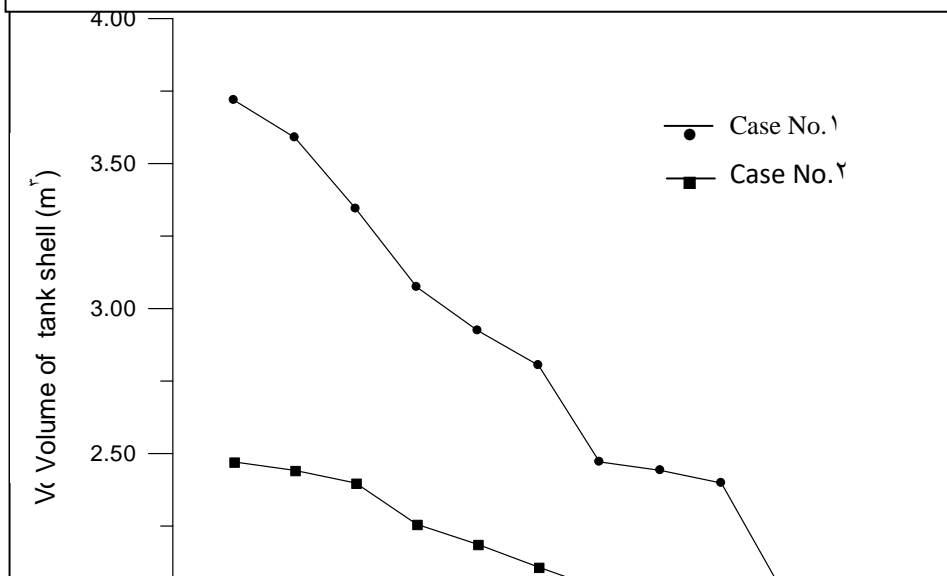


Figure (ϕ. 1ϭ): Volume of shell verses number of cycles.

Cycle No.	Volume of shell (m <sup>3</sup> )	Length (m)	Width (m)	Depth (m)
1	3.719	3.6	3.6	7.716
2	3.090	3.8	3.6	7.309
3	3.344	3.8	3.8	6.920
4	3.074	4.0	4.0	6.200
5	2.924	4.2	4.0	5.902
6	2.804	4.2	4.2	5.668
7	2.471	4.6	4.6	4.720
8	2.442	4.8	4.6	4.528
9	2.398	4.8	4.8	4.340
10	2.026	5.4	5.4	3.429
11	2.020	5.42	5.40	3.416
12	1.980	5.42	5.42	3.404

Table (ϭ. 4): Optimization results for case No. 1.

Cycle No.	Volume of shell (m <sup>3</sup> )	Length (m)	Width (m)	Depth (m)
1	2.471	4.6	4.6	4.720
2	2.442	4.8	4.6	4.528
3	2.398	4.8	4.8	4.340
4	2.206	5.0	5.0	4.000

5	2.187	0.2	0.1	3.846
6	2.108	0.2	0.2	3.698
7	2.034	0.4	0.2	3.561
8	2.026	0.4	0.4	3.429
9	2.020	0.42	0.4	3.416
10	1.980	0.42	0.42	3.404

Table (0.0): Optimization results for case No.2.

0.3.2 Closed rectangular tank :

**Closed rectangular tanks of different volume filed with water are investigated. A quarter of the tank is divided into (36) elements. The following material properties are used:**

$$E = 200000 \text{ MN/m}^2, \nu = 0.3, \sigma_y = 400 \text{ MN/m}^2$$

**The design variables are: Length L, Width W, Depth D and thickness of floor  $t_f$ , wall in x-direction  $t_l$ , wall in y-direction  $t_w$  and roof slab thickness  $t_r$ , step length = 0.1.**

**Volume of shell = ( L×W× $t_f$  )+2×( L×H× $t_l$  )+2×( W×H× $t_w$  )+( L×W× $t_r$  ), Initial values of dimensions and thicknesses are shown in table (0.6).**

Initial dimensions				
Tank volume (m <sup>3</sup> )	Length (m)	Width (m)	Depth (m)	$t_f, t_l, t_w, t_r$ (mm)
100	0.4	0.4	3.43	10
300	8.0	8.0	4.68	20

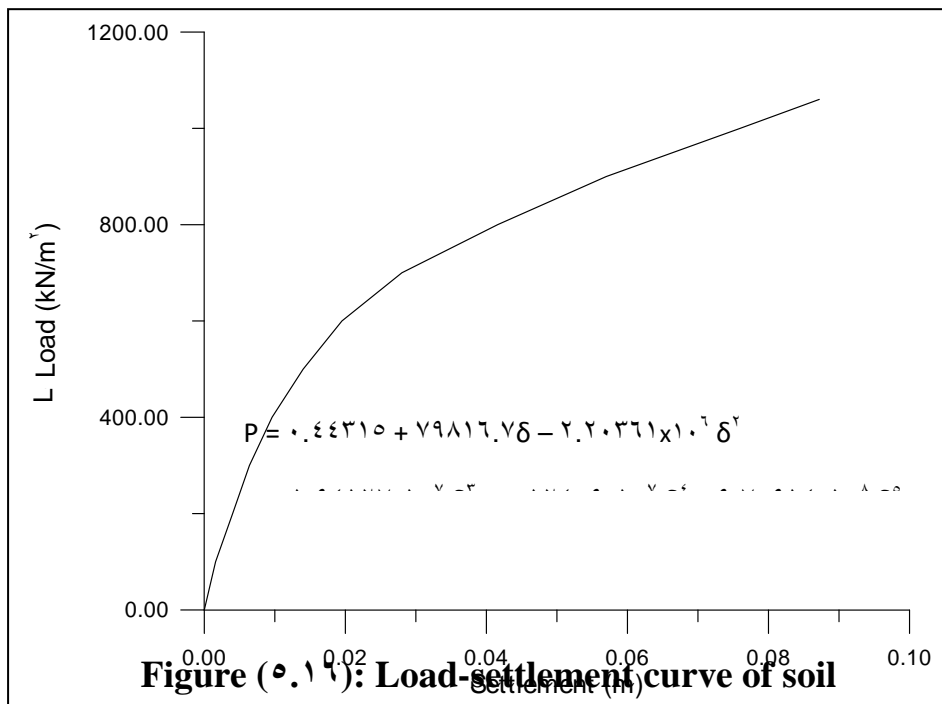
Table (0.6): Initial values of dimensions.

**For non-linear elastic foundation, different types of polynomial model are considered as shown in Figures (0.16) and (0.17) . As shown in (Table (0.7) Figure (0.18) and Figure (0.19)) it is found that the optimum solution is**

not so sensitive to the type of soil. It is clear from Figures (0.20) and (0.21) that the square shape forms the best plan shape.

Soil type	Tank volume (m <sup>3</sup> )	Length (m)	Width (m)	Depth (m)	Roof thickness (mm)	Wall thickness (mm)	Floor thickness (mm)
Dense sand	100	6.7	6.7	2.23	5.02	6.73	5.69
	300	9.8	9.8	3.12	8.82	12.1	9.49
Loose sand	100	6.7	6.7	2.23	5.28	6.92	6.08
	300	9.8	9.8	3.12	9.38	12.5	10.7

Table (0.7): Optimum dimensions for different storage capacity.



[dense sand (12)].

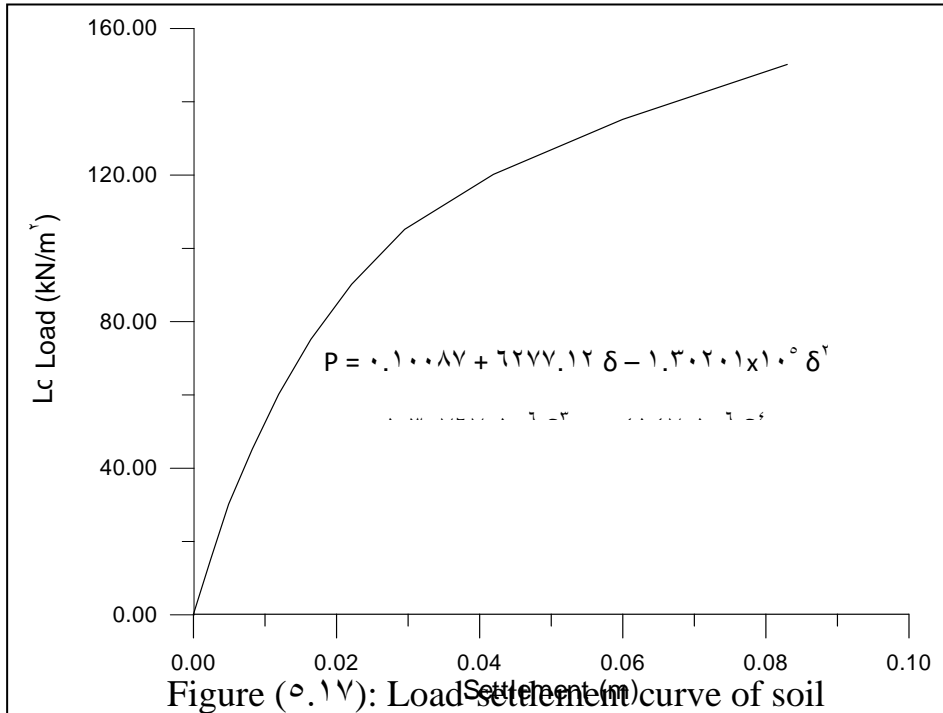
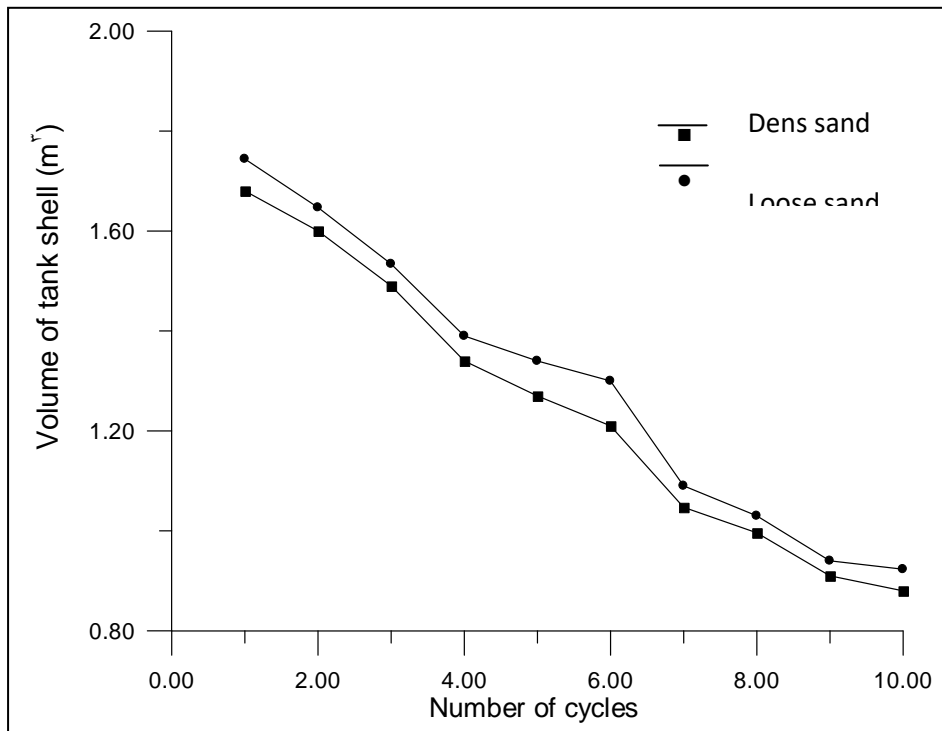


Figure (٥.١٧): Load settlement curve of soil

[loose sand (٣٤)].



(١٠٠ m) closed tank.

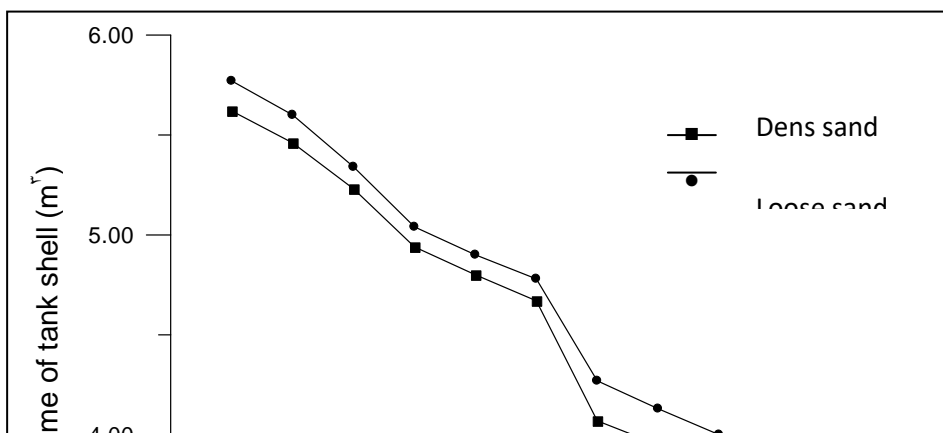
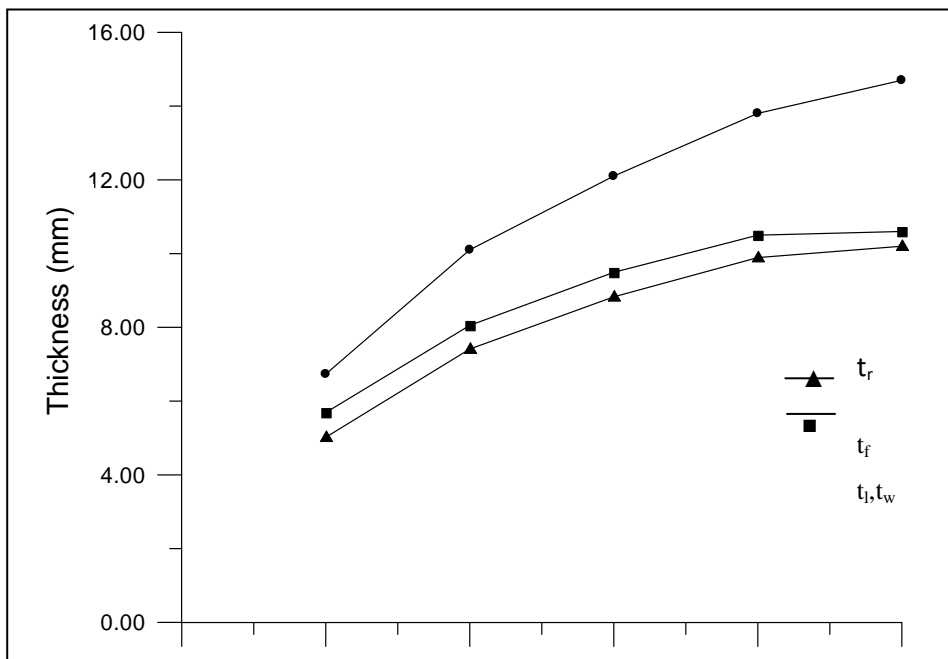
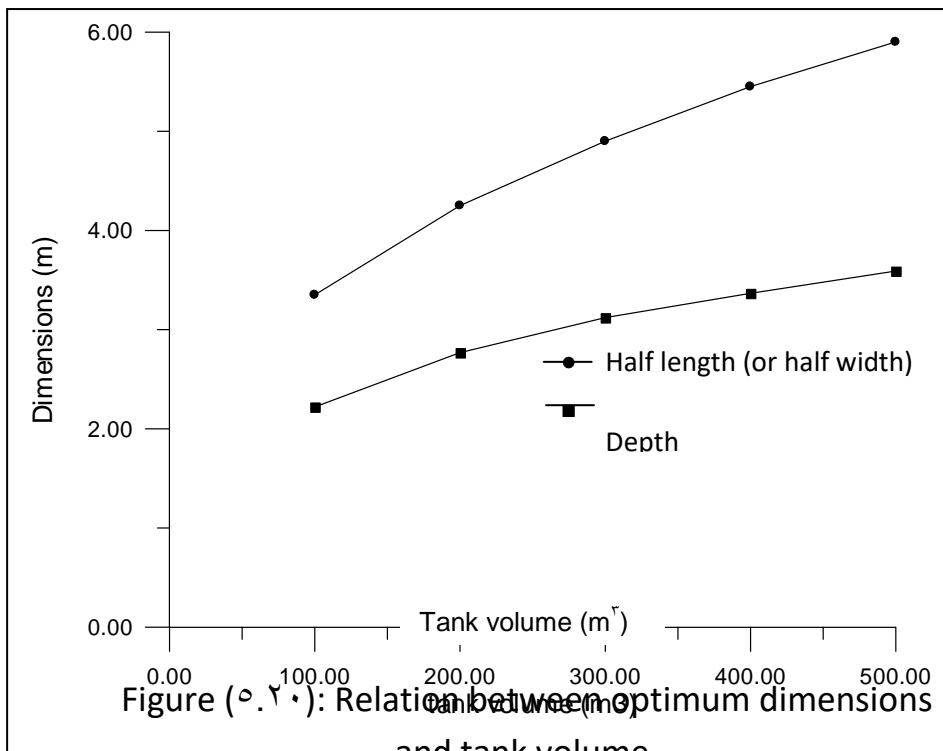
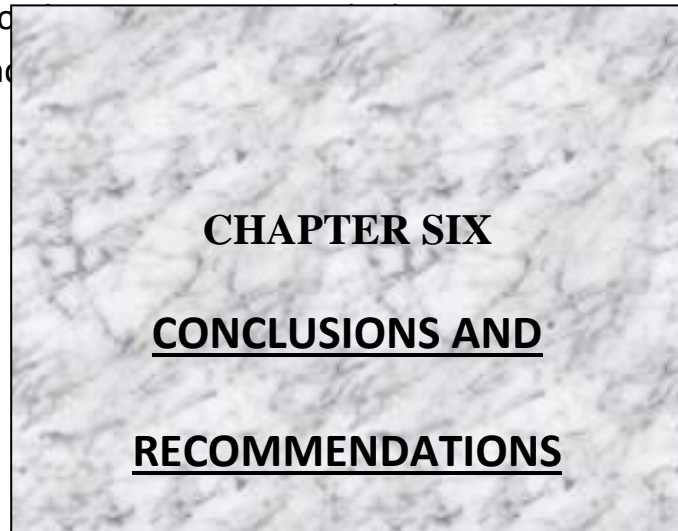


Figure (٥.١٩): Volume of shell verses number of cycles for (٣٠٠ m<sup>٣</sup>) closed tank.



Tank volume (m<sup>3</sup>)

Figure (6.21): Relation  
and



## 6.1 Conclusions

Based on the results obtained in the present study, several conclusions may be drawn. They are summarized as follows:

1-This investigation shows that the non-linear behavior of rectangular tank structures resting on elastic foundation can be accurately predicted by using the finite element method with flat shell element.

٢- The adopted three-level technique: subincrements within iterations within load increments, was used to eliminate the numerical errors that may occur in computations. Such technique has been confirmed to be efficient in the application of the incremental finite element method for non-linear analysis.

٣- The non-linear constrained optimization problem is solved by using the modified Hooke and Jeeves method. It has been shown that this method is efficient, easy to be programmed and can be used in general non-linear constrained optimization.

٤- In structural optimization by the modified Hooke and Jeeves method, an appropriate initial step length must be used to reduce the computational time. The numerical applications have shown that a step length of ٠.١ to ٠.٢ times the smallest design variable is suitable for most cases in the present study.

٥- The optimum material volume for rectangular tank, as obtained by non-linear analysis is smaller than that obtained by linear analysis and the difference is about (٢٦٪) for the considered problem in this study.

٦- The square shape of the rectangular tank forms the best plan shape.

٧- The results of the optimization in the present study shows that the length : width : depth ratio is about (٣ : ٣ : ١), the roof thickness : floor thickness : walls thickness ratio is about (١ : ١.١ : ١.٣).

٨- The optimal dimensions are not so sensitive to the type of soil.

## **٦.٢ Recommendations for future research**

The following recommendations may be suggested as an extension of the present study:

١- Optimum design studies of reinforced concrete rectangular tanks structures, a case in which the percentage of reinforcement steel will be an additional design variable.

٢- Using different types of element in the non-linear analysis problem like degenerated shell element or using a different non-linear analysis technique like closed form solutions and carrying out an optimal design based on that formulation.

٣- Study of the effect of dynamic and earthquake loading on the optimal design of rectangular tanks.

٤- As underground structures, the optimal design of rectangular tanks need to be carried out following the non-linear behavior. A special technique must be introduced for the soil and interface layer.

٥- Implementing a different optimization technique other than the modified Hooke and Jeeves method, then, comparing the results with those obtained in the present work.

٦- Optimal design of stiffened rectangular tanks based on elastic-plastic analysis. The dimensions of stiffeners may be incorporated as design variables.

## **REFERENCES**

١- Abdul-Hussain , K. "Optimum Design of Structures" M.Sc. Thesis , University of Technology, ١٩٨٥.

٢- Adidam S.R. and Subramanyam A.V. "Optimum Design of Reinforced Concrete Water Tanks" Journal of the Structural Division , ASCE, Vol.١٠٨, No.ST٦, pp.(١٢١٩-١٢٣١), June ١٩٨٢.

٣- Al-Azzawi A. A. "Finite Element Analysis of Thin and Thick Reinforced Concrete Shell Foundations" Ph.D. Thesis, University of Baghdad, ٢٠٠٠.

٤- Al-Khafaji, A.G.A. "Large Displacement and Post-Buckling Analysis of Plane Steel Structures With Non-Prismatic Members Resting on Elastic Foundation" M.Sc. Thesis , University of Babylon, ٢٠٠٢.

٥- Al-Mahaidi, Riadh S. "Stiffness Analysis of Cylindrical Tanks Resting on Elastic Media" Proceeding of Fourth Scientific Conference , Scientific Research Council , Vol. ٤, Part ١, Baghdad, ١٩٨٦.

٦- Al-Ne'aimi A.A.H and Al-Sabah A.I "Optimum Design of R/C Cylindrical Tanks With Tapered Walls" Proceeding of the ٢nd. Iraqi Engineering Conference, University of Mosul, Engineering College, ١-٣ Nov., ١٩٨٨

٧- Al-Ne'aimi A.A.H and Al-Sabah A.I "Minimum Cost Design of Underground R/C Cylindrical Tanks" Proceeding of the ٥th. Iraqi Engineering Conference , Vol.٤, Part٢, ٧-١١ Oct., ١٩٨٩.

**٨- Al-Rubai, Q. K. "Large Displacement Elastic Stability Analysis of Plane Structure Under Static Loads and Resting on Non-Linear Winkler Foundation" M.Sc. Thesis , University of Technology, ٢٠٠١.**

٩- Al-Saeq H. M. A. "Optimal Design of Plate and Shell Structures Based on Non-Linear Finite Element Analysis" M.Sc. Thesis , University of Babylon, ٢٠٠٥.

١٠- Al-Sarrai, Basheer A. M. "Analysis of Non-Prismatic Cylindrical Tanks Resting on Elastic Media" M. Sc. Thesis, University of Baghdad, ١٩٨٨.

**١١- Alwash, N. A. H. "Elasto-Plastic and Limit Analysis of Thick Plates" M.Sc. Thesis , University of Baghdad, ١٩٨٩.**

١٢- Beaufait F. W. and Hoadley P. W. "Analysis of Elastic Beams on Non-Linear Foundations" International Journal of Computers and Structures, Vol. ١٢, No. ٥, pp(٦٦٩-٦٧٦), Nov. ١٩٨٠.

١٣- Bowels J. E. "Foundation Analysis and Design" Mc Graw-Hill International Editions, ٥th Edition, ١٩٩٦.

١٤- Buchi J. F. "The Design of Walls of Open Rectangular Tanks" Concrete and Construction Engineering, July, ١٩٥١, Cited in Ref.(٤٨).

١٥- Bunday B. D. "Basic Optimization Methods" School of Mathematical Sciences, University of Bardford, Edward Arnold Pty Limited, Australia. ١٩٨٤.

١٦- Cheung Y, K. and Zienkiewicz O. C. "Plates and Tanks on Elastic Foundations An Application of Finite Element Method" International Journal of Solids and Structures, Vol. ١, pp. (٤٥١-٤٦١), ١٩٦٥.

١٧- Cheung Y. K. and Davies J. D. "Analysis of Rectangular Tanks Use of Finite Element Technique" Concrete, pp. (١٦٩-١٧٤) May, ١٩٦٧.

١٨- Cheung Y. K. and Davies J. D. "Bending Moments in Long Walled Tanks" Journal of the American Concrete Institute , pp. (٦٨٥-٦٨٩), October ١٩٦٧.

١٩- Cook R. D. "Concepts and Applications of Finite Element Analysis" John Wiley and Sons, New York, N.Y. ١٩٨١.

٢٠- Davies J. D. "The Influence of Support Conditions on the Behavior of Cylindrical Concrete Tanks" Proc. Instr. Civil Engineering , London, England, pp.(٣٧٩-٣٨٨), ١٩٦١, Cited in Ref.(٢٧).

٢١- Davies J. D. "Cylindrical Concrete Tanks on Elastic Foundation" Civil Engineering Public Works Review, Vol. ٥٦, pp.(٦١-٦٤), Jan., ١٩٦٢.

٢٢- Davies J. D. et al. "Analysis of Long Rectangular Tanks" Water and Water Engineering , pp.(٥١٠-٥١٦), Dec. ١٩٧٠, Cited in Ref.(٤٨).

٢٣- Fujikubo M. Yao T., Abdul Rahim M. Murakami Y. "Elasto plastic Optimal Design of Frame and Truss Structures Using Repeated Sensitivity Analysis", Preceding of the Third International Offshore and Polar Engineering Conference, Vol. ٤, pp. (٥٣٨-٥٤٤), ١٩٩٣.

٢٤- Ghali A. "The Structural Analysis of Circular and Rectangular Concrete Tanks" Ph.D. Thesis, University of Leeds, England, ١٩٥٧, Cited in Ref.(٤٨).

٢٥- Ghali A, "Analysis of Cylindrical Tanks with Flat Bases by Moment Distribution Method" The Structural Engineering ,. Vol. ٣٦ No.٥, pp(١٦٥-١٧٦) May, ١٩٥٨, Cited in Ref.(٤٨).

٢٦- Ghali A, "Circular Storage Tanks and Silos" Spon LTD. ١٩٧٩, Cited in Ref.(٢٧).

**٢٧- Hamdi M.J. "Optimum Design of Reinforced Concrete Cylindrical Tank Resting on Elastic Media" M.Sc. Thesis , University of Baghdad, ١٩٩٨.**

٢٨- Husain H. M. "The Analysis of Rectangular Plates and Cellular Structures" Ph.D. Thesis, University of Leeds, England, ١٩٦٤, Cited in Ref.(٤٨).

٢٩- Jaiswal O. R. , Rai D. C. and Jain S. K. "Review of Code Provisions on Seismic Analysis of Liquid Storage Tanks" Department of Civil Engineering, Indian Institute of Technology, Kanpur, ٢٠٠٣.

٣٠- Johnson, W. and Mellor, P. B. "Engineering Plasticity" Von Nostrand Reinhold Company Ltd. ١٩٧٨.

**٣١- Karkush M. O. "Non-Linear Behavior of Folded Plate Structures" M.Sc. Thesis , University of Babylon, ١٩٩٨.**

**٣٢- Kimence B. and Ergunen M.E. "Interaction Between Cylindrical and Shallow Spherical Shells on the Vlasov Model Foundation" Computers and Structures Vol. ٤٥, No. ١, pp. (٤١-٥١), ١٩٩٢.**

٣٣- Kondner R. L. "Hyperbolic Stress-Strain Response: Cohesive Soil" Journal of the Soil Mechanics and Foundations Division, ASCE, Vol. ٨٩, pp. (١١٥-١٤٣), Feb. ١٩٦٣.

੨੬- Lambe T. W. and Whitman R. V. "Soil Mechanics, SI Version" ੨nd Edition Wiley Eastern Limited, ੧੯੮੬.

੨੭- Lightfoot E. and Ghali A. "The analysis of Rectangular Tanks" Proceedings of the Institution of Structural Engineering, London, England, ੧੯੭੮, Cited in Ref.(੬੮).

੨੮- Meichoers R. and Rozvany G. "optimum Design of R/C Tanks" Journal of the Engineering Mechanics Division , ASCE, Vol. ੯੬, No.EM੬. pp. (੧ੰ੯੩-੧੧ੰ੬), Dec. ੧੯੮ੰ.

੨੯- Moy S. S. J. "Plastic Method for Steel and Concrete Structures" Department of Civil Engineering, University of Southampton, Macmillan Publishers Limited, UK. ੧੯੮੭.

**ੳ੦- Ng. et al. "Finite Strip Method for Analysis of Structures With Material Non-Linearity" Journal of the Structural Division, ASCE, Vol. ੧੧੮, No. ੳ, pp(੬੮੯-੭ੰੰ), ੧੯੯੧.**

**ੳੱ- Owen D. R. J. and Hinton E. "Finite Element in Plasticity, Theory and Practice" Pineridge Press Limited, Swansea, U.K. , ੧੯੮ੰ.**

੬ੰ- Papadrakakis M., Lagaros N. D.,Tsompanakis Y. and Plevris V. "Large Scale Structural Optimization : Computational Methods and Optimization Algorithms", Archives of Computational Methods in Engineering. Vol. ੮, pp.(ੳੳ੯-ੳੰ੧), ੲੰੰ੧.

ξ١- Portland Cement Association “Rectangular Concrete Tanks” Structural Bureau, ١٩٥١.

ξ٢- Ross C. T. F. “Finite Element Method in Engineering Science” Ellis Horwood Comp. Ltd. , New York, ١٩٩٠.

ξ٣- Save M. A. and Massonnet C. E. “Plastic Analysis and Design of Plates, Shells and Disks” North Holland Publishing Company-Amsterdam, London, ١٩٧٢.

**ξ٤- Starczewski M. “Non-Circular Pressure Vessels-Some Guidance Notes for Designers” British Engineering Technical Report , Vol. XIV, ١٩٨١.**

ξ٥- Therendran V. and Thambiratnam D. P. “Minimum Wight Design of Cylindrical Water Tanks” International Journal of Numerical Methods in Engineering , Vol. ٢٣ , pp.(١٦٧٩-١٦٩١), ١٩٨٦.

ξ٦- Timoshinko S. and Woinowsky-Krieger S. “Theory of Plates and Shells” McGraw-Hill BookCO. Inc. , NewYork, N. Y., ١٩٥٩.

**ξ٧- Uraiby S.A. “Optimum Design of Reinforced Concrete Rectangular Tank on Elastic Foundation” M.Sc. Thesis , University of Baghdad, ١٩٩٧.**

**ξ٨- Wilby C. A. “Structural Analysis of Reinforced Concrete Tanks” Journal of Structural Division, ASCE, Vol. ١٠٣. pp.(٩٨٩-١٠٠٤), ١٩٧٧.**

